



RESEARCH REPORT

HEALTH
EFFECTS
INSTITUTE

Number 98
November 2000

Final Version

Daily Mortality and Fine and Ultrafine Particles in Erfurt, Germany

Part I: Role of Particle Number and Particle Mass

H-Erich Wichmann, Claudia Spix, Thomas Tuch, Gabriele Wölke, Annette Peters, Joachim Heinrich, Wolfgang G Kreyling, and Joachim Heyder



Includes a Commentary by the Institute's Health Review Committee



HEALTH
EFFECTS
INSTITUTE

The Health Effects Institute, established in 1980, is an independent and unbiased source of information on the health effects of motor vehicle emissions. HEI supports research on all major pollutants, including regulated pollutants (such as carbon monoxide, ozone, nitrogen dioxide, and particulate matter) and unregulated pollutants (such as diesel engine exhaust, methanol, and aldehydes). To date, HEI has supported more than 200 projects at institutions in North America and Europe and has published over 100 research reports.

Typically, HEI receives half its funds from the US Environmental Protection Agency and half from 28 manufacturers and marketers of motor vehicles and engines in the United States. Occasionally, funds from other public and private organizations either support special projects or provide resources for a portion of an HEI study. Regardless of funding sources, HEI exercises complete autonomy in setting its research priorities and in reaching its conclusions. An independent Board of Directors governs HEI. The Institute's Health Research and Health Review Committees serve complementary scientific purposes and draw distinguished scientists as members. The results of HEI-funded studies are made available as Research Reports, which contain both the Investigators' Report and the Health Review Committee's evaluation of the work's scientific quality and regulatory relevance.



STATEMENT

Synopsis of Research Report 98, Part I

Daily Mortality and Fine and Ultrafine Particles in Erfurt, Germany Part I: Role of Particle Number and Particle Mass

INTRODUCTION

Epidemiologic studies have shown an association between airborne particles and mortality data, but uncertainty persists as to which aspects of the particle mixture are the driving force underlying observed associations. Further, only a small number of studies have investigated the role of ultrafine particles (particles less than 0.1 μm in diameter). Although ultrafine particles contribute little to mass concentration, they are present in urban air in high numbers and may be important in terms of health effects. One hypothesis is that these particles may be particularly toxic because their small size allows them to deposit efficiently deep in the lungs and that the higher number of ultrafine particles, and therefore their greater total particle surface area, may increase their toxicologic effects. However, the few epidemiologic studies that have tried to isolate effects of ultrafine particles have evaluated respiratory disease, not deaths.

APPROACH

Dr H-Erich Wichmann and colleagues at the National Research Center for Environment and Health (GSF) in Neuherberg, Germany, prospectively studied the association of daily mortality data with the number and mass concentrations of ultrafine and fine particles in Erfurt, Germany. Using a time-series approach, they looked at short-term changes in particle concentration and the concurrent deaths due to cardiovascular and respiratory causes. Concentrations were measured at one monitoring site, which was close to a road, and mortality was analyzed for 3.5 years. Because Erfurt had a population of roughly 200,000 people, the number of deaths was small (average 5 to 6 deaths per day). The analytic technique that the investigators developed to gather air pollution data, especially monitoring of the ultrafine fraction, was unique in the sharp detail of the size ranges.

The statistical methods were Poisson regression with a generalized additive model to smooth time trends, weather, and other variables.

RESULTS AND INTERPRETATION

The authors evaluated whether human deaths were associated in time with levels of outdoor particles (that is, whether the measured day-to-day changes in air pollution related to the day-to-day changes in deaths). If air pollution and adverse health outcomes are closely linked in time, then a daily average value of air pollution will be associated with a daily measure of health. This relation was estimated in the current study by relative risk, the relative increase in deaths given the range of particulate pollutants.

Timing of effect was evaluated by examining pollutant levels on the current day (lag 0), the prior day (lag 1), 2 days prior to death (lag 2), and so on, up to 5 days prior to death (lag 5). A lag is the assumed time period between exposure and effect and can be represented by the best single day or an average of the effect over multiple days. Currently, no biological evidence supports a particular lag. Although many investigators of time-series studies have used the best lag approach, this method can bias the results toward finding positive or negative statistically significant associations.

This study was the first to show that ultrafine particles are associated with human mortality. The investigators found comparable effects for ultrafine and fine particles and have reported a suggestion of a delayed effect for ultrafine particles versus an immediate effect for fine particles. The HEI Health Review Committee agreed with the investigators' conclusions that associations between mortality and ultrafine and fine particles were observed; however, the Committee did not agree that a consistent pattern indicating either a delayed or an immediate effect existed.

Research Report 98, Part I

This study is a major contribution to our knowledge of actual airborne particle levels, and it has provided the first evidence that ultrafine particles as well as fine particles are associated with mortality. Despite the unique analytic technique developed by the investigators, important limitations to the results remain

(specifically regarding interpretations of timing of effect). Although the results associate the ultrafine fraction with human deaths, no clear pattern of associations indicates temporal differences between ultrafine and fine particles.



CONTENTS

Research Report 98

HEALTH
EFFECTS
INSTITUTE

Daily Mortality and Fine and Ultrafine Particles in Erfurt, Germany

Part I: Role of Particle Number and Particle Mass

H-Erich Wichmann, Claudia Spix, Thomas Tuch, Gabriele Wölke, Annette Peters,
Joachim Heinrich, Wolfgang G Kreyling, and Joachim Heyder

*GSF-Forschungszentrum für Umwelt und Gesundheit and Ludwig Maximilian University,
Neuherberg, Germany*

HEI STATEMENT

This Statement is a nontechnical summary of the Investigators' Report and the Health Review Committee's Commentary.

PREFACE

Background	1	Continuing Research	2
Research Program from HEI RFA 94-2	2	References	3

INVESTIGATORS' REPORT

When an HEI-funded study is completed, the investigators submit a final report. The Investigators' Report is first examined by three outside technical reviewers and a biostatistician. The report and the reviewers' comments are then evaluated by members of the HEI Health Review Committee, who had no role in selecting or managing the project. During the review process, the investigators have an opportunity to exchange comments with the Review Committee and, if necessary, revise the report.

Abstract	5	Implications of Findings	66
Introduction	6	Acknowledgments	67
Specific Aims	7	References	67
Definitions	8	Appendix A. Assigning the Causes of Death to Categories	73
Methods	8	Appendix B. Comparison of the Distribution of the Underlying Causes of Death	74
Study Design	8	Appendix C. Comparison of Prevalent Diseases and Underlying Causes of Death	75
Study Period and Study Area	8	Appendix D. Properties of the Particle Data	77
Data	9	Appendix E. Diagnostics of Confounder Model	80
Mortality Data	15	Appendix F. Further Subgroup Results	82
Analytical Methods	18	Confounder Models Differ by Subgroup	82
Results	22	Delays Differ by Subgroup	82
Data Description	22	Appendices Available on Request	84
Regression Analysis	36	About the Authors	84
Summary of the Regression Results	51	Abbreviations and Other Terms	86
Discussion and Synthesis	55		
Ambient Air Pollution in Erfurt	55		
Health Effects of Particles	57		
Gaseous Pollutant Effects	62		
Limitations	65		
Conclusions	66		

Continued

Research Report 98, Part I

COMMENTARY Health Review Committee

The Commentary about the Investigators' Report is prepared by the HEI Health Review Committee and staff. Its purpose is to place the study into a broader scientific context, to point out its strengths and limitations, and to discuss remaining uncertainties and implications of the findings for public health.

Introduction	87	Gaseous Pollutants	92
Effects of Particle Size	87	Prevalent Versus Underlying Condition	92
Epidemiology	88	Characterization of Exposure to Ultrafine Particles	80
Technical Evaluation	88	Summary and Conclusions	92
Aims and Objectives	88	Acknowledgments	93
Study Design	88	References	93
Methods	89		
Results	90		
Discussion	91		
Lag Patterns	91		
Sensitivity Analyses	92		

RELATED HEI PUBLICATIONS

Publishing History: This document was posted as a preprint on www.healtheffects.org and then finalized for print.

Citation for whole report:

Wichmann H-E, Spix C, Tuch T, Wölke G, Peters A, Heinrich J, Kreyling WG, Heyder J. 2000. Daily Mortality and Fine and Ultrafine Particles in Erfut, Germany. Part I: Role of Particle Number and Particle Mass. Research Report 98. Health Effects Institute, Cambridge MA.

When specifying a section of this report, cite it as a chapter of this document.

PREFACE

In 1994, HEI initiated a research program to investigate the complex issues associated with the health effects of exposure to particulate matter (PM)* in the air. This program was developed in response to growing concern about the potential public health significance of reported associations between daily fluctuations in levels of PM and changes in daily morbidity and mortality in time-series epidemiology studies. These results were questioned for a variety of reasons, including the lack of support from experimental studies and the lack of a mechanism to explain how such effects would occur. To address these issues HEI undertook two research initiatives in 1994: (1) the Particle Epidemiology Evaluation Project (Samet et al 1995, 1997), which evaluated six of the time-series epidemiology studies that had reported effects of PM on mortality; and (2) a program of toxicologic and epidemiologic studies (funded from RFA 94-2, "Particulate Air Pollution and Daily Mortality: Identification of Populations at Risk and Underlying Mechanisms"), which aimed to understand better how PM might cause toxicity and what factors might affect susceptibility. In all, HEI has issued five requests for research on PM and funded 34 studies or reanalyses over the last five years.

This Preface provides general regulatory and scientific background information relevant to studies funded from RFA 94-2, including the study by H-Erich Wichmann that is described in the accompanying Report and Commentary. All of the studies from RFA 94-2 have been completed and are either under review by HEI or have been published. The *HEI Program Summary: Research on Particulate Matter* (Health Effects Institute 1999) provides information on studies funded since 1996.

BACKGROUND

Particulate matter (PM) is the term used to define a complex mixture of anthropogenic and naturally occurring airborne particles. The size, chemical composition, and other physical and biological properties of PM depend on the sources of the particles and the changes the particles undergo in the atmosphere. In urban environments, these particles derive mainly from combustion, including mobile sources such as motor vehicles and stationary sources such as power plants. The most commonly used descriptor of particle size is *aerodynamic diameter*. Based

on this parameter, ambient particles tend to fall into three size classes (often defined as modes): ultrafine or nuclei mode (particles less than 0.1 μm in diameter); fine or accumulation mode (particles between 0.1 and 2.5 μm in diameter), and coarse (particles larger than 2.5 μm in diameter). Fine and ultrafine particles are dominated by emissions from combustion processes while coarse particles are mostly generated by mechanical processes from a variety of noncombustion sources. Generally, the ultrafine and fine fractions are composed of carbonaceous material, metals, sulfate, nitrate and ammonium ions. The coarse fraction is composed mostly of mechanically generated particles and consists of insoluble minerals and biologic aerosols, with smaller contributions from primary and secondary aerosols and sea salts (US Environmental Protection Agency [EPA] 1996).

A number of early epidemiologic studies indicated that human exposure to high concentrations of PM, such as London fog, had deleterious effects (such as increased number of deaths), particularly in children, the elderly, and those with cardiopulmonary conditions (Firket 1931; Ciocco and Thompson 1961; Logan 1953; Gore and Shaddick 1968). Because of this apparent relation to increased mortality, the EPA has regulated the levels of ambient PM since 1971, when the Clean Air Act was first promulgated. This act authorized the EPA to set National Ambient Air Quality Standards (NAAQSs) for a number of potentially harmful air pollutants (including PM) in order to protect the health of the population, particularly those thought to be sensitive.

The first NAAQS for PM was based on controlling total suspended PM or particles up to 40 μm in diameter. In 1978, the standard was revised to regulate inhalable particles, or particles that can deposit in the respiratory tract and therefore have greater potential for causing adverse health effects. These are particles with an aerodynamic diameter of 10 μm or less (PM_{10}). More recent epidemiologic studies, published in the early 1990s, indicated a relatively consistent association between small short-term increases in PM levels and increases in both mortality and morbidity from respiratory and cardiovascular diseases (reviewed by the Committee of the Environmental and Occupational Health Assembly, American Thoracic Society [Bascom et al 1996]).

Some studies also suggested that long-term exposure to low levels of PM is associated with adverse effects (Dockery et al 1993; Pope et al 1995). These latter studies also pointed to a possible role of fine particles (less than

* A list of abbreviations and other terms appears at the end of the Investigators' Report.

Table 1. Current NAAQs for PM (set in 1997)

	PM ₁₀	PM _{2.5}
Daily Standard	150 µg/m ³	65 µg/m ³
Annual Standard	50 µg/m ³	15 µg/m ³

2.5 µm in aerodynamic diameter [PM_{2.5}]). In 1997, the EPA considered the evidence for the effects of fine particles sufficient to promulgate a fine particle standard while retaining the PM₁₀ standard (US Environmental Protection Agency 1997) (see Table 1). The next review of the PM NAAQS is scheduled to be completed by the year 2002.

RESEARCH PROGRAM FROM HEI RFA 94-2

The wealth of epidemiologic data published in the early 1990s suggested an association between PM and health effects, but aspects of these findings were not well understood. Problems involved uncertainties in the exposure estimates, confounding by weather or other factors, the role of copollutants, and the mechanisms by which particles may cause effects. Moreover, although the epidemiologic findings were consistent across different communities exposed to distinct mixes and levels of pollutants, they were not well supported by either human chamber studies or animal inhalation studies aimed at delineating pathologic changes that might result in death. Failure of the experimental studies to provide support for the epidemiologic findings was attributed to insufficient statistical power, use of particles not representative of ambient particles, or use of animals not representative of the individuals susceptible to increased mortality.

By the mid 1990s, it became apparent that the research to advance our understanding of the association between exposure to particles and daily mortality found in the epidemiologic studies needed to focus on identifying (1) susceptible populations, (2) mechanisms by which particles may lead to increased mortality, and (3) characteristics of the particles responsible for the effects. It was recognized that both epidemiologic and experimental studies would be required.

The HEI program initiated in 1994 was aimed at addressing these research needs. Six epidemiologic and toxicologic studies were funded through RFA 94-2, and three additional studies were added through the preliminary application process. As a group, the five epidemiologic studies investigated: (1) social and medical factors that might increase the risk of mortality when particulate pollution

increases (Mark Goldberg of the National Institute of Scientific Research, University of Quebec [see Goldberg et al 2000]); (2) components of particulate pollution that might account for its effect on mortality (Morton Lippmann of the New York University School of Medicine [see Lippmann et al 2000] and Erich Wichmann of the GSF Institute of Epidemiology and Ludwig Maximilian University [presented in this Research Report]); and (3) cause of death (Harvey Checkoway of the University of Washington [see Checkoway et al 2000] and Mark Goldberg) or possible pathophysiologic mechanisms that might lead to death in people exposed to particulate air pollution (Douglas Dockery of Harvard School of Public Health [see Dockery et al 1999]).

The four experimental studies tested the hypothesis that older animals or animals with preexisting lung or heart disease or respiratory infections are more sensitive to the acute effects of particles than healthy animals. They investigated possible mechanisms leading to mortality such as inflammation, changes in immune response, or changes in cardiac and respiratory function. Three of these studies used for the first time concentrated ambient particles (CAPs) (John Godleski of Harvard School of Public Health [see Godleski et al 2000], and Terry Gordon [see Gordon et al 2000] and Judith Zelikoff of New York University School of Medicine). In these CAPs studies, particles in the range of about 0.1 to 2.5 µm are concentrated while those greater than 2.5 µm are removed and those under 0.1 µm remain at the ambient concentration. CAPs exposures represent a significant fraction of ambient PM and provide a reasonable approach to mimicking the exposure to PM in epidemiology studies. The fourth experimental study (Günter Oberdörster of the University of Rochester School of Medicine [see Oberdörster et al 2000]) focused on evaluating the effects of different ultrafine particles that have been hypothesized to be more toxic than fine particles.

CONTINUING RESEARCH

Many of the key questions identified in the early 1990s are still relevant and much research is ongoing to address them. The research strategies have evolved, however, as results from previous studies have provided insights into which animal models and which endpoints may be the most helpful to evaluate. In addition, advances in exposure assessment and statistical methods have pointed to new approaches for conducting epidemiologic studies. Since RFA 94-2, HEI has funded a number of research projects that build on the new findings and approaches. These studies will be completed by the end of 2002.

REFERENCES

- Bascom R, Bromberg PA, Costa DA, Devlin R, Dockery DW, Frampton MW, Lambert W, Samet JM, Speizer FE, Utell M. 1996. Health effects of outdoor air pollution. Part 1. *Am J Respir Crit Care Med* 153:3–50.
- Checkoway H, Levy D, Sheppard L, Kaufman J, Koenig J, Siscovick D. 2000. A Case-Crossover Analysis of Fine Particulate Matter Air Pollution and Out-of-Hospital Sudden Cardiac Arrest. Research Report 98. Health Effects Institute, Cambridge MA.
- Ciocco A, Thompson DJ. 1961. A follow-up on Donora ten years after: Methodology and findings. *Am J Pub Health* 15:155–164.
- Dockery DW, Pope CA III, Xu X, Spengler JD, Ware JH, Fay ME, Ferris BG, Speizer FE. 1993. An association between air pollution and mortality in six US cities. *N Engl J Med* 329:1753–1759.
- Dockery DW, Pope CA III, Kanner RE, Villegas GM, Schwartz J. 1999. Daily Changes in Oxygen Saturation and Pulse Rate Associated with Particulate Air Pollution and Barometric Pressure. Research Report 83. Health Effects Institute, Cambridge MA.
- Firket J. 1931. The cause of the symptoms found in the Meuse Valley during the fog of December 1930. *Bull Acad R Med Belg* 11:683–741.
- Godleski JJ, Verrier RL, Koutrakis P, Catalano P. 2000. Mechanisms of Morbidity and Mortality from Exposure to Ambient Air Particles. Research Report 91. Health Effects Institute, Cambridge MA.
- Goldberg MS, Bailar JC III, Burnett RT, Brook JR, Tamblyn R, Bonvalot Y, Ernst P, Flegel KM, Singh RK, Valois MF. 2000. Identifying Subgroups of the General Population That May Be Susceptible to Short-Term Increases in Particulate Air Pollution: A Time-Series Study in Montreal, Quebec. Research Report 97. Health Effects Institute, Cambridge MA.
- Gordon T, Nadzieko C, Chen LC, Schlesinger R. 2000. Effects of Concentrated Ambient Particles in Rats and Hamsters: An Exploratory Study. Research Report 93. Health Effects Institute, Cambridge MA.
- Gore AT, Shaddick CW. 1968. Atmospheric pollution and mortality in the county of London. *Br J Prev Soc Med* 12:104–113.
- Health Effects Institute. 1999. Research on Diesel Exhaust (HEI Research Program Summary). Health Effects Institute, Cambridge MA.
- Health Effects Institute. 1999. Research on Particulate Matter (HEI Research Program Summary). Health Effects Institute, Cambridge MA.
- Lippmann M, Ito K, Nádas A, Burnett RT. 2000. Association of Particulate Matter Components with Daily Mortality and Morbidity in Urban Populations. Research Report 95. Health Effects Institute, Cambridge MA.
- Logan WPD. 1953. Mortality in London fog incident. *Lancet* i:336–338.
- Oberdörster G, Finkelstein JN, Johnston C, Gelein R, Cox C, Baggs R, Elder ACP. 2000. Acute Pulmonary Effects of Ultrafine Particles in Rats and Mice. Research Report 96. Health Effects Institute, Cambridge MA.
- Pope CA III, Thun MJ, Namboodiri MM, Dockery DW, Evans JS, Speizer FE, Heath CW. 1995. Particulate air pollution as a predictor of mortality in a prospective study of US adults. *Am J Respir Crit Care Med* 151:669–674.
- Samet JM, Zeger SL, Birhane K. 1995. The association of mortality and particulate air pollution. In: *Particulate Air Pollution and Daily Mortality: Replication and Validation of Selected Studies, The Phase I.A Report of the Particle Epidemiology Evaluation Project*. Health Effects Institute, Cambridge MA.
- Samet JM, Zeger SL, Kelsall JE, Xu J, Kalkstein LS. 1997. Air pollution, weather, and mortality in Philadelphia. In: *Particulate Air Pollution and Daily Mortality: Analysis of the Effects of Weather and Multiple Air Pollutants, The Phase I.B Report of the Particle Epidemiology Evaluation Project*. Health Effects Institute, Cambridge MA.
- US Environmental Protection Agency. 1996. Air Quality Criteria for Particulate Matter. Vol I. Document EPA/600/P-95/001. Office of Research and Development, Washington DC.
- US Environmental Protection Agency. 1997. Revisions to the National Ambient Air Quality Standards for particulate matter: Final rule. *Fed Regist* 52:24634–24669.

Daily Mortality and Fine and Ultrafine Particles in Erfurt, Germany

Part I: Role of Particle Number and Particle Mass

H-Erich Wichmann, Claudia Spix, Thomas Tuch, Gabriele Wölke, Annette Peters, Joachim Heinrich, Wolfgang G Kreyling, and Joachim Heyder

ABSTRACT

Increases in morbidity and mortality have been observed consistently and coherently in association with ambient air pollution. A number of studies on short-term effects have identified ambient particles as a major pollutant in urban air. This study, conducted in Erfurt, Germany, investigated the association of mortality not only with ambient particles but also with gaseous pollutants and indicators of sources. Part I of this study concentrates on particles.

Data were collected prospectively over a 3.5-year period from September 1995 to December 1998. Death certificates were obtained from the local authorities and aggregated to daily time series of total counts and counts for subgroups.

In addition to standard data for particle mass with diameters $\leq 2.5 \mu\text{m}$ ($\text{PM}_{2.5}$)* or $\leq 10 \mu\text{m}$ (PM_{10}) from impactors, a mobile aerosol spectrometer (MAS) was used to obtain size-specific number and mass concentration data in six size classes between $0.01 \mu\text{m}$ and $2.5 \mu\text{m}$. Particles smaller than $0.1 \mu\text{m}$ were labeled *ultrafine particles* (three size classes), and particles between 0.1 and $2.5 \mu\text{m}$ were termed *fine particles* (three size classes). Concentrations of the gases sulfur dioxide (SO_2), nitrogen dioxide (NO_2), and carbon monoxide (CO) were also measured.

The daily average total number concentration was $18,000 \text{ particles/cm}^3$ with 88% of particles below $0.1 \mu\text{m}$

and 58% below $0.03 \mu\text{m}$ in diameter. The average mass concentration ($\text{PM}_{2.5}$) was $26 \mu\text{g/m}^3$; of this, 75% of particles were between 0.1 and $0.5 \mu\text{m}$ in diameter. Other average concentrations were $38 \mu\text{g/m}^3$ for PM_{10} , $17 \mu\text{g/m}^3$ for SO_2 , $36 \mu\text{g/m}^3$ for NO_2 , and $600 \mu\text{g/m}^3$ for CO.

Ambient air pollution demonstrated a strong seasonality with maximum concentrations in winter. Across the study period, fine particle mass decreased, whereas ultrafine particle number was unchanged. The proportion of ultrafine particles below $0.03 \mu\text{m}$ diameter increased compared with the proportion of other particles. During the study, concentrations of SO_2 and CO also decreased, whereas the concentration of NO_2 remained unchanged.

The data were analyzed using Poisson regression techniques with generalized additive modeling (GAM) to allow nonparametric adjustment for the confounders. Both the best single-day lag and the overall association of multiple days fitted by a polynomial distributed lag model were used to assess the lag structure between air pollution and death. Mortality increased in association with level of ambient air pollution after adjustment for season, influenza epidemics, day of week, and weather. In the sensitivity analyses, the results proved stable against changes of the confounder model.

We saw comparable associations for ultrafine and fine particles in a distributed lag model where the contribution of the previous 4 to 5 days was considered. Furthermore, the data suggest a somewhat more delayed association of ultrafine particles than of fine particles if single-day lags are considered. The associations tended to be stronger in winter than in summer and at ages below 70 years compared to ages above 70 years. Analysis of the prevalent diseases mentioned on death certificates revealed that the overall association for respiratory diseases was slightly stronger than for cardiovascular diseases.

In two-pollutant models, associations of ultrafine and fine particles seemed to be largely independent of each other, and the risk was enhanced if both were considered at the same time. Furthermore, when the associations were summed for the six size classes between 0.01 and $2.5 \mu\text{m}$,

*A list of abbreviations and other terms appears at the end of the Investigators' Report.

The Investigators' Report is one part of Health Effects Institute Research Report 98, which also includes a Preface, a Commentary by the Health Review Committee, and an HEI Statement about the research project. Correspondence concerning the Investigators' Report may be addressed to Dr H-Erich Wichmann, GSF Institute of Epidemiology, Ingolstädter Landstr 1, Neuherberg, D-85764, Germany.

Although this document was produced with partial funding by the United States Environmental Protection Agency under Assistance Award R824835 to the Health Effects Institute, it has not been subjected to the Agency's peer and administrative review. Therefore, it may not necessarily reflect the views of the Agency, and no official endorsement by the Agency should be inferred. The contents of this document also have not been reviewed by private party institutions, including those that support the Health Effects Institute; therefore, it may not reflect the views or policies of these parties, and no endorsement by them should be inferred.

the overall association was clearly stronger than the associations of the individual size classes alone.

Associations were observed for SO₂, NO₂, and CO with mortality despite low concentrations of these gases. These associations disappeared in two-pollutant models for NO₂ and CO, but they remained stable for SO₂. The persistence of the SO₂ effect was interpreted as artifact, however, because the SO₂ concentration was much below levels at which effects are usually expected. Furthermore, the results for SO₂ were inconsistent with those from earlier studies conducted in Erfurt.

We conclude that both fine particles (represented by particle mass) and ultrafine particles (represented by particle number) showed independent effects on mortality at ambient concentrations. Comparable associations for gaseous pollutants were interpreted as artifacts of collinearity with particles from the same sources.

INTRODUCTION

In various climates in North America, South America, and Europe, epidemiologic studies have consistently observed short-term associations of particulate matter on daily mortality (Dockery and Pope 1994; Schwartz 1994a; Bascom et al 1996; Katsouyanni et al 1997; Pope and Dockery 1999), frequently finding the largest effect estimates on the concurrent day or one day afterward. A recent review estimated that an increase of 10 µg/m³ in PM₁₀ was associated with 0.8% increase in mortality with a summary estimate for respiratory disease mortality around 3% and for cardiovascular disease at around 1.3% (Pope and Dockery 1999). When measures of both PM₁₀ and PM_{2.5} have been available, PM_{2.5} has appeared more strongly associated with mortality than has PM₁₀ (Dockery et al 1992; Schwartz et al 1996).

Pooled analysis of data from four large western European cities (London, Barcelona, Paris, and Athens), obtained as part of the APHEA (Air Pollution and Health: A European Approach) project, suggested that the risk of mortality increased independently with increased levels of SO₂ and black smoke (Katsouyanni et al 1997). In the absence of more detailed air pollution measurements, black smoke could be regarded as a surrogate measure for ambient particles in urban air.

The objective of this study was to assess the association and role of particles of different size (with size classes ranging from 10 µm to 2.5 µm) with respect to mortality in an urban setting. In the 1980s, analysis of the association in Erfurt between ambient air pollution and mortality had identified stronger associations between total suspended

particles (TSP) and mortality than between SO₂ and mortality (Spix et al 1993a,b). Since the reunification of Germany, SO₂ concentrations have been reduced substantially due to diminished use of brown coal as fuel (Wichmann and Heinrich 1995; Brauer et al 1995; Spix et al 1993a,b; Peters et al 1996; Cyrus et al 1998). In addition, fine particle mass decreased substantially in Erfurt between 1991 and 1996, while the particle number concentration did not change (Tuch et al 1997a; Wichmann and Peters 1999a,b). Therefore, Erfurt provided an ideal location to use a refined characterization of particle size distribution to assess the effects of particulate matter on mortality.

Ambient concentrations of particles are classically characterized by their mass concentrations. Depending on particle size, however, quite substantial differences in particle number or surface area can be associated with the same particle mass concentration (Table 1; Oberdörster et al 1995). For example, although only 1 particle/cm³ with a diameter of 2.5 µm is sufficient to result in a mass concentration of 10 µg/m³, more than 2 million particles of a diameter of 0.02 µm are needed to obtain the same mass concentration.

Depending on particle size, inhaled particles are deposited in different parts of the respiratory tract. In particular, the deposition probability of ultrafine particles is rather high in the alveolar region (International Commission on Radiological Protection 1994; US Environmental Protection Agency [EPA] 1996). Despite many epidemiologic studies showing a relation between particle exposure and excess cardiopulmonary morbidity and mortality (Dockery and Pope 1994; Schwartz 1994b; Bascom et al 1996), it is important to remember that ambient particles are a mixture: The responsible properties of the particles still have to be identified, and a plausible mechanism has yet to be established to explain this association.

Some researchers have hypothesized that ultrafine particles are responsible for the associations between particle matter and health outcomes at the current low concentrations of ambient particles (Oberdörster et al 1995; Seaton

Table 1. Number and Surface Area of Spherical Particles of Unit Density at Concentration of 10 µg/m³ (Oberdörster et al 1995)

Particle Diameter (µm)	Particles (n/cm ³)	Surface Area (µm ² /cm ³)
0.02	2,400,000	3,016
0.5	153	120
2.5	1	24

et al 1995). A number of potential mechanisms might contribute to an increased toxicity of ultrafine particles:

1. For a given aerosol mass concentration, ultrafine particles have a much higher particle number and surface area compared with values for larger sized particles. Both fine particles and ultrafine particles can act as a carrier to the deep lung for adsorbed reactive gases, radicals, transition metals, or organic compounds, and the larger surface area of ultrafine particles can transport more toxic, surface-adsorbed materials than larger particles can.
2. Inhaled ultrafine particles are deposited deep in the respiratory tract. As much as 50% of inhaled 0.02 μm diameter particles are estimated to be deposited in the alveolar region of the human lung, along with somewhat lower levels being deposited in the lower tracheobronchial tree.
3. Particles not readily soluble in the fluid of the epithelial lining provide the interface between retained particles and the cells, fluids, and tissues of the lungs. Hence, the dramatically increased surface area of ultrafine particles is likely to increase surface-dependent reactions.
4. Protection of lung tissue resulting from avid particle phagocytosis by alveolar macrophages is impaired because ultrafine particles are less well recognized by these cells. In addition, many more ultrafine particles spread over the surface of the alveolar epithelium than would be the case with larger particles.
5. After deposition, ultrafine particles penetrate more rapidly into interstitial lung tissue than do larger particles. Preliminary evidence suggests ultrafine particles can be translocated to remote organs such as the liver and heart.

Recent studies in healthy and compromised laboratory animals have suggested that inhalation of particle pollutants may induce changes in cardiac rhythm or repolarization, but the implications of these results for mechanisms in humans are unclear. Others have proposed that pollution exposure induces a transient increase in blood coagulability as part of the acute phase response associated with inflammation (Seaton et al 1995). Even though animal experiments show evidence that inflammation in the lungs, as well as its translation to the systemic circulation, may be induced by instillation or inhalation of particles, the mechanism in the context of ambient particle concentrations is unclear.

So far, the only epidemiologic evidence of a systemic response was shown in our MONICA-Augsburg survey, which coincided with the Europe-wide air pollution

episode in 1985 (Peters et al 1997d). The odds for observing a plasma viscosity level above the 90th percentile doubled in men and women during this period. An 8-year follow-up revealed that the relative risk for coronary heart disease nearly tripled in the highest quintile in men compared with all other quintiles (Koenig et al 1998). This suggests that the changes in plasma viscosity were a risk factor when they occurred repeatedly over time, and they might therefore provide a link to mortality observed in time series analysis.

To date, no data on the role of ultrafine particles on mortality have substantiated these hypotheses. As summarized by Wichmann and Peters (2000), however, three panel studies have reported epidemiologic data on the health effects of ultrafine particles in persons with respiratory disease (Peters et al 1997d; Pekkanen et al 1997; Penttinen et al 1998). These studies are described in detail in the Discussion.

SPECIFIC AIMS

The study had two specific aims: Specific Aim 1 was to characterize ambient air pollution based on measurements of particles with a diameter between 10 μm and 2.5 μm obtained with a particle spectrometer and on measurements of gaseous pollutants. Specific Aim 2 was to assess the role of ambient particles in the size range of 10 μm to 2.5 μm in exacerbating mortality.

Specific Aim 1 was addressed by setting up a measurement platform that operated over 3.5 years to characterize the ambient aerosol with a particle spectrometer and with measurements of gaseous pollutants. Specific Aim 2 was addressed in an epidemiologic study based on death certificates. Daily mortality was analyzed using Poisson regression models. In these analyses the following questions were assessed.

1. Is mortality associated with ambient air pollution as was observed in the 1980s (Spix et al 1993a,b) and are stronger effects observed for particulate matter than for gaseous pollutants such as SO_2 ?
2. Do ultrafine particles have a stronger or different association with mortality than that between fine particles and mortality? This was hypothesized by Oberdörster and colleagues (1995), articulated by Seaton and coworkers (1995), and supported by Peters and associates (1997) studying lung function in persons with asthma in Erfurt.
3. Are relative risks larger for persons with preexisting cardiovascular disease, respiratory disease, or both,

than for all-cause mortality based on pathomechanisms relating inhalation of particles to exacerbation of preexisting disease?

DEFINITIONS

For the purpose of this study, we used several definitions. Particles were described according to size: Ultrafine particles were below 0.1 μm in diameter, fine particles had a diameter between 0.1 and 2.5 μm , and coarse particles had a diameter above 2.5 μm . Furthermore, we looked at two parameters: number concentration (NC), the concentration of the number of particles in 1 cm^3 , and mass concentration (MC), the weight of particles measured in 1 m^3 .

METHODS

STUDY DESIGN

The study followed the usual design of a short-term effects–mortality study: Daily death counts, daily pollution data, and daily confounder data (such as weather and influenza information). In this study we collected all data prospectively.

Death certificate data were obtained from the local health authorities, who allowed us to copy each certificate with the name and address concealed. The additional information on the death certificate enabled us to do more than simply count total deaths. We hoped to find any indications, if any existed, that definable subgroups of the population were more sensitive to air pollution effects. We had no means to verify information on an individual basis, however.

A site was selected for our air pollution measurements based on site characteristics and practical considerations. There we measured size-stratified particle number and mass, particle mass by various impactors, gaseous pollutants, and weather. In addition, air pollution data from official sites in the city were obtained later. Health confounder data (eg, influenza information) were obtained from an independent source. Analysis of data involved state-of-the-art Poisson regression methods.

To reach Specific Aim 2, we tried to isolate the particle size that was most responsible for the short-term effects that have been observed. Secondarily, we looked for sensitive subgroups and delays in health effect that might indicate possible pathomechanisms. To accomplish this, we restricted the death data to Erfurt residents dying in Erfurt, made efforts to obtain certificate information as completely as possible, chose a site for ambient aerosol measurements with a rather typical mix of emissions and

pollutants for Erfurt, and made efforts to obtain pollution data as completely as possible.

Concurrently, we obtained data on gaseous pollutants and particle composition to help get an idea of sources responsible for different size fractions by comparing effect sizes and observing correlations. These latter results will be published separately in Part II of this report (Wichmann et al 2000).

STUDY PERIOD AND STUDY AREA

Erfurt, capital of the German state of Thüringen, lies in the southern part of the former German Democratic Republic and has roughly 200,000 inhabitants.

Germany in general has a rather mild, oceanic climate, but places to the east and south such as Erfurt are further inland. Consequently, they have a somewhat more continental climate. Two climatic consequences of the geography of the study location are rather cold winters and generally higher emissions of air pollutants in winter. Energy consumption from air conditioning in summer is not an issue because air conditioning is not very prevalent. Also, summer smog was observed only to a relatively small extent.

The city of Erfurt is surrounded by mountains several hundred meters higher than the city itself on three sides. The terrain is open to the north and northwest of the city. Several high buildings placed in the direction of this opening are likely to reduce the air exchange rate. Therefore temperature inversions, which are frequent during winter, can cause elevated levels of ambient pollutants in the city.

Before reunification, ambient air in Erfurt was among the most polluted in eastern Germany. This was not due to heavy industry but rather to a typical mix of industry, home heating (primarily with surface coal), and light traffic with high emissions per car. All air pollutants were frequently trapped in the city by inversions. Since 1990, the pollution profile has changed toward a mix much like that of cities in western Germany. In Erfurt in 1998 domestic heating was based mostly on natural gas, and traffic was dense with a rather modern fleet.

The population of Erfurt does not differ in any major way from that of the general German population (Table 2). Except for the youngest age group (births in eastern Germany dropped dramatically after reunification), the age distributions in both sectors and in Erfurt are quite similar. In particular, the fractions of persons aged 70 years and above are almost identical. As in Germany as a whole, everybody in Erfurt has access to good health care. Specifically, there was no major change over the study years.

Table 2. Age Distribution of German Population in 1995 (Percentage of Total Population in Each Area)

Age group (years)	Western Germany	Eastern Germany	Thüringen	Erfurt
0–4	5.37	2.87	2.92	2.94
5–9	5.62	6.36	4.98	6.32
10–14	5.19	6.98	6.88	6.65
15–19	5.10	6.66	7.09	6.59
20–24	5.91	5.43	5.49	5.75
25–29	8.45	6.91	6.58	7.52
30–34	8.97	8.38	7.90	8.76
35–39	7.85	7.92	8.35	8.02
40–44	6.88	7.80	7.92	7.95
45–49	6.30	5.69	7.06	6.21
50–54	6.11	6.35	5.41	6.73
55–59	7.22	7.69	7.60	7.48
60–64	5.39	5.88	6.26	5.36
65–69	4.91	5.08	5.10	4.64
70–74	4.21	3.99	4.17	3.62
75–79	2.46	2.27	3.05	2.14
80–84	2.31	2.15	1.64	1.97
85+	1.78	1.58	1.58	1.36
% ≥70	10.76	9.99	10.44	9.09

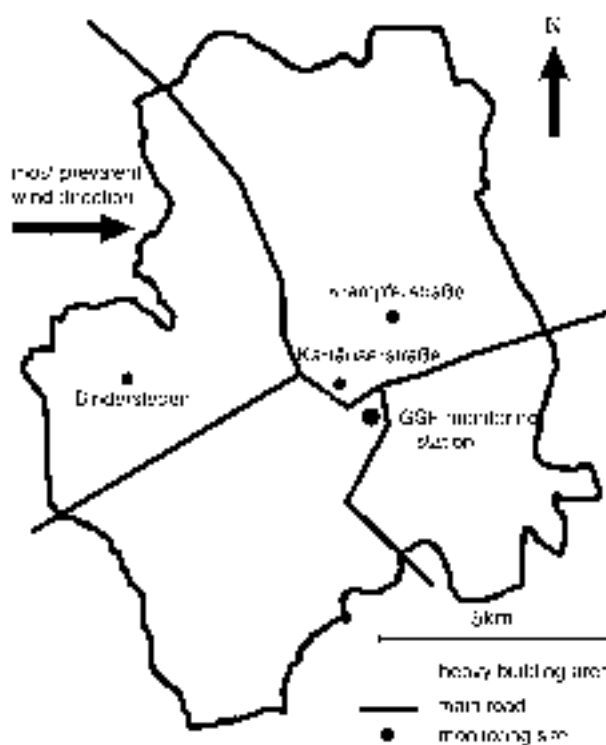
Differences in numbers of physicians and hospital beds between areas can be explained structurally: Thüringen as a whole is rather rural; Erfurt is the largest city in Thüringen and its capital, so specialties and special hospitals tend to accumulate there (Table 3).

The disadvantage for statistical power of a relatively small place (ie, Erfurt) was far outweighed by the fact that the geography allowed assessment of population exposure at a single site (the GSF monitoring station; Figure 1). The

Table 3. Hospital Beds and Physicians per 100,000 Inhabitants

Year	Germany	Thüringen	Erfurt
Hospital Beds			
1995	746	762	852
1996	725	763	858
1997	NA ^a	757	855
Physicians			
1995	334.7	287.5	413.2
1996	340.6	293.9	411.5
1997	344.5	297.1	418.4

^a NA = data not available.

**Figure 1.** Map of Erfurt showing measuring stations.

use of a single station was unavoidable because of the cost and degree of maintenance required by the air pollution measurement equipment. The measurement site was located in a mixed area (residential and offices, with a school and hospital) 2 km from the center of the city and approximately 50 m from a major road. The air pollutant mixture at this location was primarily influenced by traffic emissions and domestic heating and thus was typical for Erfurt. The location was selected because a fixed meteorologic station was already there.

DATA

Air Pollution Measurements

Mass concentration of a complex and dynamic urban aerosol represents only a crude characteristic of air pollution. Therefore, we decided to collect additional information on the study's ambient aerosol (such as the size distribution of the particle number concentration) from which daily number concentrations of preset size ranges could be calculated (Tuch et al 1997a, 1999). Based on parallel measurements of the number-size distribution and PM_{2.5} mass concentration and two simplifying assumptions (namely, spherical shape and invariable density of all

particles), we attempted to estimate daily mass concentrations of the same set of size ranges. The former assumption was justified because even chain aggregates of particles round to some extent during aging and because the instruments we used determined particle properties associated with the volume-equivalent diameter of the particle. We were aware that the second assumption was very crude. However, we learned that the mass distribution was dominated by the fraction of fine particles, for which we were able to determine a mean apparent density. Beside these

physical characterizations of the ambient aerosol, we also approached the chemical composition, which is covered in Part II of this report.

Gaseous pollutants SO_2 , NO_2 , and CO were measured at the state station of Thüringen (Krämpferstrasse in Figure 1). Furthermore, SO_2 measurements were obtained at the second state station (Kartäuserstrasse in Figure 1). SO_2 and NO_2 measurements were also obtained at the GSF monitoring station. Meteorologic variables were measured at the GSF monitoring station and in Bindersleben (Figure 1).

Table 4. Aerometric Measurements

Item	Period	Frequency	Duration	Measurement in Days		Raw Data Available (%)
				Scheduled	Available	
GSF Site						
NC _{0.01–0.5} , 13 bins (TSI30713760 DMA/CPC)	9/95–12/98	Hourly, every day	5 min	1,203	1,166	96.9
NC _{0.01–2.5} , 45 bins (PMS LAS-X OPC)	9/95–12/98	Hourly, every day	5 min	1,203	1,166	96.9
PM _{2.5} mass (non-denuded Harvard impactor)	9/95–2/96	Every other day	24 hr	1,158	1,096	94.7
	3/96–12/98	Every day	11 am–10:50 am			
PM ₁₀ mass (non-denuded Harvard impactor)	9/95–2/96	Every other day	24 hr	1,171	1,133	96.8
	3/96–12/98	Every day	24 hr			
PM _{2.5} sulfate, H ⁺ (PSA) (denuded Harvard impactor)	9/95–12/98	Every other day	24 hr, 11 am–10:50 am	604	594	98.3
Berner impactor, 8 size classes, elemental composition by PIXE	9/95–7/97	About once a week	24 hr	91	90	98.9
	8/97–12/98	6 days/week	11 am–10:50 am	418	389	93.1
SO ₂	9/95–12/98	Hourly, every day	10 min	1,218	1,137	93.3
NO ₂	6/97–12/98	Hourly, every day	10 min	556	535	96.2
Wind speed, direction, temperature, and relative humidity	9/95–12/98	Hourly, every day	10 min	1,203	1,170	97.2
Krämpferstrasse, Kartäuserstrasse Site						
TSP by beta attenuation at 3 sites (2 used)	8/95–12/98	Hourly, every day	30 min	1,249	1,242	99.4
				1,096	1,071	97.7
SO ₂	8/95–12/98	Hourly, every day	30 min	1,249	1,246	99.8
NO ₂	8/95–12/98	Hourly, every day	30 min	1,249	1,236	99.0
CO	8/95–12/98	Hourly, every day	30 min	1,249	1,219	97.6
Bindersleben (airport) Site						
Temperature and relative humidity	8/95–12/98	Every day	24 hr	1,249	1,249	100.0

Measurement Methods, Quality Control The environmental measurements were set up to meet the requirements of this study. The MAS was the main instrumentation. In addition, standard measures of air quality (such as gravimetric particle mass, gaseous pollutants, and weather) were obtained throughout the study to provide both standard exposure variables and quality control for the MAS measurements.

The two MAS units were commercially available instruments covering different size ranges. Particles ranging from 0.01 to 0.5 μm in size were measured using a differential mobility analyzer (DMA). Particles ranging from 0.1 to 2.5 μm in size were classified by an optical laser aerosol spectrometer (LAS-X). The MAS provided number concentrations as a function of particle diameter. From those data, numbers of certain size ranges were calculated. After making certain assumptions, a mass estimate could then be derived. (For more details, see section on Estimation of Mass Concentration Distributions.)

From the beginning of the study, we ran two standard $\text{PM}_{2.5}$ impactors and one PM_{10} impactor side by side with the MAS. The first $\text{PM}_{2.5}$ impactor was originally scheduled to operate only every other day, but after March 1996 it operated on a daily basis. The second $\text{PM}_{2.5}$ impactor provided a sample for sulfate and acidity analysis every other day. The additional $\text{PM}_{2.5}$ impactor was primarily introduced as a quality control for the MAS, and therefore this time schedule did not interfere with the daily approach of the study. PM_{10} samples were collected every day and yielded additional information for data analysis. PM_{10} measurements were therefore automatically scheduled from midnight to midnight. In addition, we obtained gaseous pollution data and Berner impactor samples for analysis by proton-induced x-ray emission (PIXE) to obtain metal composition data. These data are presented in Part II.

Data from the GSF monitoring site were almost complete (availability 93% to 95%; Table 4). Missing data were due to laboratory calibration, instrument maintenance and, in some cases, instrument failure. Some additional data were not considered usable for analysis after internal plausibility checks.

From the three state-run stations in Erfurt, we could obtain concurrently daily data on TSP and gaseous pollution: one was specifically close to traffic (and was not used in this study); two others were an inner city and a background station (Krämpferstrasse and Kartäuserstrasse, respectively; see Figure 1). The Krämpferstrasse station, off a large street, ran a complete set of pollutants. Placement of this station was not too different from that of the GSF station, which was about 2 km away. The Kartäuserstrasse

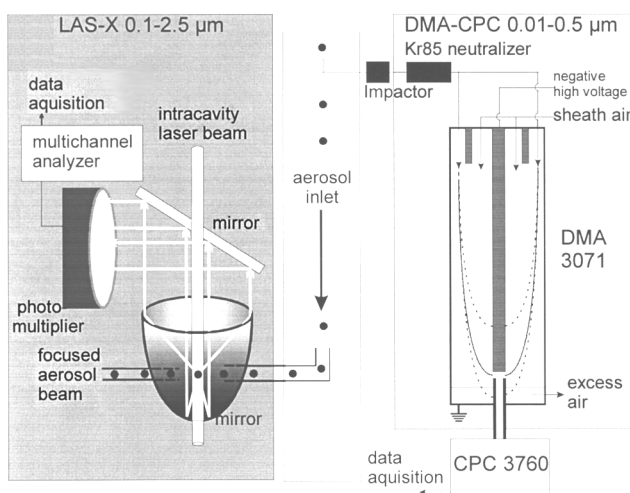


Figure 2. Mobile aerosol spectrometer (MAS). The aerosol is sucked through the central chimney into the aerosol inlet. The right-hand instrument (DMA-CPC or DMPS) classifies particles in the size range 0.01 to 0.5 μm (used up to 0.1 μm). The left-hand instrument (LAS-X) sizes particles in the range 0.1 to 3.0 μm (used up to 2.5 μm).

station was about 1 km away from the GSF station in a residential area.

Mobile Aerosol Spectrometer The properties of electrical and mechanical mobility, impaction, sedimentation, diffusion, and light scattering are commonly used to determine particle size; the choice of specific properties depends on the size range of the particles. Because the diameter of fine particles ranges from 0.1 to 2.5 μm , different physical measuring principles need to be applied.

The MAS, described previously (Brand 1989; Brand et al 1991, 1992; Tuch et al 1997a, 1999), consisted of two different, commercially available instruments covering different size ranges (Figure 2). Particles ranging from 0.01 to 0.5 μm were measured using a DMA (model 3071; TSI, Aaden, Germany) combined with a condensation particle counter (CPC) (TSI model 3760). This instrument set and the software developed by Brand (1989) together compose the *differential mobility particle sizer* (DMPS). Particles ranging from 0.1 to 2.5 μm were classified by LAS-X (PMS, Leonberg, Germany). The MAS had already been deployed in an earlier 6-month campaign measuring the ambient urban aerosol in Erfurt, Germany, during winter of 1991–1992 (Tuch et al 1997a). The DMPS mobility analyzer allowed separation of particle fractions of uniform electrical mobility from a polydispersed aerosol, the charge distribution of which was equilibrated by a ^{85}Kr source. The particle number was counted by CPC. The raw count rate was used to calculate particle number in the selected size range, taking into account the charging probability of the particles with use of the Knutson approximation

(Knutson 1976), diffusional losses in the mobility analyzer (Reineking and Porstendörfer 1984, 1986), and the counting efficiency (Zhang and Liu 1991). The numbers of the separate particle fractions were measured as a function of particle diameter in 13 discrete size ranges between 0.01 μm and 0.5 μm using the inversion algorithm of the mobility analyzer provided by the company but as adapted to the 13 selected channels. The 4 upper channels, with particles between 0.1 μm and 0.5 μm , were used for the mobility calibration, for quality checks of the overlapping spectra obtained from the mobility analyzer and the LAS-X, and for proper operation of the impactor.

The LAS-X classified particles according to the light scattered inside the cavity of a laser into 45 size-dependent channels. The intensity of light scattered by a particle depends on particle diameter as well as the shape and optical properties, such as the refractive index of the particle material (Hinds and Kraske 1986; Szymanski and Liu 1986; Reisert et al 1991; Kim 1995). The counting efficiency of the LAS-X was 1.0 for particles ranging from 0.1 to 1.0 μm and decreased only slightly, to 0.95, for particles up to 2.5 μm in diameter (Hinds and Kraske 1986; Brand 1989; Gebhart et al 1989).

Electrical Mobility Calibration of LAS-X Data In a previous attempt, Hering and McMurry (1991) showed that the Los Angeles area ambient aerosols scattered less light than did the polystyrene latex particles on which the manufacturer's calibration was based. They found that the light scattering of the ambient aerosols was similar to that of oleic acid aerosol particles and determined a new calibration curve, which was used for a later air monitoring survey (Eldering et al 1994). To classify ambient aerosol particles of unknown refractive indices by the LAS-X in the present study, a more vigorous calibration procedure was applied: It used the DMA to provide monodispersed fractions of the ambient aerosol with known mobility-equivalent diameters of 0.1 to 0.5 μm (Liu et al 1974; Brand et al 1991, 1992). These particle fractions were then used to calibrate the LAS-X in terms of mobility-equivalent diameters and to eliminate the dependency on refractive index. This procedure was termed *electrical mobility calibration* of the optical particle spectrometer. The electrical mobility calibration curve was extrapolated for particles 0.5 to 2.5 μm . Beside the full spectrum, including the mobility calibrated data, the original data of DMPS and LAS-X were stored. With respect to correct sizing and resolution, the LAS-X was checked biweekly using monodispersed 0.304- μm latex aerosols. Aerosolized latex particles were diffusion dried and classified by the mobility analyzer before entering the LAS-X. The resulting spectrum was checked for the appropriate channel of LAS-X (range #1, channel #6: 0.30 to 0.32 μm) and for width (ie, one or at most two channels).

Aerosol Sampling Both DMPS and LAS-X were located in a laboratory van. With an air-flow velocity of approximately 1.0 m/sec, a sample flow was sucked into the van through a chimney with diameter of 22 cm and height approximately 4.0 m above the ground. Each instrument of the MAS sampled isokinetically from this main air stream (Tuch et al 1997a). The aerosol flow rates of the DMA and LAS-X were 610 $\text{cm}^3 \text{min}^{-1}$ and 60 $\text{cm}^3 \text{min}^{-1}$, respectively.

Limits of Particle Counting The lower and upper limits of particle counting were predominantly determined by CPC: 0.01/ cm^3 (electronic noise) and 1,600/ cm^3 (speed of electronics) in a given channel. The lower and upper limits of the LAS-X were 10^{-3}cm^{-3} and $3 \times 10^4 \text{cm}^{-3}$, respectively. For the LAS-X, the error for coincident particle counting was 30%. An experimentally determined coincidence correction was applied in the software of the MAS to correct the LAS-X determined number (Brand 1989).

Time Resolution The typical measuring time for a complete size distribution was 5 to 6 minutes. During this time the analyzer switched the high voltage 13 times to count the particle number of the corresponding size interval. Similarly, within this same time interval, the LAS-X switched between 3 size ranges (0.1 to 0.25 μm , 0.25 to 0.5 μm , 0.5 to 2.5 μm) to collect spectral data in 15 channels of each range.

Data Acquisition and Performance Control of the measurements, data acquisition, and evaluation were performed by a personal computer. After the measuring time for a complete size distribution was finished, the size distribution was displayed for 30 seconds to allow an operator to control the size distribution. When operated in automatic mode, the next measurement started immediately after this break. An hourly average was considered valid if 66% of the data were available.

The quality of MAS measurements was ensured throughout the study by several tests with laboratory aerosols and several side-by-side measurements of ambient aerosol comparing results of identical instruments as well as a different type of aerosol spectrometer. Furthermore, both performance and data handling were checked during a site visit from HEI. The auditors found the procedures and equipment satisfactory and requested no changes (Wichmann 1997). (For details, see Appendix G: Quality Control MAS.)

Estimation of Mass Concentration Distributions The MAS provided number data as a function of particle diameter. From these data, the particle volume distribution as a function of particle diameter was calculated assuming spherical particles. To calculate the mass distribution, an estimate of the particle density was required. An apparent mean density of 1.5 g/cm^3 was given in the literature (Joshi 1988). This value was further supported from extensive

measurements of the bulk density of ambient aerosol particles collected at different locations in Germany under different meteorologic conditions (Hänel and Thudium 1977). These measurements varied around 2.0 g/cm^3 . Bulk material densities usually were higher than the apparent density of aerosol particles, which may be porous, aggregated, or both.

In addition, the apparent mean density of the ambient aerosol particles in Erfurt was estimated from the number distributions measured by MAS and the daily $\text{PM}_{2.5}$ measurements: The differential volume distribution was calculated from each particle number distribution with the presumption of spherical particles. From the volume distributions, a daily mean particle volume concentration was calculated. These MAS data obtained over the entire study time were graphed as scatterplots against the corresponding daily $\text{PM}_{2.5}$. The slope of the regression line provided the apparent mean density of ambient particles, and the scatter indicated the variability over time.

Using this estimated apparent mean density, integral masses of all counted particles ($\text{MC}_{0.01-2.5}$) and of the relevant subclasses $\text{MC}_{0.1-0.5}$, $\text{MC}_{0.5-1.0}$, and $\text{MC}_{1.0-2.5}$ were calculated from the differential mass distributions. Note that the estimated apparent density was a mean over the entire particle size spectrum. The authors were well aware that the density in certain fine particle size ranges might differ from this apparent mean density.

Other Particulate Data Ambient $\text{PM}_{2.5}$ and PM_{10} concentrations were measured using filter-based methods. The measurements were conducted with the Harvard impactors (Marple et al 1987) without predenuder. The sample volume was determined with a gas meter, and sample flow was checked with a calibrated rotameter. The initial volume on the gas meter, sample, and start time of the sample were recorded in a field form at the beginning of each measurement. Air was then sampled for 24 hours through a size-selective inlet that excluded large particles from the air stream. The particles of interest, those less than the cut size (2.5 or 10 μm , respectively), were deposited on preweighed Teflon membrane filters (PTFE) (Gelman Sciences GmbH, Dreieich, Germany) with a pore size of 2.0 μm . The remaining particles, which were collected on the impaction plates, were discarded and not analyzed. The impaction plates were impregnated with light mineral oil. The oil provided a sticky surface from which the particles would not easily bounce. Volume, flow rate, and stop time were recorded in the field form. The exposed filters were then weighed again. The entire procedure of weight determination followed a protocol derived previously (Chow 1995).

The $\text{PM}_{2.5}$ filters were changed every day at 10:50 am. The measurement of $\text{PM}_{2.5}$ started at 11:00 am. The PM_{10}

filters were changed every day at the same time, and measurements were started by a radio-controlled clock at midnight.

The $\text{PM}_{2.5}$ and PM_{10} concentrations were calculated from the mass difference prior to and after the sampling period and the respective sample volume. Because the sampled mass on the filters was very small, extensive care was taken to provide accurate filter weighing. Before weighing, the filters were equilibrated at $21 \pm 2^\circ\text{C}$ and $35 \pm 5\%$ relative humidity for 24 hours. Note that during the first year of the study, no air conditioning system was available to maintain the required weighing conditions and weighing could only be done when the requirements were met. Upon request of the site visitors, the weighing room was air conditioned for the rest of the study. An analytical balance with a reading precision of 1.0 mg was used (model M5P V001; Sartorius, Göttingen, Germany).

Internal and external quality control measures were introduced to ensure reliable weighing of the filters. Internal quality controls included the following:

1. The accuracy of the microbalance was checked with certified mass prior to each session of weighing filters. The measured weight was recorded in a control chart;
2. Two blank Teflon filters were weighed each day that sample filters were weighed. Weighing was cancelled for the respective day if the weight of one filter differed by more than 5 μg from the target weight, and the cancellation was documented;
3. Two exposed and aged Teflon filters were weighed each day that sample filters were weighed. Weighing was cancelled for the respective day if the weight of one filter differed by more than 5 μg from the target weight, and the cancellation was documented; and
4. Weighing conditions in the laboratory (eg, temperature, relative humidity) were documented on a control chart.

Note that weighing of blank and exposed filters was introduced after the first six months of the study based on comments from the site visitors. External quality was controlled in collaboration with other researchers. Five blank and five exposed filters were circulated by the coordination center of the ULTRA I study (*Exposure and Risk Assessment for Fine and Ultrafine Particles in Ambient Air*). The filters were weighed at three laboratories including one in Erfurt. The determined weight of each filter differed by less than 5 μg among the different laboratories. The ULTRA I study was funded by European Union (EU) and had as its aim the performance comparison of three different aerosol spectrometers characterizing laboratory test and ambient

aerosols. Ultrafine particle levels were determined in three European cities during the winter of 1995–1996. (For details, see Appendix G: Quality Control MAS, available on request.)

The TSP data came from the city of Erfurt. TSP was sampled using beta attenuation with no cutoff. Stochastically, the cutoff was around 15 μm (Spix and Wichmann 1996). TSP data used in this study were measured at the Kartäuserstrasse and Krämpferstrasse stations. Data from the Krämpferstrasse station were available from the beginning of our study, and data from the Kartäuserstrasse station were available since January 1996. Although the stations are about 1.5 km apart and in differing surroundings, the correlation between them was very high (0.91) and the annual averages were almost identical. The measurements from Kartäuserstrasse and Krämpferstrasse were used to form a mean series with a level correction for missing values by month of year. The mean series was correlated with both original series with $r = 0.98$.

Gaseous Pollutants SO_2 was measured at three stations, NO_2 at two stations, and CO at one station (see Table 4). Standard techniques were used because they were mandatory for the official net for ambient air control in Germany and the EU (Abshagen et al 1984; TA Luft 1986; EU 1991, 1994). Details of our analyses will be published in Part II of this report.

Meteorologic Data Temperature, relative humidity, wind speed, and wind direction were obtained at the GSF measurement site. The combined temperature and relative humidity sensors (RCI Rösler, Offenbach, Germany; model FT3205-M, PT100, and capacitive sensor) were mounted in the chimney outside the measurement station. Readings from these automatic instruments were frequently verified against readings from standard thermometers and a psychrometer located in the measurement field. Additional data on temperature and relative humidity came from an official measurement site operated by the Deutscher Wetterdienst located at the airport (ie, Bindersleben station as shown in Figure 1). Wind speed and wind direction (Albin Sprenger, Frankfurt, Germany; model E 14051.61 H) were determined 5 m above ground. These instruments were checked against two additional instruments in the measurement field operated by the University of Applied Sciences of Erfurt. Note that both wind speed and wind direction reflected only local conditions at the measurement site because the inner city wind field was heavily influenced by local buildings.

Selection of Cutpoints and Accumulated Particle Indicators For this study, we developed particle indicators based on selected cut points. These cut points were

based on considerations of particle behavior, particle origin as an aerosol, and particle deposition in the respiratory tract, the last of which is an important dose metric for health outcome. Because the diffusion coefficient increases drastically with decreasing particle size, 0.1 μm is commonly used to distinguish ultrafine particles (all particles with diameter less 0.1 μm) from fine particles (particles with diameter from 0.1 to 2.5 μm). Finally, coarse particles are those with diameter above 2.5 μm .

In our study, the ultrafine particles ranged from 0.01 to 0.1 μm . We subdivided this range into three sections: particles 0.01 to 0.03 μm , 0.03 to 0.05 μm , and 0.05 to 0.1 μm . We introduced the range of 0.05 to 0.1 μm because this fraction consisted of agglomerates of smaller primary particles mainly resulting from combustion processes. We distinguished the lower range into particles between 0.01 to 0.03 μm and 0.03 to 0.05 μm because of increasing analytical uncertainty caused by the electrical charging probability for particles below 0.03 μm .

Fine particles ranged from 0.1 to 2.5 μm . We subdivided this range into three sections: particles between 0.1 to 0.5 μm , 0.5 to 1.0 μm , and 1.0 to 2.5 μm . Due to deposition in the lungs of particles between 0.1 to 0.5 μm , we distinguished this particle range size range from those particles above 0.5 μm . Particle diffusion is the predominant deposition mechanism below 0.5 μm , whereas sedimentation is the dominant deposition mechanism for particles between 0.5 and 2.5 μm in the respiratory tract. Both mechanisms overlap and contribute to lung deposition equally at 0.5 μm . Impaction starts to play a role only for high breathing air flows or for particles above 2.5 μm . We also made provisions to subdivide into the range of the accumulation mode (eg, from 0.1 to 1 μm).

Assuming the sphericity of the particles and the apparent mean density mass concentration, the mass concentrations estimated in various size ranges confirmed that the particle mass of the ultrafine fraction was negligible. Due to the very low particle number either in $\text{NC}_{0.5-2.5}$, or even lower in $\text{NC}_{1.0-2.5}$, the particle mass of these fractions was found to be 10% to 20% and less than 10% of the fine particle mass concentration, respectively. In addition, $\text{PM}_{2.5}$ provided the gravimetrically measured fine particle mass concentration. The coarse particles were represented by the difference between PM_{10} , TSP, and $\text{PM}_{2.5}$, but coarse particles were not analyzed separately in this study. The sizes are summarized in Table 5.

As shown in Table 5, ultrafine particles were mainly represented by number, whereas fine particles were represented by mass. Thus, discussion about the particle number implied discussion of ultrafine particles, whereas discussion about the particle mass implied discussion of fine

particles. The 6 size ranges of ultrafine particles and fine particles combined were considered for total mortality regression. For ultrafine particles, only the number data were used and for fine particles, only the mass data. For subgroups and sensitivity analyses, we only considered representatives: ultrafine particles ($NC_{0.01-0.1}$), fine particles ($MC_{0.01-2.5}$, which for practical purposes is identical to $MC_{0.1-2.5}$), and PM_{10} impactor.

Figure 3 summarizes what is known about particle size distribution and in what way size distribution is connected to more common measures of particle number and mass. The percentage values were based on 1995–1998 data from Erfurt (see later discussion of Tables 7 and 8).

MORTALITY DATA

Collection Methods and Quality Control

Access to death certificates is restricted in Germany due to data privacy rules. The basis for access is the *Bundesstatistikgesetz* (a federal law about statistical data), which

Table 5. Size Ranges Used for This Study and Contribution to Number and Mass Concentration

	Contribution ^a	
Size (μm)	Number	Mass
Ultrafine particles		
NC _{0.01–0.03}	88%	3%
NC _{0.03–0.05}		
NC _{0.05–0.1}		
Fine particles		
MC _{0.1–0.5}	12%	97%
MC _{0.5–1.0}		
MC _{1.0–2.5}		
Total ultrafine and fine particles		
0.01–2.5	100%	100%
Coarse particles		
PM _{10–2.5}	—	20%
TSP–PM ₁₀	—	30%

^a Based on the data from Erfurt 1995 to 1998: contribution of ultrafine and fine particles to number and mass in the size range of 0.01–2.5 μm and contribution of coarse particles to mass of total aerosol size distribution.

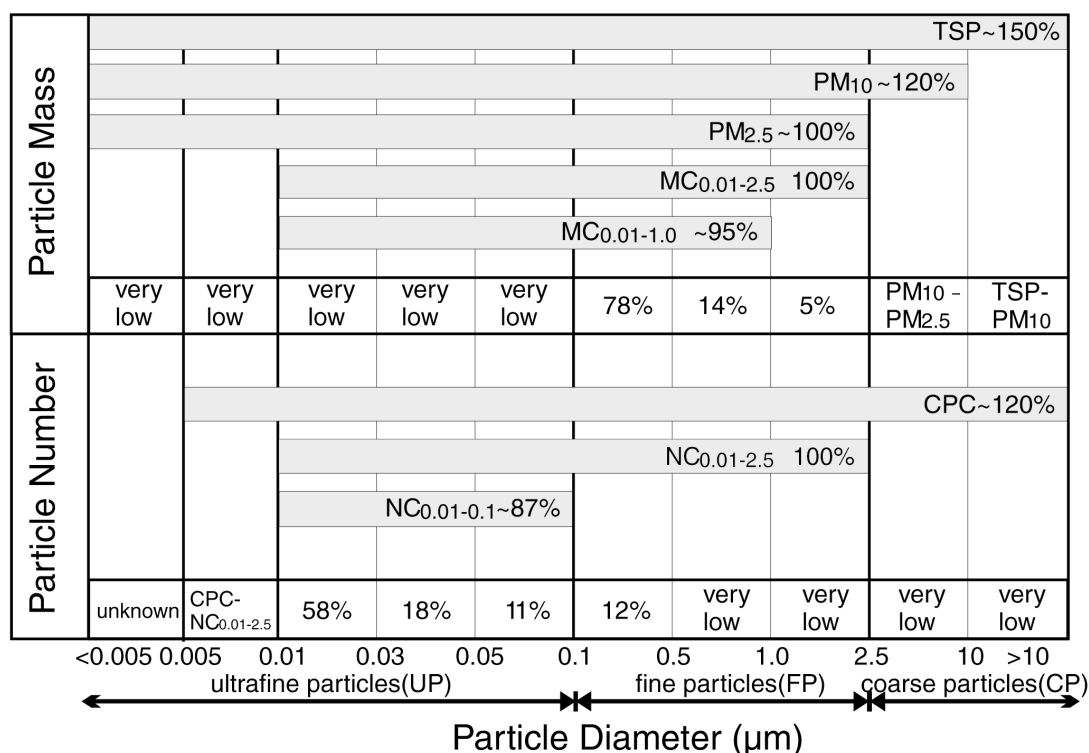


Figure 3. Particle size distribution in relation to common measures of particle number and particle mass.

regulates access to individual death certificate data for scientific purposes.

In our study, all locally available death certificates were collected and copied without the name and address of the deceased. This was a condition for our access. Thus, we were unable to approach next of kin or to obtain further information. Infant deaths were excluded. Copying was done on the site of the local health authority. Our copier stood close to the room where the certificates were filed, and certificates did not leave the premises. The anonymous copies of the death certificates were stored in lockers in our office in Erfurt.

Following suggestions made during the quality control audit in 1997, we slightly revised our original standard operating procedures for data entry and control. (The revised version is included in Appendix H.) Data quality was ensured by double entry and extensive internal plausibility checks.

For death certificates, we waited at least 3 months to obtain complete records. To be sure we did not miss any, we checked our lists against the older records in the Gesundheitsamt several times during the study. (Certificates were filed in the order of day of death.) (Details are recorded in Appendix H.) Our data entry and data control methods were deemed adequate by external audit during a site visit in April 1997.

The following information was recorded for each subject:

- date of birth;
- gender;
- date of death;
- time of death (not always available);
- place of death (type and city area);
- place of residence (city area); and
- immediate, underlying, and contributing causes of death.

The death certificate forms had a space for time between onset of disease and death, but this was almost always blank. Before reunification, doctors in eastern Germany were required to fill in *International Classification of Diseases* (ICD) codes themselves. They still do this although the certificates are recoded officially before being entered into the database. We collected the certificates before recoding took place. Data from the official database tended to become available after a delay of more than 1 year. The change from ICD, *Ninth Revision* (ICD-9), to the *Tenth Revision* (ICD-10) in January 1996 required an adaptation of data entry and control. However, only a small number of

certificates used in the study were coded by ICD-10 (less than 5%).

Although we were not able to check the reliability of the cause of death information against the patient's medical reports, we did have experts check the internal consistency and agreement of codes with written information. A random 10% subsample of the first 2,000 ICD-9 certificates was passed to the Academy of Public Health in Düsseldorf (the institution that teaches coding principles to official coders), and these experts recoded our certificates as far as they deemed necessary. Most errors made by physicians concerned the placement of the information with very few concerning the actual codes. When errors involved the codes, most corrected codes were within the same ICD group. We have used the cause information only in broad classes (for details, see the section on Selection of Subgroups for Analysis).

After quality control reviewing and recoding, about 10.2% of cases ended up in a different underlying death category (see Table 6). A large fraction reflected persons with diabetes mellitus who died from cardiovascular disease. In these cases, the physicians tended to list the cardiovascular disease as underlying rather than the correct underlying cause, diabetes. (Diabetes was included in our "other natural causes" category.) For cardiovascular causes, complicated rules regarding myocardial infarction, congestive heart disease, and ischemic heart disease led to many reorderings within this class (see Appendix C).

Note that, without any nosologic experience, we always accepted the ordering of causes as given by the certifying physician. This was not problematic for the rather large group of certificates with only one cause of death given, but there were also certificates with two or three codes given in the first three lines (lines 4 and 5 are always "contributing causes"). The physicians frequently tended to get the order wrong, often placing information in reverse order (ie, from underlying to immediate). Nevertheless, we used the last of the first three lines of information for categorizing "underlying." This accounted for a large fraction of the recoded certificates as well.

When we disregarded the placement of information and just looked for any mention of a cardiovascular or respiratory disease, these "prevalent conditions" were even more rarely reassigned: only 3.4% of all prevalent conditions were found in a different category after recoding (Table 6). This occurred because the mistakes exclusively regarding ordering of information no longer counted. Based on this, the prevalent disease categorization seemed more valid because it used all information on the certificates (not excluding any) and because it was insensitive to the (rather frequent) ordering mistakes made by the certifying

Table 6. Quality Control: Review and Recoding of 200 Death Certificates by Experts at Akademie für Öffentliches Gesundheitswesen

New Codes	Old Codes ^{a,b}	
	Cardiovascular or Respiratory	Other Natural
Underlying cause of death		
Cardiovascular or respiratory	52.0	2.8
Other natural	7.4	37.9
Prevalent conditions of deceased		
Cardiovascular or respiratory	65.0	1.1
Other natural	2.3	21.5

^a By percentage of total sample.

^b Note the shifts between classes of death after recoding. Off-diagonal elements signify a shift.

physicians. Although this was not optimal, we considered this a still acceptable level of quality regarding the cause of death information. The quality control validation study for the ICD-9 coding was planned to be repeated for ICD-10 as soon as there were enough ICD-10 data available, but ICD-10 coding remained an exception. We collected a total of 6,091 death certificates between August 1995 and December 1998 from individuals with last residence in Erfurt and place of death Erfurt.

Selection of Subgroups for Analysis As criteria for setting up subgroups, we chose age at death and cause of death. Both criteria had been suggested and used in studies before and described sensitive subgroups of interest. Because the number of deaths per day was limited, few subgroups were possible. Age was split into the groups < 70, 70–79, and ≥ 80 years. Further sensitive subgroups were based on cardiovascular disease and respiratory disease; individuals in these groups may be most sensitive to the effects of air pollution. (The causes of death we defined as cardiovascular or respiratory are given in Appendix G.) Deviating from definitions presented by other researchers, we included lung cancer among the respiratory causes. This was slightly unusual, but we reasoned that the causes for lung cancer (mostly smoking) would have caused chronic respiratory problems (eg, chronic obstructive pulmonary disease [COPD]) in the individual long before lung cancer, although the presence of COPD was rarely mentioned on the death certificate when lung cancer was the cause of death. Results of an autopsy always had precedence over inspection of the corpse, but autopsies were very rare (3%).

As the underlying cause, we used the information on the third line of the certificate. When nothing was available there, we used the second line. If this were blank, we used the information on the first line. Information in lines 4 and 5 was always considered to reflect contributing causes. Very frequently, only one cause was given. Underlying cause of death was considered in the “cardiovascular or respiratory” subgroups versus “other natural.” The underlying cause of death was of less interest because it used only a fraction of the cause of death information available.

The other classification we used ignored information placement and just recorded prevalent diseases. A person was considered to have a cardiovascular or respiratory condition regardless of whether this was recorded as underlying, intermediate, immediate, or contributing cause of death. Under this classification far more cases were considered as cardiovascular or respiratory than when considering underlying causes alone (see also the section Cause of Death, Age at Death, Place of Death; see Table 17). Note that each person was assigned to a category only once; “other causes” persons could have any other cause recorded, but no cardiovascular or respiratory ones. Note that the “prevalent diseases” always included the underlying cause.

Finer categorizations of prevalent diseases (eg, cardiovascular or respiratory disease) were both possible and of interest. From the literature, we knew that patients with cardiovascular or respiratory problems are affected by exposure to particles. Animal experiments and epidemiologic studies have shown specific effects for cardiovascular endpoints. (This is investigated in the category “cardiovascular diseases only,” excluding individuals with recorded respiratory causes; see also Appendix C: Comparison of Prevalent Diseases and Underlying Causes of Death.) Other studies have shown effects on respiratory endpoints. Because the subgroup of “respiratory diseases only” (persons without an additional cardiovascular disease recorded) was too small to study (see Table 17), however, all cases with respiratory causes were considered together (see also Appendix C). For comparison and completeness, all cases without cardiovascular or respiratory disease recorded were aggregated into the “other natural diseases” subgroup. The data for total deaths included all natural deaths.

For technical reasons, establishment of subgroups required two passes of analysis because we always included all cases in distinct, non-overlapping classes: one splitting by “cardiovascular or respiratory” versus “other natural,” and one splitting more finely by “cardiovascular but not respiratory,” “respiratory,” or “other natural.”

Nonnatural causes were not included. For the purpose of the study, *nonnatural* included either an ICD code 800 or S00 in the first three lines or a tick in the *nonnatural* box. These criteria did not always agree: For instance, dying from sepsis secondary to injury (ICD = 038) was “nonnatural,” whereas dying from therapy complications (ICD = 902) was considered “natural.” To be certain, we excluded both.

We could additionally have split into subgroups by type of place of death. However, “hospital” was a very mixed category when it described risk groups because it included chronically ill persons, acutely ill persons, emergencies, and persons dead on arrival. Generally the categories “hospital,” “at home,” and “institutions” differed considerably in cause and age distribution, factors that we considered more relevant in describing risk groups (see Tables 18 and 19).

Differentiating by regions within Erfurt based on ZIP codes (*Postleitzahlen*) will be considered in future analyses. In addition, time of death information was almost complete, but its reliability, especially during the night, was questionable.

Other Data

The descriptive data on city and state, age distribution, health care, and cause of death distribution were taken from official federal, state, or community statistical publications.

Influenza data were obtained from an external source because the state does not maintain surveillance on influenza epidemics in Germany. In 1994, the pharmaceutical industry set up an institute, the Arbeitsgemeinschaft Influenza (AGI), which has since built up a sentinel system with weekly report of acute respiratory cases. The institute collects data from September to April each year. Additionally, AGI collects all available information on virus isolations, compiling rather good information on which viruses are causing an increase in numbers of cases. As acute respiratory subjects are collected as an indicator, peaks are not always due to influenza viruses; they can also represent an outbreak of rather more harmless respiratory viruses or bacteria. Data for Thüringen were available but only from a few physicians, so we used the weekly time series for all of Germany (AGI 1996, 1997, 1998).

ANALYTICAL METHODS

Standard Analyses

Model Building, Model Fit We assumed the data, given the mean model, to be Poisson distributed with some

possible overdispersion. Raw mortality data were usually autocorrelated. If the residuals were still autocorrelated after fitting a confounder model, appropriate corrections were used.

The model building was done using the GAM procedure in S-Plus with a quasi link. GAM allows fitting nonparametric smooths of the independent variables such that no assumptions about the shape of dose response curves have to be made. The quasi link allows extension of the canonical log link for overdispersion. Data description and graphic presentation of results were performed with SAS, version 6.12. An approximation of a distributed lag procedure was obtained with a SAS-IML program.

The modeling principle had two steps: first, the confounder model was fitted; then the pollutants were fitted. The confounder model consisted of the following elements:

1. **Season.** Season was preferably fitted by a polynomial spline smooth to ensure a smooth curve. The degrees of freedom (*df*) were chosen by visual inspection of the plotted fit. Variations in the size, shape, and placement of the winter hump each year were permitted, but several extra humps per year were not permitted.
2. **Influenza.** The epidemics (1 or 2 per winter) were fitted separately. They were shifted up to 3 weeks in both directions, with the best shift decided by Akaike Information Criterion (AIC). This was done because deaths follow epidemics with some delay and because a given epidemic may have hit Erfurt before or after it affected the rest of Germany. If there were strong epidemics, it was advisable to fit them before the seasonal model; otherwise, the seasonal model attempted to pick up those humps and became distorted. Actual influenza epidemics that have an effect on mortality tended to be visible to the naked eye in the raw mortality series. Only such winters should be considered for a correction. Our data referred to actual influenza in some winters and mere respiratory infections in others, so each winter and epidemic were considered separately.
3. **Day of week.** When a strong day-of-week pattern or the usual day-of-week pattern (Mondays high, weekends low) occurred, indicators for weekdays were included.
4. **Meteorology.** Available data were temperature and relative humidity or dew point. Following the suggestion by Samet and colleagues (1997), we attempted to include immediate and delayed temperature effects simultaneously. The shape of the effect was determined by a locally weighted smoothing scatterplot

(LOESS) with the span chosen so that the shape was either monotonous or concave or convex. Major local maxima were not considered biologically plausible. LOESS was preferred over a cubic spline as it somewhat retained potential turning points. Humidity effects were also included. Interactions were an option. We expected the final model to have as little autocorrelation and overdispersion as possible.

The standard analysis tested each pollutant alone. Although we could have fit those by a spline or LOESS curve, this made results difficult to report other than by a graph and impossible to sum up in a single risk estimate. Thus, these analyses were done only as a sensitivity comparison. Different shapes of the dose response curve were considered by transformations of the independent variable. Relevant transformations were no transformation or log transformation. Log transformation was not chosen for distributional reasons, but rather because it corresponded to the assumption of a flattening dose response curve. We may have had some prior assumptions regarding delays of associations, but they came from a single study (not mortality), so we did not use them. Instead, we allowed each pollution indicator to select its best fitting delay.

We did not start by making assumptions about the maximum delay of associations. For each pollutant, the association of the log-transformed and untransformed pollutant was checked at least up to lag 5 or 6. The best lag was chosen by its absolute t value (which due to the large sample size corresponds to selection by smallest P value). By lag 6, there were never any associations; when there was a hint, we went looking for one beyond this.

Because different potential mechanisms of an association of ultrafine particles or fine particles might have different time scales, we looked for the best delay per size range. The best transformation and the best delay were chosen by the largest absolute t value. As we had 3 ultrafine particles and 3 fine particle categories, a pattern would have to emerge for these results to make sense.

Cumulative associations were as much of interest for this issue as single-day associations of air pollutants. The idea behind distributed lag models, models including associations of several lags simultaneously, is that one might miss some of the association by just looking at one specific lag. Fitting distributed lags was an adaptive process aimed at maximizing the association in the direction that was perceived as relevant. The advantage of this method over just fitting an unweighted average over k days is clear with an example. Assume a case of associations that spread out over the last 3 days of the time period; including the fourth and fifth days dilutes the association and gives a distorted picture. The maximization range of

lags and the relation of the lags are both an information and a result in themselves.

The regression procedure we used (GAM in S-Plus) had several advantages but did not allow fitting restricted distributed lags models. We used an ad hoc method based on polynomial distributed lags to make up for this. The method proceeded as follows:

1. Choose an order of the polynomial p (we usually started with $p = 3$) and a maximum lag q (we usually started with $q = 5$);
2. Define a set of $p + 1$ working variables, Z_{it}

$$Z_{it} = \sum_{j=0}^q j^i X_{t-j}, \quad i = 0, \dots, p$$

and fit them jointly in the usual Poisson regression model to obtain $p + 1$ parameter estimates $\beta_0, \beta_1, \dots, \beta_p$.

3. Solve the set of polynomial equations by assuming

$$\begin{aligned} \beta_i &= \beta c_i \\ \beta w_j &= \beta \sum_{i=0}^p c_i q^i. \end{aligned}$$

This is not identifiable unless the weights are forced to unity

$$w'_j = \frac{\beta w_j}{\sum_{k=0}^q \beta w_k}, \quad \sum w'_j = 1$$

If some of the weights, especially at the ends, are negative, try again with a restricted range of lags (for example, 1 to 5). Reduce the order of the polynomial down to 2 or 1, as necessary. (Sometimes this led to the conclusion that the single lag model was the best.)

4. Define a new working variable Z_t ,

$$Z_t = \sum_{j=0}^q w_j X_{t-j}$$

and fit this in the model to obtain β .

5. Determine the interquartile range (IQR) and the relative risk as usual.

To put the process into simple words: Using an algorithm borrowed from polynomial distributed lags, we determined a net of weights for a certain lag window. The weights had to add up to 1 and to follow a parabolic shape (U-shaped, J-shaped, L-shaped). They were not constrained to be positive. These weights were then used to obtain a new variable, the weighted mean over a number of previous days, which was then used for further computations. The weight curve and the lag window were optimized for maximum association.

This procedure simulated the fitting of polynomial distributed lag models as they are used in linear regression. It gave us information regarding the lag range in which most of the association was to be found. The advantage this has over an unrestricted distributed lag model or just looking at results by different lags one by one was that it somewhat smoothed random spikes.

Polynomial distributed lag models provide a flexible approach for estimating the relative effects of multiday exposures, but the estimates are influenced by both the data and the investigator's specification of the order of the polynomial. The trade-off for concise summaries of the temporal patterns of these models was reduced statistical efficiency. However, as what we used was not an integrated polynomial distributed lag procedure, the *P* values were necessarily underestimated. For this reason, the *P* values from different polynomial distributed lag models may be compared as a rough ranking of goodness of fit, but should not be directly compared to those from single-day lag models nor interpreted as confirmatory results.

We present results as relative risks per interquartile range. Confidence intervals (CIs) were obtained as the exponential of the (parameter \pm 1.96 standard deviation) times the interquartile range. Interpretation was based on the pattern of results: *P* values and CIs; comparison of the values of the point estimates; and ranking the point estimates. Ultimately, interpretation of the estimates provided by polynomial distributed lag models required comparing the observed pattern of associations with predictions based on prior knowledge. This process is at least as important for interpretation as the statistical characteristics of the fitted model. We should ask ourselves: Do the results form a consistent pattern? Is the pattern consistent with what we know about the correlations among pollutants? Is the pattern biologically plausible?

As a final step, we attempted to accumulate the associations by fitting a restricted joint model of all sizes simultaneously, similar to describing the joint association of different delays by a distributed lag model. We might call this a *polynomial distributed size range model*, a formal way of describing a pattern in the results across particle sizes, and a sum of the associations across the size categories, giving a cumulative association. (For further discussion of modeling aspects, see Katsouyanni et al 1996; Pope and Dockery 1999; Samet et al 1995, 1997; Schwartz et al 1996b.)

Selection Processes Although the elements of the confounder model were fixed beforehand, decisions had to be made as to the details. The seasonal model was fitted based on visual inspection of the fitted time series and the

residual time series. AIC is not an appropriate criterion for this. Large samples (long time series with many cases per day) fit a seasonal pattern with many small humps, whereas small samples (short time series with few cases per day) fit very smooth seasonal variations. The season itself, however, should have had the same effect in both series.

For other decisions, such as choosing a shift for an influenza epidemic, a delay for the temperature model, or the inclusion or exclusion of a temperature humidity interaction, the AIC was a helpful measure. Samet and Zeger (Samet et al 1997) suggested adding a penalty for overdispersion, and this was included. Note that the AIC comparison was valid only when the data basis was the same; this was occasionally a problem when some values were missing.

Further criteria evaluated during the fitting process were the partial autocorrelation function (PACF) and the overdispersion of the residuals. Where it occurred, autocorrelation should be reduced by the inclusion of the confounders. However, either a negative autocorrelation, especially one consistently negative over the first several lags, or an overdispersion factor much below one suggests the possibility of overfitting. Although they were informal criteria, time series plots, fitted plots, and residual plots were important at each step. They helped to check both lack of fit and overfitting, especially with regard to season and influenza. Raw data patterns of more than a week or two should show up in the fitted curve but should be gone in the residuals. No new patterns should be created in the residuals (ie, overfitting).

For the single-day pollutant models a necessary decision was whether to transform the data or not. Choosing no transformation ("id") or a log transformation tends to change the shape of the dose response curve only at the ends of the distribution, which can influence goodness of fit considerably. The best fit was selected on the basis of either AIC or the *t* value, which tended to almost always agree. They did occasionally disagree when the parameter in question was very close to zero. In these cases we usually presented the smaller *P* value, but the choice was inconsequential.

AIC could not be used when comparing the delays. Because of missing values, the data basis was slightly different from delay model to delay model, so we used the (absolute) *t* value. No upper limits were set when selecting the best lags. We started with lag 0, and at least 2 days of lag were always checked (mostly up to 6 lags). Lags were evaluated until no associations were observed, which always occurred by lag 6. This procedure is relevant because the different mechanisms under discussion here have different time scales.

Sensitivity and Exploratory Analyses

Sensitivity Analyses for Total Mortality and One-Pollutant Models A wide range of sensitivity analyses were performed to be certain that we did not miss anything or misinterpret a result.

The idea of sensitivity analyses is to assess whether results are valid or spurious, whether they are strongly influenced by decisions made during the confounder modeling process, and whether some further insights may be gained. The first question (result validity) was initially addressed by comparing parametric and nonparametric fits of the same pollutant. The standard analysis of the pollutants is parametric (see above). All pollutants were fitted alternatively by a LOESS model. Except for the tails of the distribution (the outer 10%), the agreement between the parametric model and the smoothed model should be rather good. Otherwise, the parametric model was quite inappropriate.

The question of the confounder modeling process was tackled by variations of the meteorologic, seasonal, and influenza corrections. An investigation of the day-of-week correction was related to the same question. Mortality was known to have a day-of-week pattern, and we observed air pollution to have one. The specific day-of-week correction in the confounder model was based on model fit. Variations thereof may have had considerable influence if what we saw was solely caused by the phase shifts of the different day-of-week patterns. The question of gaining further insight into the data was finally approached by looking at separate effects by day of week, season, and study winters.

The effect seen for all days was necessarily an average of different subsets of days or periods of differing character, and we wanted to see whether certain subsets might drive or dilute this observed effect. A different regression estimate for the slope by different subsets of study time could mean that different populations were at risk. This was considered unlikely, except perhaps in the context of influenza epidemic periods and, maybe, seasons. Different composition and consequent toxicity of a given amount of air pollution seemed likely, especially for the weekday–weekend comparisons. The dose response curve may have a truly different slope at different ranges, such as a threshold (ie, a flat curve below a certain value). Finally, the signal-to-noise ratio of the independent variables was lower in periods with lower pollution (for example in summer) than otherwise, and thus the parameter would have been biased toward the null.

These models were fitted alternatively:

1. If a choice had to be made between two rather different but almost equally well-fitting meteorologic models, they were exchanged.
2. Epidemics were added and removed.
3. Interactions were included with epidemics.
4. Many more degrees of freedom were allowed for the seasonal model.
5. Day-of-week indicators were added and removed.
6. Models were done with effects by season, study winter, and day of week.

Multisize models were considered in the form of the polynomial distributed size range models.

Two-Pollutant Models Two-pollutant models are another special type of sensitivity analysis. Two-pollutant models, especially SO₂ and a particulate pollution indicator, have been widely used. SO₂ and particles tend to be more or less highly correlated (were they uncorrelated, a two-pollutant model would be no problem but also unnecessary). Often one parameter tends to increase in size for one pollutant and decreases for the other. This observation is usually interpreted as the first one being the real pollutant and the second one as an acting proxy. This effect can also be obtained when disparate measurement error is present in these two variables. Measurement error in this context means not only actual measurement problems but also less representative measurements for actual exposure of the sensitive group. This may be caused, for example, by high spatial variability of a variable or a low and highly varying penetration indoors. The two-pollutant analysis favors the more reliably measured exposure variable.

Having thus pointed out the caveats regarding the usefulness of such models for the decision “What is to blame?” we would like to point out that two-pollutant models might have more uses than that: We can learn about joint effects from two-pollutant models. To judge those, we also need to include the interaction term between the two pollutants regardless of whether it is significant. We can then compute relative risks for a day with both pollutants low and compare them with those for days with one or both pollutants high. Thus we learn about the independent effects, effects in the absence of the respective other pollutant, and the joint effect on days with high levels of both pollutants.

From a more technical point of view, note that an interaction term close to zero (eg, additive risks) corresponds to the two relative risks for only one pollutant elevated multiplied because of the log linear risk model. For a small relative risk (RR), this is roughly $RR_1 \times RR_2 \approx RR_1 + RR_2 - 1$.

Note also, that days with one pollutant (very) low and the other one (very) high may actually not occur at all because the pollutants are positively correlated. Finally, keep in mind that days with pollution levels above the 75th percentile of one pollutant and above the 75th percentile of another one occur in fewer than 25% of the total number of days if the pollutants are correlated. Although such analysis is formally possible for more than two pollutants, presentation of results becomes very difficult and was not attempted in this study.

Sensitivity Analyses for Subgroups Subgroups were analyzed together. Data sets always contained the counts for all age groups or all cause-of-death classes of one type, with classes identified by an indicator variable. Although we were aware that transformations and delays may differ between classes, the model obtained from the total data set was used for reasons of simplicity.

Whether different parameters were necessary for the different subgroups was determined one by one by defining interactions with the indicator variables. Decisions were made on the basis of an improvement of fit beyond the loss of degrees of freedom. At least a minor AIC improvement was required for such a set of interactions to be allowed to stay in the model. Subgroup indicator variables were always included in the model, giving different offsets for the subgroups. The interaction terms with those indicator variables basically described differences in the slope of an effect by subgroup. Different pollution parameters were always determined for each group. Further differences in lag or transformation by subgroup were considered as a sensitivity analysis. To reduce the number of models that needed to be run, such in-depth analyses were only done for a few selected variables, based on external hypotheses and the performance in the joint model (eg, the all-cases model).

RESULTS

DATA DESCRIPTION

Particle Data

Data Availability Measurements in Erfurt were conducted from September 1, 1995, until December 21, 1998 (1,208 days). Data for 15 days during the summer of 1996 (June 1 to June 15) are missing due to routine MAS laboratory calibrations. CPC measurements for quality control are available for February 25, 1996, to May 31, 1997, and for October 1, 1998, to December 31, 1998. Gravimetric PM_{2.5} measurements were scheduled every other day during the

first three months of the study and every day from then onward. Data for TSP, SO₂, NO₂, and CO were obtained from the Erfurt city stations for August 1, 1995, to December 31, 1998. Measurements of SO₂ and NO₂ and meteorologic data were gathered at the GSF station in principle every day from September 1, 1995, to the end of the study period. The NO₂ instrument of GSF did not work properly until it was repaired in June 1997. Table 4 summarizes the raw data availability for each component measured in Erfurt. A daily average was only considered valid if the respective measurement was available for at least 16 hr/day.

Internal consistency of all data, including data obtained from the city, was checked carefully for the following observations:

1. All particulate mass data (MC_{xx-xx}, PM_{2.5} impactor, sulfates, PM₁₀, TSP) had a tendency to show similar time series.
2. Both SO₂ devices had a similar time course.
3. Mass and count data for the same particle size were highly correlated, especially for ultrafine particles.
4. Neighboring size data were highly correlated.
5. Some variables that are not directly related were highly correlated (for example, NO₂ and CO, CO and ultrafine particles).
6. Scatterplots of all variables against all variables were inspected, and time series were plotted together.

Unlikely values were identified and deleted from the work file. In case of doubt, a number was deleted rather than retained. The following descriptions of results were based on the resulting work file.

MAS Data MAS-derived particle number distributions were determined in 58 distinct size channels throughout the study. A typical particle number distribution averaged from 40 measurement days is shown in Figure 4. Note that the highest particle counts were observed for very small particles. The derived particle mass distribution calculated from this number distribution centered at larger particle diameters (about 0.4 μm).

Particle Number Concentrations Descriptive statistics of daily average number concentrations derived from MAS measurements in selected size are summarized in Table 7. This table, containing data obtained over the whole study period, comprises information on the relative contribution of each size range to the total particle number.

The time series of the total daily average particle number as determined by MAS is shown in Figure 5. This figure includes the time series of the daily average number concentrations in sizes 0.01 to 0.1 μm (shown as NC_{0.01–0.1}),

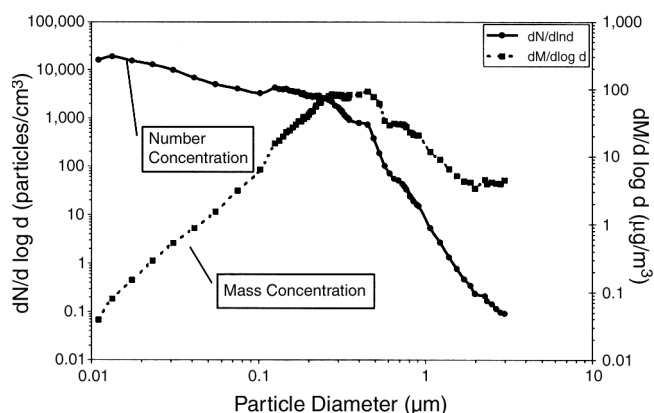


Figure 4. Typical particle number and mass distribution averaged from approximately 10,000 single measurements (40 measurement days), Erfurt.

the range that drove total number. The time series of particle number in the subsize ranges contributing to most of the ambient aerosol particles is shown in Figure 6. These time series showed a clear seasonal pattern. All numbers in the selected particle size ranges were higher during the winter seasons of the study than they were during the summer seasons.

Among the particle ranges, ultrafine particles showed a clear day-of-week pattern with high concentrations Monday through Friday (with lower concentrations on Friday) and low concentrations on the weekend (Figure 7). In Germany, Friday is only half a working day for many people and frequently taken off. On average, Sunday values were 37% below the mean. The pattern did not look different after correction for seasonality.

Table 7. Daily Average Particle Concentrations in Erfurt from September 1995 to December 1998^a

Parameter (% of Total)	N	% Missing Days	Mean ± SD	Median	Percentile	
					5th	95th
Number Concentration (particles/cm ³) ^b						
NC _{0.01–0.03} (57.9)	1,127	6.7	10,410 ± 7,077	8,230	2,703	24,609
NC _{0.03–0.05} (18.3)	1,142	5.5	3,285 ± 2,394	2,573	891	8,585
NC _{0.05–0.1} (11.3)		5.5	2,023 ± 1,577	1,547	547	5,354
NC _{0.1–0.5} (11.8)	1,133	6.2	2,123 ± 1,515	1,688	637	5,088
NC _{0.5–1.0} (< 0.5)	1,103	8.7	19 ± 26	9	1.5	72
NC _{1.0–2.5} (< 0.5)	1,097	9.2	0.7 ± 0.7	0.4	0.1	2.2
NC _{0.01–0.1} (87.5)	1,132	6.3	15,773 ± 10,321	14,769	4,415	36,468
NC _{0.01–2.5} (100)	1,074	11.1	17,966 ± 11,373	14,769	5,687	41,367
Mass Concentration (µg/m ³) ^c						
MC _{0.01–0.03} (0.2)	1,141	5.6	0.04 ± 0.03	0.03	0.01	0.1
MC _{0.03–0.05} (0.5)	1,142	5.5	0.1 ± 0.09	0.1	0.03	0.3
MC _{0.05–0.1} (1.8)	1,143	5.4	0.5 ± 0.4	0.4	0.1	1.2
MC _{0.1–0.5} (78.4)	1,130	6.5	20.1 ± 16.1	15.3	5.1	15.7
MC _{0.5–1.0} (14.1)	1,102	8.8	3.7 ± 5.2	1.6	0.4	14.3
MC _{1.0–2.5} (5.1)	1,096	9.3	1.3 ± 1.2	0.9	0.2	3.6
MC _{0.01–1.0} (94.9)	1,073	11.2	24.9 ± 21.0	17.9	6.1	67.1
MC _{0.01–2.5} (100)	1,069	11.5	25.8 ± 21.4	18.8	6.6	70.2
Other Particle Mass (µg/m ³)						
PM _{2.5}	1,081	10.5 ^d	26.3 ± 20.8	20.2	7.5	68.6
PM ₁₀	1,115	7.7	38.2 ± 26.4	31.0	11.3	92.8
TSP	1,246	0.2 ^e	48.9 ± 28.1	42.0	19.4	103.8

^a Measurements from midnight to midnight, except for PM_{2.5} (11 am to 10:50 am next day). For some parameters, data obtained in August 1995 were available.

^b Number in parentheses indicates the percentage of total NC_{0.01–2.5}.

^c Number in parentheses indicates the percentage of total MC_{0.01–2.5}.

^d During the first months, measurements were scheduled only every other day.

^e Mean series from the two highly correlated city stations.

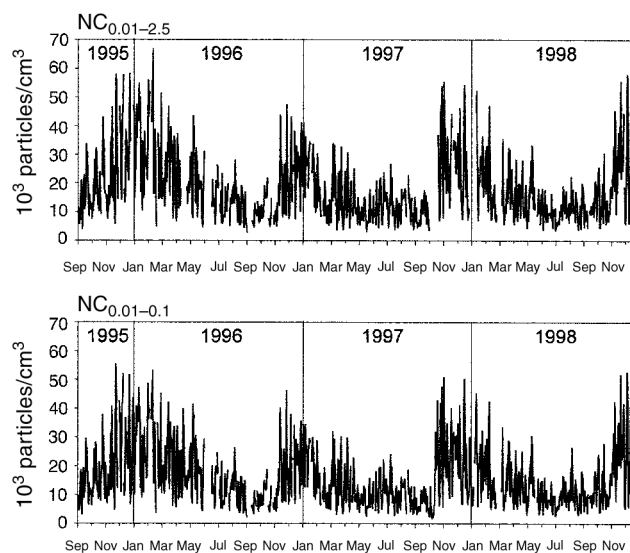


Figure 5. Time series of daily average total particle number ($NC_{0.01-2.5}$) and ultrafine number ($NC_{0.01-0.1}$).

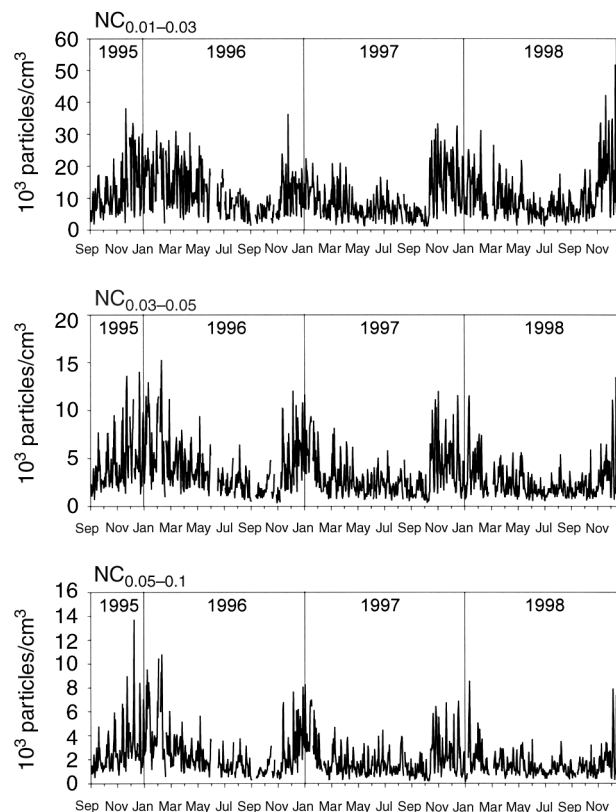


Figure 6. Time series of daily average particle numbers in the size ranges contributing most to total particle number.

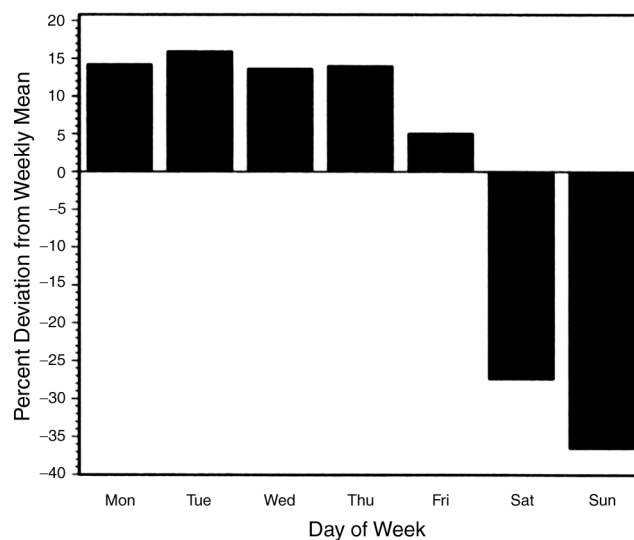


Figure 7. Day-of-week pattern of $NC_{0.01-0.1}$ with percentage deviation from mean per weekday compared with the grand mean.

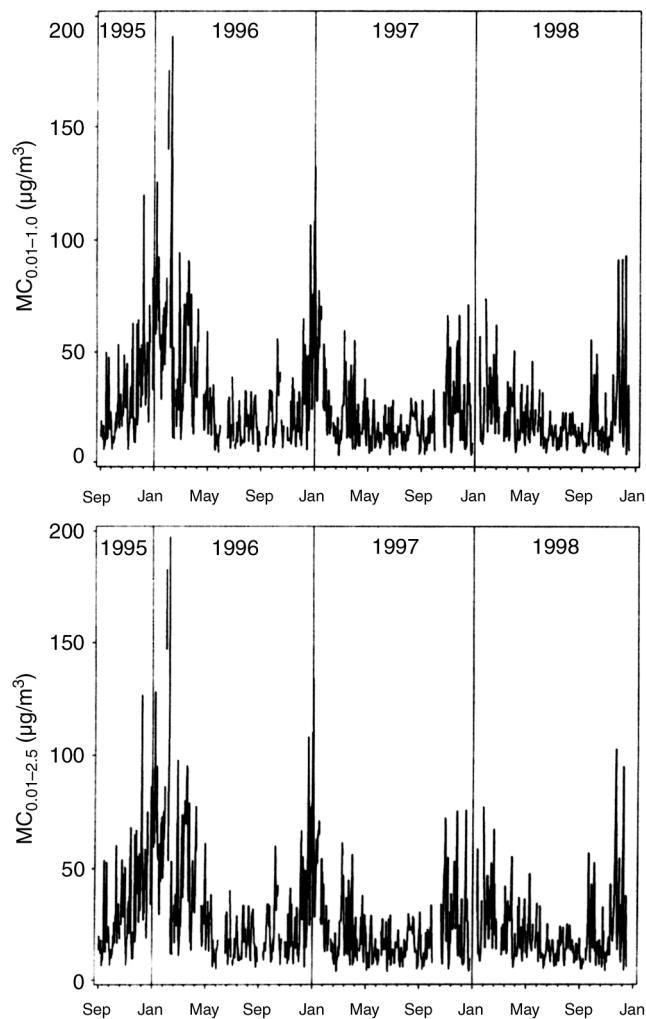


Figure 8. Time series of $MC_{0.01-2.5}$ and $MC_{0.01-1.0}$.

The short-term temporal properties of the data examined via PACF showed an AR(1) pattern with $r \approx 0.65$. Some additional large partial autocorrelation seen at lags 5 to 7 was clearly due to the day-of-week pattern. After deseasonalization, this pattern was basically retained. The AR(1) parameter was roughly 0.45; further lags were small and negative up to lag 4. The small peak at lags 6 and 7 remained. The deseasonalization applied for descriptive purposes may have been slightly overcorrecting, which would explain the negative autocorrelations. Clearly some of the autocorrelation seen in the raw data was due to trend and season, but a given day's values still depended heavily on the previous day's levels. The day-of-week pattern was not removed by deseasonalization (see Appendix D). Diurnal variation is presented in detail in Part II of this report as part of the discussion of sources.

Particle Mass Concentrations Particle number distributions were converted into particle volume distributions. When a comparison with $PM_{2.5}$ was performed, daily particle volume concentrations were calculated from 11:00 am to 10:50 pm. The mean apparent density over the entire 1,081 days was 1.53 g/cm^3 , which was in excellent agreement with the literature value of 1.5 g/cm^3 .

Descriptive statistics of daily average particle mass derived from MAS measurements in selected size ranges are summarized in Table 7. This table, which includes data obtained over the whole study period, comprises information on the relative contribution of each size range to the total particle mass. The apparent density (1.53 g/cm^3) used to convert the particle number distribution to particle mass distribution was obtained from a previous comparison of volume distribution derived by MAS measurements and gravimetrically derived $PM_{2.5}$ (Tuch et al 1997a). Time series plots of $MC_{0.01-2.5}$ ($PM_{2.5}$ equivalent) and $MC_{0.01-1.0}$ are shown in Figure 8. The time-series plot of size ranges contributing to most of the mass of ambient aerosol particles is shown in Figure 9.

The day-of-week pattern of this representative measure of fine particle mass (Figure 10) is different from that for ultrafine particles (see Figure 7). Values for fine particle mass were higher than average from Tuesday through Friday and lower on the weekend and on Monday. The fine particle pattern did not look different after correction for seasonality.

The short-term temporal properties again indicated an AR(1) model with some further autocorrelation at lags 4 to 5. There was no noticeable peak at lag 7. The 7-day partial autocorrelation was actually zero after deseasonalization. Possibly the weekday pattern was dominated by a few peak periods in winter. If this were true, the skewed nature of the distribution of these values would influence the

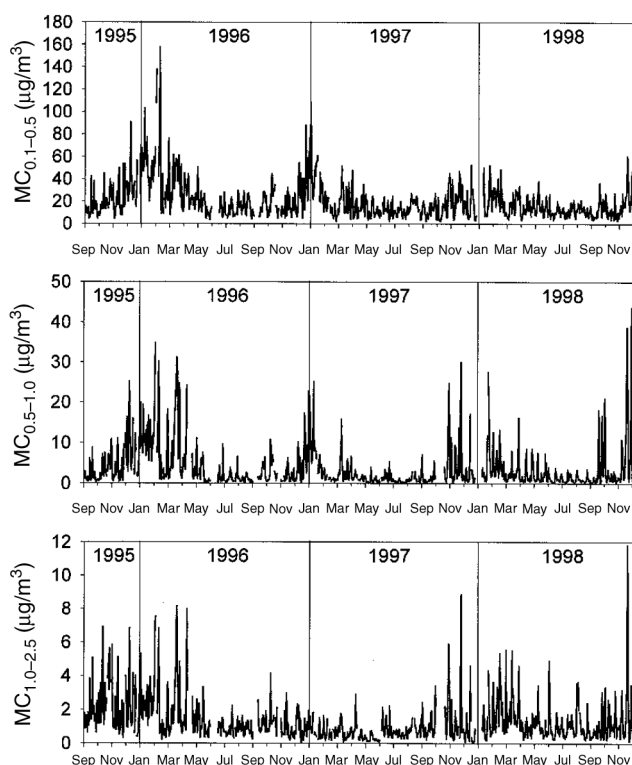


Figure 9. Time series of daily average particle mass in the size ranges contributing most to fine particle mass.

day-of-week analysis based on raw data but not as much as the PACF (which was based on log transformed data). Also, given the shape of the curve, the day-of-week pattern may have been addressed by the small autocorrelation term at lags 4 to 5. The dip at lag 2 may indicate that the (purely

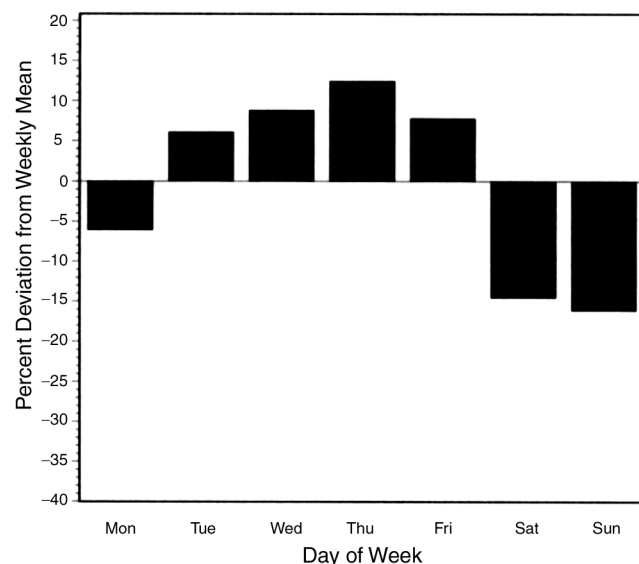


Figure 10. Day-of-week pattern of $MC_{0.01-2.5}$, with percentage of deviation from mean per weekday compared with the grand mean.

descriptive) deseasonalization was somewhat overdone. Note that the seasonality was more pronounced during the first winter of the study than during the last, so it was difficult to find a smoothing level that did justice to both periods (see Appendix D).

Reliability of MAS Measurements Two endpoints were available to check the quality of MAS measurements. First, the total particle number derived from the CPC used in the MAS was monitored by an integral counting CPC. Differences between these two instruments were dominated by particles smaller than 0.1 μm in diameter. Second, the fine particle mass measured by $\text{PM}_{2.5}$ impactor was compared with the fine particle mass derived from the MAS. This parameter was primarily influenced by particles larger than 0.1 μm in diameter.

A CPC 3022A was used to monitor the total particle number in parallel with the MAS during 545 days of the study. The correlation between concentrations derived from these two instruments was high ($r^2 = 0.9$, slope = 0.83, intercept = 542), indicating that the MAS-derived number data were comparable to data derived from a more conventional instrument (the CPC 3022A) throughout the study. The size of the intercept could be attributed to the wider range of the CPC 3022A (0.003 to 10 μm). The plot of MAS-derived total particle $\text{NC}_{0.01-2.5}$ versus CPC-derived integral particle number is shown in Figure 11.

The calculated values for $\text{MC}_{0.01-2.5}$ (11:00 am) correlated highly with gravimetric $\text{PM}_{2.5}$ measurements ($r^2 = 0.90$, slope = 0.98, intercept = 2.3), as shown in Figure 12. This clearly indicates that $\text{MC}_{0.01-2.5}$, fine mass concentration derived from MAS measurements, is equivalent to $\text{PM}_{2.5}$, fine mass concentration measured by impactor.

There were two uncertainties in the estimated apparent density. First, the shape of the particles was assumed to be spherical. Second, all particles were assumed to have the same density regardless of constituent compounds. The

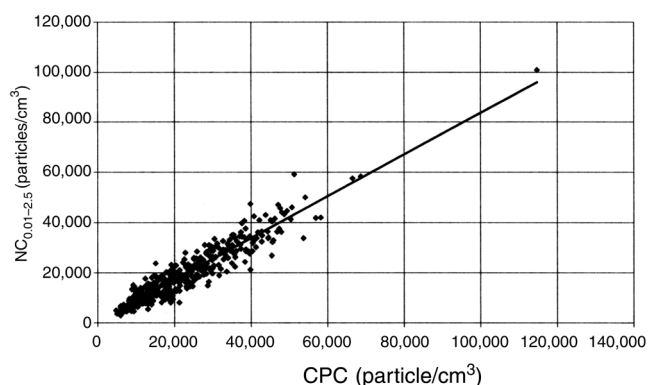


Figure 11. Daily average MAS-derived total particle number concentration versus CPC-derived total particle number concentration during 545 study days. Note: Fitted line $\text{NC}_{0.01-2.5} = 542 + 0.83 \text{ CPC}$.

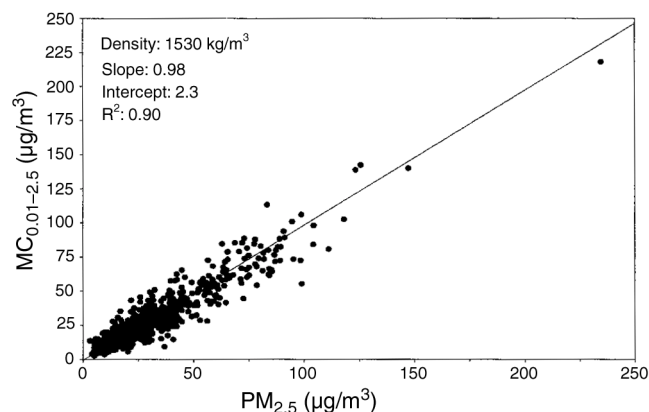


Figure 12. Daily average MAS-derived $\text{MC}_{0.01-2.5}$ versus gravimetrically derived $\text{PM}_{2.5}$ during 1,081 study days. Note: Fitted line $\text{MC}_{0.01-2.5} = 2.3 + 0.98 \text{ PM}_{2.5}$. All points refer to the measurement period from 11 am to 11 am the next day.

first assumption was justified by the facts that even chain aggregates of particles round up to some extent during aging and that the instruments determined particle properties associated with the volume equivalent diameter of the particle. We were aware that the second assumption was rather crude, but the following aspects need to be taken into account: The bulk density of major compounds of ambient aerosol as given in Table 8 varied between roughly 1 and $2.5 \times 10^3 \text{ kg/m}^3$. The density of aerosol particles was usually lower than the bulk material density (Willeke and Baron 1993), and ambient particles are usually a mixture of several compounds.

From these considerations the measured apparent density appeared to be plausible. Furthermore, this assumption applied in particular to particles between 0.1 and 0.5 μm diameter size because this fraction dominated the volume distribution. Particles in this size range may contain combustion products as well as ammonium, sulfate, and nitrate salts. Although the composition of particles between 0.5 and 2.5 μm size may shift toward salt and

Table 8. Bulk Densities of Common Compounds of Ambient Aerosol Particles^a

Aerosol Compound	Density (10^3 kg/m^3)
Elemental Carbon	
Graphite	2.2
Coal	1.2–1.8
Organic Carbon	0.8–1.5
Ammonium sulfate + nitrate	1.8
Fly ash	0.7–2.6
Aluminosilicate	1.8–2.2

^a Willeke and Baron (1993).

crystal compounds, their bulk densities are still in the same range (1.5 to $2.5 \times 10^3 \text{ kg/m}^3$; see Table 8). Based on the apparent mean density of $1,530 \text{ kg/m}^3$, their mass fraction was in the range of 10% of the total mass. If the mean density of particles $0.5 \text{ }\mu\text{m}$ to $2.5 \text{ }\mu\text{m}$ in diameter was as high as $2 \times 10^3 \text{ kg/m}^3$, their average mass fraction would increase from 10% to 12.5%, which is considered to be a moderate shift and within the error range of 5% to 10%.

There was more uncertainty about ultrafine particles, which mainly originated from combustion processes and were predominantly composed of elemental carbon with varying fractions of organic carbon. Although particles of elemental carbon may have a density in the range of $1.5 \times 10^3 \text{ kg/m}^3$, depending on their agglomeration and porosity, addition of a large variety of organic compounds of densities ranging from 0.5 to $2.5 \times 10^3 \text{ kg/m}^3$ may change particle density considerably. Yet even an error of a factor of 2 of the apparent particle density would still indicate negligible contribution of ultrafine particles to the fine particle mass. As it turned out, however, the mass distribution was dominated by the fine particle fraction, for which we were able to determine a mean apparent density. Both endpoints of the particle number distribution suggest that the overall performance of the MAS throughout the study was appreciably good.

External Quality Control of MAS Measurements Three intercomparisons of particle size spectrometers were done during this study. Two of these intercomparisons were performed in Erfurt, and the third included tests with laboratory aerosols in Petten, The Netherlands. These intercomparisons proved a good agreement between different instruments assessing the particle number distribution (Tuch et al 1999).

Other Particle Data Along with MAS-derived measurements of particle numbers and masses, $\text{PM}_{2.5}$, PM_{10} , sulfate, or particle strong acidity (PSA) concentrations in $\text{PM}_{2.5}$ samples were determined at the central GSF measurement site. (Note that sulfate and PSA are discussed in Part II of this report.) Additional information on TSP was available from the two city-run measurement sites (Krämpferstrasse and Kartäuserstrasse). Table 7 includes descriptive statistics of particulate masses measured in Erfurt during the whole study period. The time series of impactor-derived $\text{PM}_{2.5}$ and PM_{10} , and TSP data measured by beta attenuation (mean series from Krämpferstrasse and Kartäuserstrasse) are shown in Figure 13. The day-of-week pattern of PM_{10} looked similar to that for fine particles ($\text{PM}_{2.5}$ impactor); furthermore, the PACF was somewhat similar.

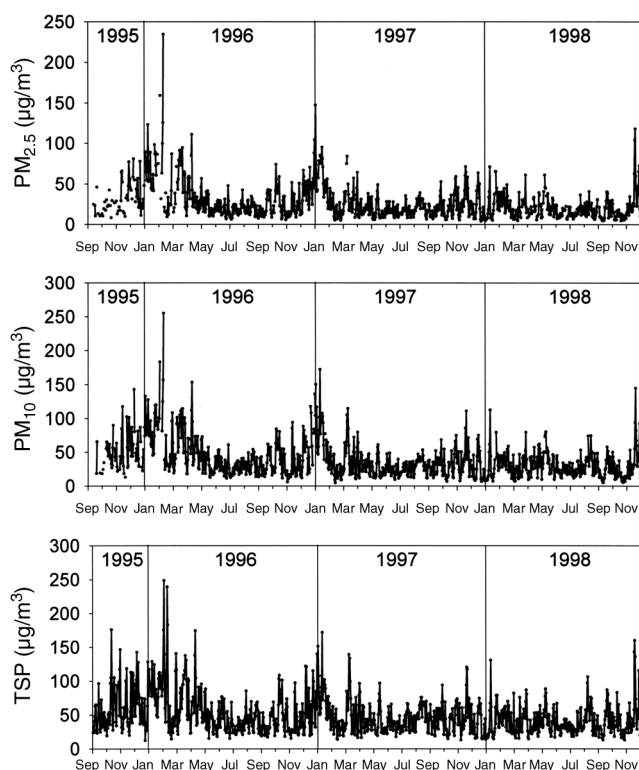


Figure 13. Time series of daily average $\text{PM}_{2.5}$, PM_{10} , and TSP concentrations.

Reliability of Other Particle Data The correlation matrix of $\text{PM}_{2.5}$, $\text{PM}_{2.5}$ impactor, PM_{10} , and TSP is shown in Table 12. All particle pollutant data were highly correlated, indicating a comparable exposure assessment at all measurement locations. Note that the correlation between PM_{10} and TSP measured from midnight to midnight was necessarily higher than their correlations with $\text{PM}_{2.5}$ impactor (measured from 11:00 am to 10:50 am the next day) because PM_{10} and TSP included part of the coarse fraction of the aerosol that originated from different sources than $\text{PM}_{2.5}$, in addition to the shift of the measurement period.

After the data had gone through these checks from a technical point of view, they were additionally inspected from an epidemiologic point of view. This was especially important for the MAS data, which had properties allowing identification of potentially false measurements. The number and mass of the same particle size were usually highly correlated. The same applied for consecutive size ranges of number and mass. A high correlation suggested a rather tight data cloud in a scatterplot. Points far outside of this cloud were likely to be measurement errors. For example, the combination of a very high $\text{NC}_{0.03-0.05}$ value with a very low $\text{NC}_{0.01-0.03}$ value was unlikely, and one of the values could be false. Which one of the two axes (x or y) provided the errant point was mostly determined

by comparing its relation in the respective other plot. Such points were excluded from the analysis. When it was unclear which recorded measurement was false, both points were excluded from the analysis. When the scatterplot showed a rather wide cloud, this was naturally handled more generously and outlying points had to be very far out to be considered unlikely. Close inspection of the time series revealed a few short periods with doubtful measurements, which were then excluded from the analysis. A similar procedure could be applied, though less strictly, when comparing different particle and gaseous measurements and our own measurements with the official site measurements. On top of missing data due to technical problems and scheduled down time, another 1% to 5% of data were thus excluded from the analyses.

Gaseous Pollutants

The data for gaseous pollutants are described in detail in Part II of this report. At this point, we present a brief summary. We had SO₂ data available from our station and the two city-run stations. The agreement among them was very good (high daily correlation and similar levels), so we chose to use the GSF data. The NO₂ data were more complete at the Krämpfertsrasse station, so we chose to use them. For the period of parallel measurements, there was good agreement between the GSF and Krämpfertsrasse stations. CO data were available only from the Krämpfertsrasse station. (See Table 9.)

Meteorologic Data

Temperature and relative humidity data were available from the central GSF monitoring site. Additional data on temperature and relative humidity were obtained from the official station at Erfurt airport (Bindersleben; see Figure 1).

Descriptive statistics of weather data are summarized in Table 9. The GSF monitoring site was located in the center of the city, whereas the airport station was located at a slightly higher altitude outside the city. Temperatures in the city were usually slightly higher than those recorded at the airport. In the end, we decided to use the GSF measurements in the analysis as more representative of the city, although the airport data were more complete. The time series plots of daily average temperature and relative humidity measured at the GSF station during the study period are shown in Figure 14.

Analysis of Air Pollution

The correlation of different air pollutants gave various kinds of information. For one, highly correlated data were assumed to be generated under similar circumstances and may have been generated by the same sources. On the other hand, air pollutants that were not correlated in the analysis would have allowed easier separation of effects in the epidemiologic model. Traditionally, raw correlation coefficients are presented but they tend to be relatively high for variables with similar seasonal patterns. We added two types of seasonally corrected air pollutants, namely correlation coefficients corrected for season in a model taking care of the seasonal pattern of the pollutants and correlation coefficients corrected for the confounder model used later in the regression analyses. These models were applied to the log of the pollution variables, and then residuals were correlated. While the correlation coefficients corrected for season were mostly aimed at giving the short-term correlation between two variables, the correlation coefficients corrected for the confounder model were aimed at indicating the separability of effects in regression models.

Table 9. Daily Statistics of Gaseous Pollutants and Meteorologic Parameters in Erfurt

Parameter	N	% Missing Days	Mean ± SD	Median	Range
Gaseous Pollutants					
SO ₂ (µg/m ³) ^a	1,137	6.7	16.8 ± 18.7	10.9	0.03 to 134.8
NO ₂ (µg/m ³) ^b	1,205	1.1	36.4 ± 15.3	35.0	7.0 to 119.0
CO (mg/m ³) ^b	1,188	2.5	0.6 ± 0.5	0.5	0.1 to 2.5
Temperature (°C)					
GSF site	1,174	2.3	8.8 ± 8.1	9.5	−17.3 to 28.2
Bindersleben (Airport)	1,218	0	7.7 ± 7.6	8.4	−18.2 to 27.0
Relative Humidity (%)					
GSF site	1,173	2.3	77.6 ± 11.4	78.5	39.4 to 99.7
Bindersleben (Airport)	1,218	0	80.2 ± 11.7	82.0	32.0 to 99.0

^a GSF site.

^b Krämpfertsrasse, Kartäuserstrasse.

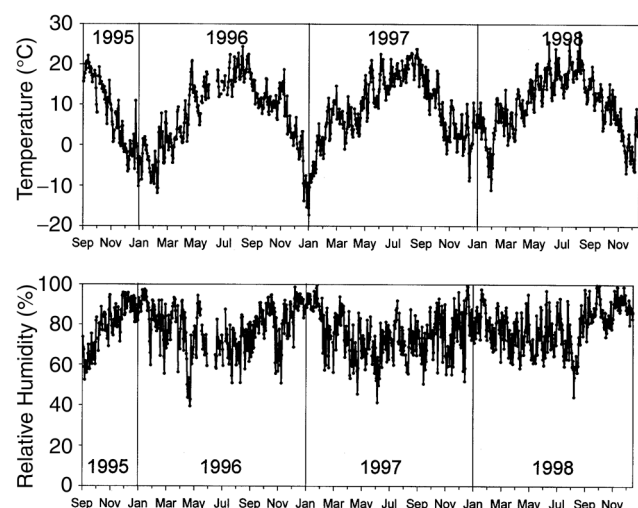


Figure 14. Time series of daily average temperature and relative humidity (obtained at GSF monitoring site).

Correlation Between Particle Number Parameters Correlation coefficients between particle numbers in size ranges contributing most to the total numbers are given in Table 10 as based on log transformed raw data. (For season and confounder model corrected data, see Tables D.1 and D.2.) All correlation coefficients were significant at $P < 0.01$.

All correlation coefficients showed a similar pattern. Correlation coefficients between nearby size classes were relatively high. The farther the size ranges were apart, the weaker was the correlation between size classes. The total particle number was driven by ultrafine particles. Thus, the correlation between total particle number determined by the MAS and number fractions for particles smaller than $0.1 \mu\text{m}$ was high.

Table 10. Correlations Between Daily Average Number Concentrations by Particle Number^a

	$NC_{0.01-0.03}$	$NC_{0.03-0.05}$	$NC_{0.05-0.1}$	$NC_{0.01-0.1}$
$NC_{0.01-0.03}$	1			
$NC_{0.03-0.05}$	0.86	1		
$NC_{0.05-0.1}$	0.74	0.93	1	
$NC_{0.01-0.1}$	0.99	0.94	0.85	1
$NC_{0.01-2.5}$	0.96	0.95	0.88	0.99

^a Log transformed raw data.

Both season and confounder model corrected correlations tended to be slightly weaker than those for the raw data. As expected, some of the positive correlation came from the similarity of the seasonal pattern, but the short-term correlation was still high. Because the confounder model also included corrections for day-of-week and temperature, the correlations had causes beyond those external factors. On the other hand, ultrafine particles and accumulation mode particles were sufficiently uncorrelated that we thought that we might be able to differentiate their effects in regression analysis.

Correlation Between Particle Mass Parameters Correlation coefficients between particle masses in size ranges contributing most to fine particle masses (Table 11) were based on log transformed raw data. Season corrected and confounder model corrected data are presented in Tables D.1 and D.2. All correlation coefficients were significant at $P < 0.01$.

All correlation coefficients showed a similar pattern. Correlations between size ranges in the accumulation mode of the aerosol (that is, 0.1 to $1.0 \mu\text{m}$) were relatively high. Correlations for $MC_{0.01-1.0}$ and $MC_{0.01-2.5}$ were practically

Table 11. Correlations Between Daily Average Number and Mass Concentrations by Particle Mass^a

	$MC_{0.1-0.5}$	$MC_{0.5-1.0}$	$MC_{1.0-2.5}$	$MC_{0.01-1.0}$	$MC_{0.01-2.5}$
Mass concentration					
$MC_{0.5-1.0}$	0.84	1			
$MC_{1.0-2.5}$	0.52	0.68	1		
$MC_{0.01-1.0}$	0.99	0.89	0.58	1	
$MC_{0.01-2.5}$	0.99	0.90	0.62	1.00	1
Number concentration					
$NC_{0.01-0.03}$	0.47	0.41	0.27	0.48	0.48
$NC_{0.03-0.05}$	0.64	0.51	0.34	0.64	0.64
$NC_{0.05-0.1}$	0.77	0.58	0.38	0.76	0.76
$NC_{0.01-0.1}$	0.57	0.47	0.30	0.57	0.57
$NC_{0.01-2.5}$	0.64	0.53	0.35	0.64	0.64

^a Log transformed raw data.

identical. The correlation between the accumulation mode and coarser particles (0.1 to 1.0 μm and 1.0 to 2.5 μm , respectively) was weaker, suggesting that these particles might have different sources. The very high correlation between total particle mass determined by the MAS and particle mass in the size 0.1 to 0.5 μm suggested that the fine particle mass was driven by particles in this size range, as noted in the data description (see Table 7). Correction for season made little difference here.

Correlation Between Particle Number and Mass Correlation coefficients between particle mass in size ranges contributing most to fine particle mass and particles in the size ranges contributing most to particle number given in Table 11 are based on log transformed raw data. Season corrected and confounder model corrected data are presented in Tables D.1 and D.2. All correlation coefficients were significant at $P < 0.01$.

Correlation coefficients for number and mass of identical size ranges were close to unity. The correlation got weaker for size classes further apart. For example, a weak correlation was observed between $\text{NC}_{0.01-0.3}$, which contributed most to total number of suspended particles, and $\text{MC}_{0.1-0.5}$, which contributed most to the fine particle mass. This low correlation had the potential to allow separation of the effects of particle number and mass on human health.

Correlation Between MAS-Derived Parameters and Other Particle Data The correlation coefficients between MAS-derived particle number and mass and other particle mass concentrations are given in Table 12 based on log transformed raw data. Season corrected and confounder model corrected data are in Tables D.1 and D.2. All correlation coefficients were significant at $P < 0.01$.

Note that this table compared daily average MAS data (measured from midnight to midnight) with the $\text{PM}_{2.5}$ impactor values (measured from 11:00 am to 10:50 am the next day). The correlation coefficient between the MAS- and impactor-derived mass was slightly weaker than the one obtained during the time period used for quality control. Correlation coefficients increased with decreasing distance from a selected size range, 0.1 to 0.5 μm , but even TSP and PM_{10} were driven by the mass in this size range.

Correlation Between Particle Data and Gaseous Pollutant Data The correlations between particle data and gases are given in the Results discussion on Two-Pollutant Models and shown in Table 12. Generally CO and NO_2 seemed to have time series similar to that of ultrafine particles, whereas SO_2 seemed to have time series similar to particle mass. A more detailed analysis of the correlation structure of the gaseous pollutants is given in Part II of this report.

Table 12. Correlations Between Parameters Derived from Mobile Aerosol Spectrometer, Other Particle Data, Gaseous Pollutants, and Weather^a

	$\text{PM}_{2.5}$ (11 am)	PM_{10}	TSP	SO_2	NO_2	CO	Temperature	Relative Humidity	Wind Speed
$\text{NC}_{0.01-0.03}$	0.46	0.45	0.42	0.44	0.58	0.53	-0.48	0.15	-0.32
$\text{NC}_{0.03-0.05}$	0.64	0.63	0.60	0.58	0.64	0.70	-0.52	0.13	-0.50
$\text{NC}_{0.05-0.1}$	0.72	0.71	0.69	0.62	0.63	0.68	-0.48	0.14	-0.50
$\text{NC}_{0.01-0.1}$	0.55	0.54	0.51	0.51	0.61	0.61	-0.51	0.16	-0.39
$\text{NC}_{0.01-2.5}$	0.61	0.61	0.58	0.56	0.66	0.64	-0.53	0.19	-0.42
$\text{MC}_{0.1-0.5}$	0.87	0.87	0.85	0.61	0.60	0.62	-0.47	0.25	-0.42
$\text{MC}_{0.5-1.0}$	0.75	0.74	0.73	0.53	0.48	0.56	-0.54	0.40	-0.28
$\text{MC}_{1.0-2.5}$	0.46	0.55	0.58	0.32	0.29	0.28	-0.13	0.07	-0.18
$\text{MC}_{0.01-1.0}$	0.87	0.87	0.85	0.62	0.60	0.62	-0.51	0.30	-0.40
$\text{MC}_{0.01-2.5}$	0.87 ^b	0.87	0.86	0.61	0.59	0.62	-0.50	0.30	-0.39
$\text{PM}_{2.5}$	1	0.89	0.84	0.63	0.59	0.62	-0.44	0.22	-0.49
PM_{10}	0.89	1	0.91	0.61	0.62	0.58	-0.34	0.14	-0.51
TSP	0.84	0.91	1	0.55	0.66	0.57	-0.26	0.12	-0.48
SO_2	0.63	0.61	0.55	1	0.46	0.59	-0.45	0.14	-0.38
NO_2	0.59	0.62	0.66	0.46	1	0.71	-0.35	0.16	-0.48
CO	0.62	0.58	0.57	0.59	0.71	1	-0.63	0.33	-0.51

^a Log transformed raw data.

^b Based on $\text{MC}_{0.01-2.5}$ (11 am), the correlation coefficient is 0.89.

Correlation Between Particle Data and Meteorologic Data

Table 12 summarizes the correlation coefficients between particle parameters and weather data. Note that the meteorologic parameters were not log transformed, only the particle data. All particle parameters increased with a decrease in ambient temperature, which was simply a function of season. Higher wind speed transported particulate air pollution out of the city, leading to a decrease of all particulate parameters with increasing wind speed. Note that winters were usually windier than summers. Increases in relative humidity were more or less associated with increases in all particle parameters. Relative humidity tended to be higher in winter.

Summary of Results on Air Pollutants The majority of the total particle number (58%) was in the lowest size category, between 0.01 and 0.03 μm in diameter. About 18% of particles fell in the second size category, between 0.03 and 0.5 μm , and 11% of particles were between 0.05 and 0.1 μm . In total, 88% of the particle number fell in the ultrafine particle fraction with diameter below 0.1 μm (Figure 15).

In contrast, mass had a completely different pattern. Only 3% of all particles were found in the ultrafine particle fraction. The majority of the mass (78%) was found in the larger diameter range between 0.1 and 0.5 μm . About 14% of particle mass was found in the size range between 0.5 and 1.0 μm , and 5% of particles were between 1.0 and 2.5 μm . The particle mass below 1.0 μm represented 95% of $\text{PM}_{2.5}$.

In addition to the MAS-derived measurements, we made gravimetric measurements: $\text{PM}_{2.5}$ impactor, PM_{10} impactor, and TSP (β -attenuation). From our parallel measurements in Erfurt, we found that $\text{PM}_{2.5}$ impactor values were nearly identical to $\text{MC}_{0.01-2.5}$. PM_{10} was approximately 1.5 times

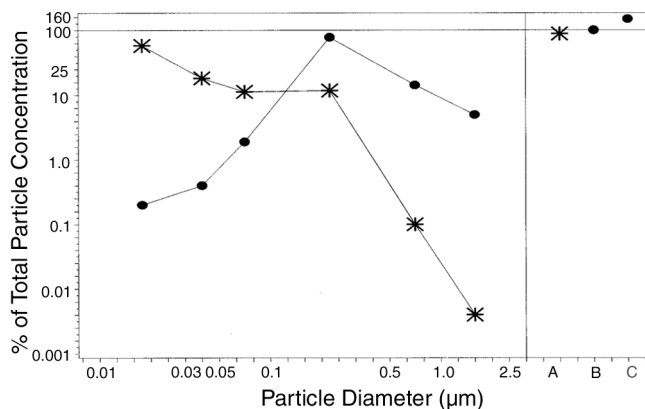


Figure 15. Size distribution of particle number and particle mass in percentage of total. Stars refer to percentage of total number ($\text{NC}_{0.01-2.5}$), dots to percentage of total mass ($\text{MC}_{0.01-2.5}$). Log scales. A = $\text{NC}_{0.01-0.1}$, B = $\text{MC}_{0.01-0.1}$, C = PM_{10} .

$\text{PM}_{2.5}$, with TSP approximately 1.9 times $\text{PM}_{2.5}$. We also had an additional measurement of particle number, the total particle count (by CPC), which in Erfurt represented approximately 1.2 times $\text{NC}_{0.01-2.5}$.

The day-of-week pattern (comparing Monday through Friday to Saturday through Sunday) was stronger for particle number than for particle mass. Weekend ultrafine particle levels were only 60% of the weekday concentrations; $\text{PM}_{2.5}$ was approximately 83%; PM_{10} was 81% (Figure 16). Furthermore, there was a strong seasonal difference for the particle concentrations. Summer concentrations were only 45% of the ultrafine particles found in the winter concentrations. For fine particles, this trend was even more pronounced, with 36% for $\text{PM}_{2.5}$ and 55% for PM_{10} (see Figure 16).

Over the three winters studied, 1995/1996 to 1997/1998, both $\text{PM}_{2.5}$ and PM_{10} showed a continuous decrease, from 100% to 65% to 58% for $\text{PM}_{2.5}$, and from 100% to 69% to 48% for PM_{10} . In contrast, ultrafine particles decreased from 100% in the first winter to 70% in the second winter, followed by an increase to 82% in the third winter. Even more remarkable, the lowest particle size fraction, $\text{NC}_{0.01-0.03}$, was 64% of $\text{NC}_{0.01-0.1}$ in the first winter, 61% in the second winter, and 68% in the third winter.

In terms of correlations among the different size fractions, the strongest correlation coefficient within number was found between $\text{NC}_{0.01-0.03}$ and $\text{NC}_{0.01-0.1}$ (the full size range of ultrafine particles). Within mass, the strongest correlation coefficient was found between $\text{MC}_{0.1-0.5}$ and $\text{MC}_{0.01-2.5}$ (the full size range of fine particles). These sub-categories represented the majority of particle number and particle mass, respectively. Correlation between $\text{NC}_{0.01-0.1}$ and $\text{MC}_{0.01-2.5}$ was weak. The raw coefficient was 0.57, which was reduced to 0.42 after correction for season and confounders. This low coefficient between ultrafine number concentration $\text{NC}_{0.01-2.5}$ and fine mass concentration $\text{MC}_{0.01-2.5}$ indicated that both gave quite independent information and would allow a separation of effects in the setting of the study in Erfurt.

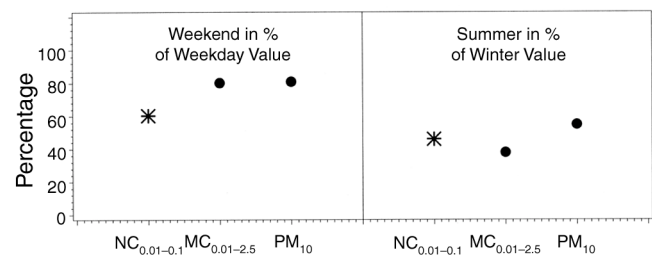


Figure 16. Percentage of total particle data by weekday and season. Summer: April to September; winter: October to March.

The (raw) temporal correlation of the gaseous pollutants showed none of the gases were highly correlated with any particle indicator (see Table 12). Particle number indicators were somewhat correlated with NO₂ and CO. SO₂ did not show a very pronounced day-of-week pattern, but CO and NO₂ did so in a manner similar to that of NC_{0.01–0.1}.

Mortality Data and Influenza Data

Cause, Age, and Place of Death We collected information on a total of 6,793 cases (Table 13). The data were almost complete, especially for the most relevant information. We compared the underlying causes of death from the study with official records of underlying causes in Germany and in Thüringen (see Appendix B). We had no information on Erfurt residents dying far from Erfurt, which might partly explain the slightly lower total death rate in Erfurt (Germany 1,001.9/100,000, Thüringen 1,117.5/100,000, Erfurt approximately 972.1/100,000). Other discrepancies, especially concerning myocardial infarction and ischemic heart disease, were likely caused by the fact that we determined the underlying cause of death from the certificates as completed by the physician and not after official recoding, the basis for official statistics. The underlying cause officially recorded may have differed from the one we found in the last of the three first lines of the certificate. Note that broader categories of cardiovascular disease showed good agreement between Erfurt and Germany as a whole, so the discrepancies we saw were most likely to represent shifts by coding. As we noted in Methods, each individual was assigned to only one class per categorization.

Among all natural deaths, 62% had an underlying cardiovascular or respiratory cause. Many more persons had some cardiovascular or respiratory condition, even when it was not listed as the underlying cause of death. In total, a cardiovascular or respiratory condition was recorded for 81% of all cases. Roughly 19% of all cases would not have been classified as either respiratory or cardiovascular when only looking at the underlying cause. In the finer classification shown in Table 14, note that in 11% of cases the classification by underlying cause of death missed the respiratory contribution to a cardiovascular cause or vice versa. Of the underlying respiratory causes, about half of the cases had a cardiovascular contribution. Actually, respiratory cases without cardiovascular contribution were quite rare, although the “both” category as based on all information on the certificates was quite large.

To describe the population further, we listed more finely stratified causes of death within the broad categories. Specifically, we showed the underlying causes and the observed diseases in the underlying cause of death class,

Table 13. Mortality, Missing Value Information, and Usability of Information

	N	%
Last Place of Residence		
Erfurt	6,756	99
Outside	33	0
Missing	4	0
Place of Death		
Erfurt	6,466	95
Outside	326	5
Missing	1	0
Place Where Case Either Lived or Died		
Died in Erfurt	6,764	100
Lived and Died Both in Erfurt	6,453	95
Neither in Erfurt	24	0
Both Informations Missing	0	0
Type of Death		
Natural ^a	6,368	94
Not Natural ^b	425	6
Missing ^c	0	0
Usable Information		
Natural Deaths of Erfurt Residents	6,091	90
Cause of Death Missing		
Underlying Cause of Death	4	0
Any ICD Information	4	0
Determination of Cause of Death		
Autopsy	206	3
Autopsy Among Natural Deaths	175	3
Place of Death Missing^d		
	0	0
Age (Date of Birth)		
Missing for Natural Deaths in Erfurt	5	0
Hour of Death		
Missing	76	1

^a Ticked “natural” or “unknown” and ICD code for natural death.

^b Ticked “not natural” or an ICD code for non-natural death.

^c Information not ticked and no ICD code.

^d “Unknown” is usually coded as “other;” those are $\approx 4\%$.

as well as both in the prevalent disease class. Percentages of prevalent diseases had to add up to more than 100% because up to five causes could be recorded on the certificate (see Appendix C).

Within the recorded causes in each category, the most frequent underlying causes of death in the category “cardiovascular or respiratory underlying cause” were chronic ischemic heart disease, congestive heart disease, atherosclerosis, and stroke. All of those are chronic conditions or

Table 14. Percentage of Deaths by Prevalent Condition and Underlying Cause of Death

Prevalent Condition	Percentage of Underlying Cause of Death				Total
	Cardiovascular	Respiratory	Cardiovascular and Respiratory	Other Natural	
Cardiovascular but not respiratory	45	0	0	14	59
Respiratory but not cardiovascular	0	4	0	2	6
Cardiovascular and respiratory	6	5	2 ^a	3	16
Other natural only	0	0	0	19	19
Total	52	9	2 ^a	38	100

^a A few causes were classified as affecting both the cardiovascular and respiratory systems (such as cor pulmonale).

the consequence of chronic conditions. The most frequent underlying respiratory causes were lung cancer and pneumonia, followed by COPD (which contributed only 3%). Because only a handful of cases were certified as having died from influenza, the category pneumonia and influenza consisted almost entirely of pneumonia cases. The most frequent conditions generally recorded as underlying cause of death (ie, cardiovascular or respiratory) were congestive heart disease, chronic ischemic heart disease, stroke, atherosclerosis, diabetes (which was not defined as cardiovascular but was connected to it), acute myocardial infarction, and hypertension. The most prevalent respiratory conditions in those with an underlying cardiovascular or respiratory cause of death were pneumonia, lung cancer, and COPD.

The most frequent underlying causes in the “other natural underlying cause of death” group were cancer (49%), diabetes, and digestive tract diseases, the last of which were very frequently alcohol related. For the psychiatric disorders, the most frequent diseases in the “other natural underlying cause of death” category were cancer (54%), diabetes, congestive heart disease, chronic ischemic heart disease, and digestive tract and urogenital tract diseases. Note that a rather large group of persons with congestive and chronic ischemic heart disease had “other natural” underlying causes as well.

The most frequent prevalent conditions among those with some cardiovascular or respiratory condition were congestive heart disease, chronic ischemic heart disease, diabetes, stroke, atherosclerosis, acute myocardial infarction, and pneumonia as well as cancer. These subjects were mostly recorded with underlying causes of death as chronic ischemic heart disease, congestive heart disease, and atherosclerosis, but also lung cancer. Pneumonia was recorded very rarely as the underlying cause of death in these subjects (3%). Among those with no cardiovascular or respiratory condition recorded, the most frequent prev-

alent diseases were cancer (71%), digestive tract and alcohol-related diseases and diabetes (the last of which was rarely found without a cardiovascular disease). The most frequently recorded underlying causes in this group were cancer and alcohol-related diseases.

The place of death was ticked on the certificate by category. Institution could mean any type of home for handicapped, elderly, or other groups of persons; most institutions were retirement homes (Table 15). While many “other cause” subjects died in a hospital (these represented mostly cancers), cardiovascular and respiratory deaths occurred more at home or in an institution. The transport deaths were too few to analyze (see Table 15). Persons with deaths due to cardiovascular and/or respiratory conditions seemed to die at an older age than other persons, who consisted largely of individuals with cancer, alcohol-related disease, or diabetes. As “institution” typically referred to a retirement home, the average age at death was higher there (Table 16).

The distribution of hour of death did not differ much by place, cause, or age at death. No particular period of the day stood out, except perhaps between 7:00 am and 10:00 am, when slightly more deaths seemed to occur than at other times. This may have been a recording bias. The data were analyzed aggregated to time series (Table 17). Figure 17 shows the time series of deaths. The effect of an influenza epidemic late in 1995 can be seen clearly as a tall spike.

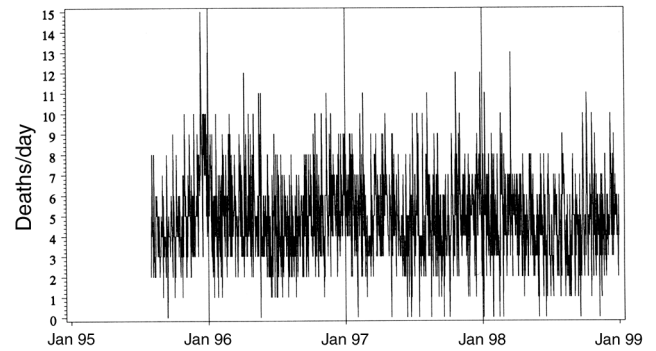
Temporal Properties of the Data The total deaths series was slightly overdispersed (1.06). We thought it likely that a model including influenza and season would correct for this completely. Only a slight day-of-week pattern was observed (Figure 18). Figure 19 displays the seasonality of the mortality data. The influenza winter 1995/1996 was excluded here, and the data set (represented by Figure 19) was restricted to the two full years from summer 1996 to summer 1998.

Table 15. Distribution of Place of Death and Cause of Death

Place of Death	Prevalent Condition		Underlying Cause of Death		Total
	Cardiovascular or Respiratory	Other	Cardiovascular or Respiratory	Other	
Hospital	75%	25%	55%	45%	2,825 (46%)
Home	83%	17%	65%	35%	2,053 (34%)
Institution	91%	9%	73%	27%	1,021 (17%)
Transport	87%	13%	69%	31%	16 (<1%)
Other	84%	16%	71%	29%	176 (3%)

Table 16. Age at Death and Cause of Natural Deaths Within Erfurt

	Mean Age \pm SD	Age Range ^a
Total	74.8 \pm 13.6	2 to 107
Prevalent Condition		
Cardiovascular or Respiratory	76.7 \pm 12.5	2 to 107
Other	66.8 \pm 15.1	2 to 100
Underlying Cause of Death		
Cardiovascular or Respiratory	77.3 \pm 12.2	2 to 107
Other	70.7 \pm 14.7	2 to 100
Place of Death		
Hospital	72.0 \pm 13.5	2 to 100
Home	74.5 \pm 13.4	14 to 107
Institution	84.6 \pm 8.0	16 to 102
Transport	73.1 \pm 10.6	53 to 87
Other	66.2 \pm 16.5	6 to 99

^a Infant deaths were excluded from data collection.**Figure 17.** Daily death counts.**Table 17.** Deaths Per Day from Natural Causes Among Erfurt Residents^a (1,249 Days; August 1995 to December 1998)

Category	Mean Deaths/Day	Variance	Overdispersion	Range
Total	4.88	5.19	1.06	0–15
Age Group (years)				
< 70	1.48	1.52	1.03	0–7
70–79	1.25	1.32	1.05	0–7
≥ 80	2.15	2.19	1.02	0–8
Prevalent Condition				
Cardiovascular or respiratory	3.95	4.06	1.03	0–13
Cardiovascular but not respiratory	2.87	2.75	0.96	0–10
Respiratory	1.08	1.18	1.09	0–7
Respiratory not cardiovascular	0.29	0.28	0.96	0–3
Respiratory and cardiovascular	0.79	0.85	1.08	0–5
Other natural condition	0.93	0.98	1.05	0–6
Underlying Cause of Death				
Cardiovascular or respiratory	3.03	3.17	1.05	0–12
Other natural	1.85	1.87	1.01	0–8

^a All died in Erfurt.

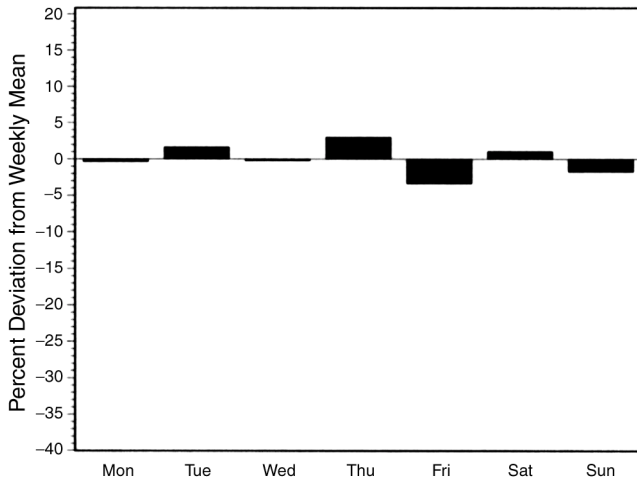


Figure 18. Weekly pattern of raw mortality.

The partial autocorrelation function had a small peak at 7 days lag, indicating a slight day-of-week pattern. However, neither the visible peak at 3 days lag nor the similar small peaks at 9 and 10 days lag were explained by this pattern. All in all, there was no distinct pattern and no strong autocorrelation (Figure 20). We felt it likely that corrections for season and day-of-week would take care of this, and no correction of the error model for dependent residuals would be needed.

Influenza Data The first Erfurt analysis (using data from 1980–1989) showed the importance of proper influenza correction in some years. A report system for influenza in eastern Germany has been discontinued, and West German influenza data has always been a problem. Fortunately, since 1992, AGI's sentinel system has provided an acceptable indicator for an influenza epidemic. The AGI

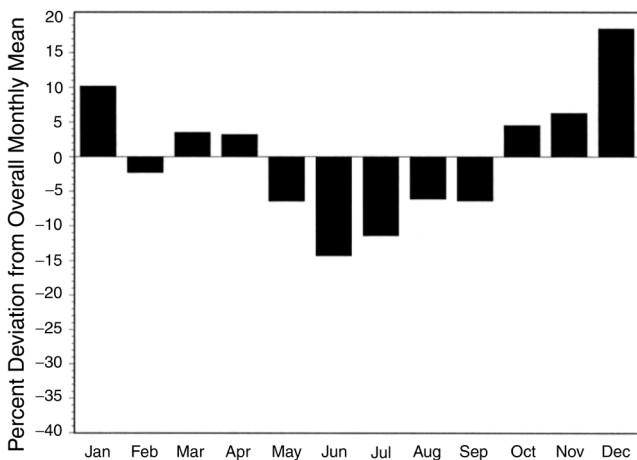


Figure 19. Monthly pattern of raw mortality (July 1996–June 1998).

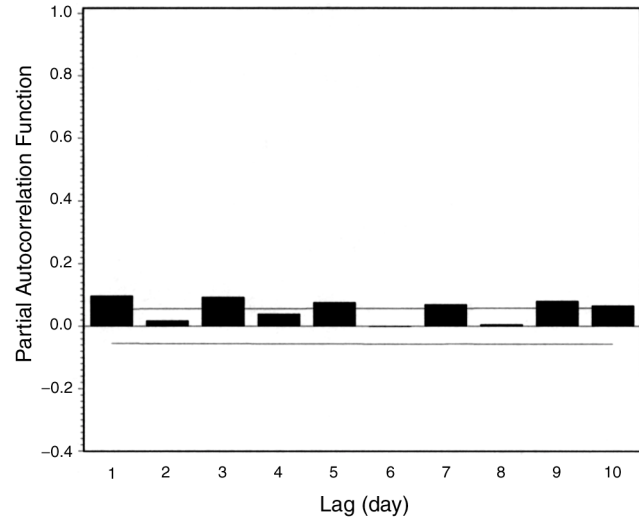


Figure 20. Partial autocorrelation function of raw mortality data. Lines indicate the 95% confidence limits.

also collects information on virus isolations from virologic laboratories from all over Germany to characterize the observed periods of epidemic activity.

As shown in Figure 21, a two-wave epidemic occurred in the winter of 1995/1996. The first wave was due to an IA (H3N2) virus. Note that the usual drop in physician visits over Christmas was not observed in 1995 because of the severity of the epidemic. The second wave, early in 1996, could mostly be attributed to an IA H1N1 virus, with some IB activity later. The IA (H1N1) virus was prevalent in Germany before 1957, so a large fraction of older persons was immune. No major epidemics occurred during the winters of 1996/1997 and 1997/1998. The increases in counts were identified as being caused mostly by less severe respiratory infections and, only to a moderate extent, to influenza infections (AGI 1996, 1997, 1998).

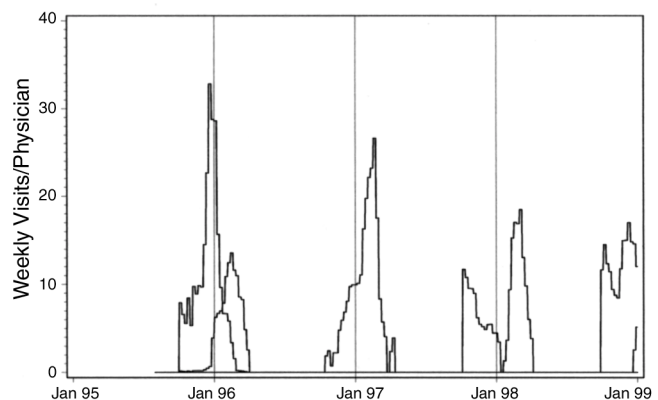


Figure 21. Time series of influenza data (from weekly numbers of physician visits for acute respiratory symptoms per physician in Germany).

Data Reliability We had no means of checking the reliability of influenza data other than judging the plausibility of the time series graph. This, however, seemed to be fine. In all years of the study except the first (1995), when a major epidemic took place over the winter, there was a considerable drop around Christmas and New Year's in subjects with acute respiratory symptoms seen by a doctor (a time when physicians and patients alike prefer to stay home). In the relevant graphs, this period was replaced with the mean of the weeks before and afterward because we did not expect a similar drop in mortality. Data for Thüringen were available but, at least for the first season, they were based on only a handful of physicians and obviously unreliable. We chose to use the all German data, which were based on a large number of reporting physicians.

Mortality data can be unreliable in two ways: they can be incomplete, and the information on individual certificates can be unreliable. We previously described the steps we took to ensure completeness. We were fairly certain that fewer than 1% of all possible cases were missing, if any were missing at all. If this dropped off toward the end of the study, the trend and season corrections should have taken care of it.

As to the certificate information, we considered day of death and date of birth as very reliable: the first would be off by at most one day (ie, for persons found dead in the morning who might have died before midnight). Place of death was also quite reliable, insofar as the place recorded was the actual place where a physician certified the death. In terms of whether this location was where the person actually died, "home" or "institution" could usually be believed, whereas some of the "hospital" deaths may actually have occurred at home or during transport. Time of death was probably unreliable. The efforts we made to assess the reliability of the cause of death information as far as possible without extraneous information are described previously. As a result, we consider the quality of this information to be acceptable, especially regarding the prevalent causes.

Summary of Mortality Data Description Because Erfurt is a relatively small city, the number of daily deaths was low. Total mortality due to natural causes was approximately 5 deaths/day. Out of these, 4 deaths/day were attributable to cardiovascular or respiratory causes. The study showed, that the information extracted from the death certificates, data necessary to identify prevalent conditions, was very important. Otherwise, one could only have used the underlying cause of death data, which were less informative for our purposes. Given information on the prevalent conditions, it was possible to consider separately

cardiovascular causes and respiratory causes as compared with other natural causes.

For mortality, no day-of-week pattern was observed. However, a clear seasonal pattern showed that the number of deaths during the winter (December to February) was approximately 20% above the number during the summer (June to August). One important factor during the winter was the occurrence of influenza epidemics, which may have had a strong influence on mortality.

REGRESSION ANALYSIS

The regression results of the relation between particles, gaseous pollutants, and total mortality are described first using the standard one-pollutant model. Then, a sensitivity analysis is described.

Total Deaths Analysis

Confounder Model Predetermined components of the confounder model were trend and season, epidemics, calendar effects (if applicable), and meteorology. The elements were usually fitted in that order. However, the effect of the 1995–1996 influenza epidemic was so clearly visible, it was obvious that the seasonal model would be distorted without taking care of the epidemic first.

The influenza data of 1995–1996 could be separated into two distinct waves (prior to any regression analysis) based on the knowledge that two different virus strains had been observed. It was also known that the first epidemic headed more or less from east to west and the second from west to east, so different shifts of physician data (Germany as a whole) against mortality data (Erfurt) were to be expected. Shifts of 3 weeks in both directions were considered. In agreement with prior knowledge, the first wave fitted best shifted by 7 days to the left with the second shifted 11 days to the right. A LOESS model was chosen for each wave because this did not make any assumptions about the shape of the dependency between case counts and mortality counts. The resulting shapes became somewhat steeper for the very high counts (that is, for the worst epidemic weeks) but they did not deviate much from a linear curve. The effect of the epidemic, especially the first wave, was considerable (Figures E.2 and E.4).

The mortality curves for the next two winters did not suggest an epidemic. The influenza data (reported as acute respiratory cases) did not fit conclusively into the mortality series, and so they were not included. (The last study winter saw a rather severe epidemic, but this started only later, in January 1999.) The least bad fits identified in those attempts were used for sensitivity analyses later. The overdispersion after this step was 1.007. The data became now

practically uncorrelated with a remaining small peak at 7 days lag (see Appendix E).

We handled season and trend by including a smoothed function of time so these two could be taken care of in one step. Using 14 *df* for a spline smoother described a shape with only 1 peak/winter and 1 valley/summer while still allowing those to differ in placement and shape each year (see Appendix E). The partial fits for season and epidemics (Figures E.2, E.4, and E.5) did not look very different from the ones done after all confounders were included. The overdispersion after this step was 0.98. This might actually indicate some slight overcorrection, but because the model was definitely not overdefined (see Figure E.2), we accepted that. We did not judge this to be seriously underdispersed. The partial autocorrelation factor pointed to the same conclusion (Appendix E). The 7-day peak was gone. Possibly the day-of-week pattern, such as there was, was only visible in winter, which would have dominated the raw data.

As mentioned before, the day-of-week pattern did not quite follow the usual shape (see Figure 18). Inclusion of indicators for each day cost more degrees of freedom than it improved model fit. Finally, a model with an indicator for “Monday–Thursday” versus “Friday–Sunday” was chosen as a compromise for not correcting for day-of-week at all, which seemed inappropriate given the rather strong day-of-week pattern in the air pollutants. The parameter was not significant, estimating the Monday–Thursday mortality at about 1.6% above that for the rest of the week. The overdispersion after this step was 0.98, and the PACF stayed practically unchanged (Appendix E).

The suggestion by Samet and colleagues (1997) to include temperature and lagged temperature jointly in the model had worked on previous preliminary analyses of Erfurt data. They were included in our model. Delayed temperature fit almost identically well whether we used the temperature of 3 days previously or the temperature mean of lags 1 to 3. The latter, because we took the mean of available data even when some were missing, allowed the use of slightly more data points, whereas the first fit slightly better. The first (ie, temperature of 3 days previously) was chosen, and the consequences were investigated in the sensitivity analysis.

The same day temperature (corrected for delayed temperature effects) had an almost linearly increasing shape, describing the immediate adverse effect of warm weather. The delayed effect mirrored this, but for cold weather. Indicator variables for unusually warm days were tried in several forms but failed to improve the model, quite likely due to the lack of an actual heat wave during the study

period. (See Figures E.7 and E.8 for the shape of the association, which was not influenced by relative humidity.)

Humidity could be included as relative humidity or dew point temperature (a function of humidity and temperature). Both were highly correlated with temperature, dew point temperature even more so, which was probably why the relative humidity fits were slightly better. It did not make much difference which delay we chose, so an (insignificant) parameter for relative humidity was left in the model for the sake of completeness and tradition. Interaction terms between temperature and humidity did not improve the model any further and were discarded.

The partial fit (after correction for all other confounders) of the 1995–1996 influenza epidemic showed that actually the LOESS fit was almost linear. The second wave of the epidemic had an effect only during its peak time, with none before or after (seen as low numbers on the x-axis). Note that the before-period for the second wave of the epidemic fell mostly during the first wave and thus was corrected. The temperature fits (partial, after correction for all other confounders) showed nicely how the immediate and the delayed effect split the cold (delayed) and the warm (immediate) short-term effects between them (Appendix E). The total fit (raw, fitted, residuals) is displayed in Figure 22. The overdispersion after this final confounder modeling step was 0.99, which was very good (close to 1.00). Note that some temperature data were missing, but this was mostly due to calibrations; concurrent MAS data were missing as well. The residual day-of-week pattern was only marginally different from the raw pattern and not very conclusive.

The PACF of the Pearson residuals after confounder correction more or less varied around 0. The AR(1) term was practically 0, and among the next lags were a few small negative ones (Appendix E). There was no indication of undercorrection. There may actually have been some

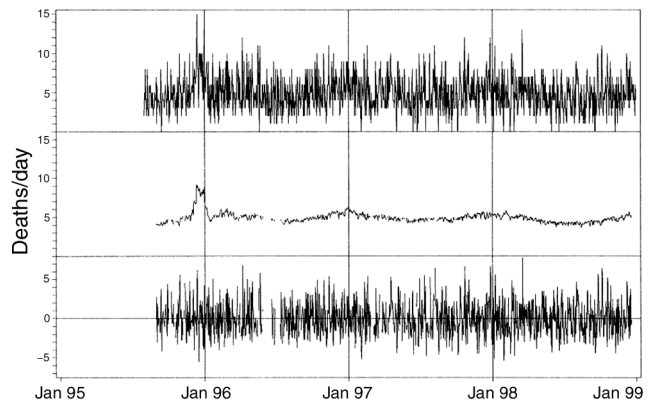


Figure 22. Mortality series after fitting the confounder model. From top to bottom: raw data, fitted data, residuals.

Table 18. Regression Results for Particle Number Concentration, Particle Mass Concentrations, and Gaseous Pollutants

	Interquartile Range (IQR)	Lag (Days)	TR	Relative Risk/IQR	CI	<i>P</i>
Particle Number Concentration (particles/cm³): Best Single-Day Lag						
NC _{0.01–0.03}	5,177–14,065	4	log	1.048	1.000–1.099	0.05
NC _{0.03–0.05}	1,603–4,127	4	id ^a	1.031	0.998–1.066	0.07
NC _{0.05–0.1}	993–2,518	1	log	1.043	0.999–1.089	0.06
NC _{0.01–0.1}	8,042–20,732	4	log	1.046	0.997–1.097	0.07
NC _{0.01–2.5}	9,659–22,928	4	log	1.041	0.991–1.093	0.11
Particle Number Concentration (particles/cm³): Polynomial Distributed Lag^d						
NC _{0.01–0.03}		0–5	id	1.030	0.997–1.065	0.06
NC _{0.03–0.05}		0–4	id	1.038	1.000–1.077	0.05
NC _{0.05–0.1}		0–5	id	1.040	0.997–1.085	0.07
NC _{0.01–0.1}		0–4	id	1.041	1.001–1.082	0.04
NC _{0.01–2.5}		0–4	id	1.036	1.003–1.069	0.03
Particle Mass Concentration (µg/m³): Best Single-Day Lag						
MC _{0.1–0.5}	9.8–25.2	0	id	1.026	0.995–1.058	0.10
MC _{0.5–1.0}	0.81–4.03	0	id	1.015	0.996–1.034	0.13
MC _{1.0–2.5}	0.56–1.55	3 ^b	id	0.977	0.954–1.001	0.06
MC _{0.01–1.0}	11.3–31.0	0	id	1.028	0.996–1.060	0.09
MC _{0.01–2.5}	12.0–31.9	0	id	1.031	1.000–1.063	0.05
Particle Mass Concentration (µg/m³): Polynomial Distributed Lag^d						
MC _{0.1–0.5}		0–5	id	1.035	0.999–1.071	0.05
MC _{0.5–1.0}		0–5	id	1.028	1.004–1.052	0.02
MC _{1.0–2.5}		0–5	log	1.048	1.011–1.087	0.01
MC _{0.01–1.0}		0–5	id	1.040	1.002–1.080	0.04
MC _{0.01–2.5}		0–5	id	1.049	1.011–1.088	0.01
Other Particle Mass (µg/m³): Best Single-Day Lag						
PM _{2.5}	13.0–31.5	3 ^c	id	0.970	0.941–1.000	0.05
PM ₁₀	19.9–47.6	0	id	1.035	1.001–1.069	0.04
TSP	28.8–61.9	1	log	1.023	0.981–1.067	0.28
Other Particle Mass (µg/m³): Polynomial Distributed Lag^d						
PM _{2.5}		0–1	id	1.022	0.988–1.058	0.20
PM ₁₀		0–4	id	1.036	1.004–1.069	0.03
TSP		0–1	log	1.022	0.965–1.083	0.46
Gaseous Pollutants: Best Single-Day Lag						
SO ₂ (µg/m ³)	5.5–19.8	0	log	1.060	1.011–1.112	0.02
NO ₂ (µg/m ³)	26.0–46.0	4	id	1.029	0.992–1.067	0.12
CO (mg/m ³)	0.3–0.8	4	log	1.055	1.003–1.110	0.04
Gaseous Pollutants: Polynomial Distributed Lag^d						
SO ₂ (µg/m ³)		0–3	log	1.074	1.022–1.129	0.01
NO ₂ (µg/m ³)		1–4	id	1.035	0.995–1.077	0.09
CO (mg/m ³)		1–4	log	1.076	1.017–1.138	0.02

^a With log transformation fit was only slightly less well: lag = 4, TR = log, RR = 1.040, CI = 0.994–1.089, *P* = 0.09.^b The second best fit was lag = 0, TR = id, RR = 1.019, CI = 0.997–1.042, *P* = 0.1.^c The second best fit was lag = 0, TR = id, RR = 1.019, CI = 0.991–1.049, *P* = 0.19.^d The weights are given in Table 20.

minor overcorrection, but as no element of the model, except for relative humidity perhaps, was redundant in a major way, this had to be accepted. There was no need to correct for residual autocorrelation in the regression.

Standard Analyses Analyses of total mortality were performed for MAS data, other particles, and gaseous pollutants. For nearly all of them we saw clear possible associations (Table 18).

MAS Data The particle numbers in the different size classes showed the strongest associations with a lag of 4 days (Tables 18 and 19). The increase of 4.6% for ultrafine particles ($NC_{0.01-0.1}$) was borderline significant by the interquartile range with no clear preference for any size class below 0.1 μm .

If one considers polynomial distributed lags, the associations were similar. Here the increase for $NC_{0.01-0.1}$ was 4.1% by the interquartile range, which is significant (Table 18).

Because the polynomial distributed lags were not available together with the GAM function in S-Plus, the modeling was done manually as previously described. The variance estimate did not account for the degrees of freedom lost by the estimation of weights used to combine the lags; thus, the *P* values and the CIs were slightly underestimated. Here the point estimates were of greater interest than the CIs.

The idea behind a distributed lag model compared with a single-day model is the assumption that the same air pollution event may cause its effect with a different delay in different individuals. Then, the true effect is evident when adding up the effects over several delays, which would then be larger than the single-day effect. This was not the case here. The reason was obvious when we looked at the weight pattern. Instead of the monotonous decrease one usually has in mind for such processes, we saw a duality. The original 4-day delay association was supplemented by a slightly smaller immediate association, while the days in between did not show an association. Note that the third-order polynomial shape was predetermined and may not quite have described distribution of the association over the lags. The implication was the duality of both an immediate and a delayed association, with the delayed one somewhat stronger in the case of ultrafine particles. Note that the weights should never be compared vertically in Table 20, only horizontally. The actual values are meaningless; only their relative relations within one model are of interest.

The results for particle mass in different size classes are also shown in Tables 18 and 19. $MC_{0.1-0.5}$ contained the majority of the mass and had an increase of 2.6% for the interquartile range on the same day. The larger masses had

no clear associations. The particles in the size range 1.0 to 2.5 μm added very little to the total mass, so $MC_{0.01-1.0}$ and $MC_{0.01-2.5}$ were almost identical. The increase for fine particles, $MC_{0.01-2.5}$, was 3.1% per interquartile range, borderline significant and slightly smaller than the increase for ultrafine particles, $NC_{0.01-0.1}$ (4.6%). The polynomial distributed lag models showed the opposite, a slightly stronger increase for $MC_{0.01-2.5}$ (4.9%) than for $NC_{0.01-0.1}$ (4.1%) per interquartile range (Table 18).

Other Particles The standard model results for impactor measurements use $PM_{2.5}$, PM_{10} , and TSP as indicators for particulate mass. They basically repeated the MAS-derived mass estimate (Tables 18 and 19). Associations were largest on the same or next day: The same-day association from the $PM_{2.5}$ impactor where filters were changed at 11:00 am instead of midnight shows the best fit, with a negative parameter after 3 days (the 3-day parameter was negative for practically all particulate indicators) and the second best on the same day. The PM_{10} parameter was just significant. Note that all these measures of particle mass were highly correlated. The polynomial distributed lag models emphasized the immediate (same-day or one-day) lag of larger particles. Overall, they showed a slightly smaller increase than $MC_{0.01-2.5}$.

Gaseous Pollutants In the standard regression results for gaseous pollutants (Table 18), a strong immediate association was found for SO_2 in contrast to NO_2 and CO, which showed delayed associations (lags of 4 days). In the polynomial distributed lag model, the associations became slightly stronger. The immediate association of SO_2 was complemented by a weaker, delayed association at 3 days lag. The strong delayed association (lag 4 days) of NO_2 and CO was accompanied by a smaller, earlier association (lag 1 day). The whole range of single-day lags between 0 and 5 days is presented in Table 19. SO_2 showed a significant immediate association. (Note that the association of SO_2 was only strong for the log transformed data—not for the untransformed data.) A second significant association of SO_2 was found at a lag of 3 days. NO_2 and CO had their strongest associations at 4 days lag.

Sensitivity Analyses, Exploratory Analyses As the sensitivity analyses were rather extensive, representatives were chosen instead of presenting analyses for all variables: ultrafine particles were investigated by their aggregated size category $NC_{0.01-0.1}$, fine particles by $MC_{0.01-2.5}$, and total mass by PM_{10} . Analyses were performed for gaseous pollutants as well. Distributed lag analysis was performed for a smaller selection of the sensitivity variations, especially those that might give more insight into the short-term temporality of associations.

Table 19. Regression Results for Total Mass and Number Concentrations and for Gaseous Pollutants: Total Mortality, All Single-Day Lags and Transformations^a

Lag (Day)	TR	RR/IQR	CI	P
NC_{0.01–0.1}				
0	id	1.022	0.982–1.065	0.22
0	log	1.019	0.969–1.072	0.30
1	id	1.003	0.966–1.042	0.39
1	log	1.026	0.979–1.075	0.22
2	id	0.984	0.946–1.022	0.28
2	log	0.994	0.948–1.042	0.39
3	id	1.009	0.970–1.050	0.36
3	log	1.021	0.973–1.071	0.28
4	id	1.035	0.995–1.077	0.10
4	log	1.046	0.997–1.097	0.07
5	id	1.005	0.967–1.044	0.39
5	log	1.012	0.967–1.059	0.35
MC_{0.01–2.5}				
0	id	1.031	1.000–1.063	0.06
0	log	1.040	0.992–1.089	0.11
1	id	1.013	0.982–1.045	0.29
1	log	1.016	0.969–1.064	0.32
2	id	1.000	0.969–1.032	0.40
2	log	0.998	0.951–1.047	0.40
3	id	0.978	0.947–1.009	0.15
3	log	0.985	0.939–1.032	0.32
4	id	1.004	0.974–1.035	0.39
4	log	1.006	0.962–1.053	0.38
5	id	1.006	0.977–1.037	0.37
5	log	1.023	0.977–1.071	0.25
PM₁₀				
0	id	1.035	1.001–1.069	0.05
0	log	1.030	0.987–1.075	0.16
1	id	1.016	0.984–1.050	0.25
1	log	1.020	0.978–1.064	0.26
2	id	0.997	0.964–1.030	0.39
2	log	0.993	0.951–1.036	0.38
3	id	0.976	0.944–1.010	0.15
3	log	0.988	0.947–1.031	0.34
4	id	1.003	0.971–1.035	0.39
4	log	1.002	0.962–1.044	0.40
5	id	0.995	0.964–1.028	0.38
5	log	1.007	0.966–1.049	0.38

*(Table continues next column)***Table 19 (continued).** Regression Results for Total Mass and Number Concentrations and for Gaseous Pollutants: Total Mortality, All Single-Day Lags and Transformations^a

Lag (Day)	TR	RR/IQR	CI	P
SO₂ (µg/m³)				
0	id	1.020	0.994–1.046	0.13
0	log	1.060	1.011–1.112	0.02
1	id	0.993	0.967–1.019	0.35
1	log	1.019	0.974–1.067	0.29
2	id	1.020	0.994–1.047	0.13
2	log	1.019	0.973–1.068	0.29
3	id	1.008	0.982–1.034	0.33
3	log	1.049	1.002–1.098	0.05
4	id	1.000	0.975–1.025	0.40
4	log	1.000	0.956–1.046	0.40
5	id	1.016	0.991–1.042	0.18
5	log	1.038	0.992–1.086	0.11
NO₂ (µg/m³)				
0	id	1.003	0.965–1.043	0.39
0	log	0.989	0.951–1.029	0.35
1	id	1.015	0.977–1.054	0.30
1	log	1.020	0.982–1.059	0.24
2	id	1.004	0.966–1.044	0.39
2	log	1.002	0.963–1.042	0.40
3	id	1.015	0.977–1.054	0.30
3	log	1.012	0.974–1.052	0.33
4	id	1.029	0.992–1.067	0.12
4	log	1.020	0.983–1.059	0.23
5	id	1.005	0.969–1.041	0.39
5	log	1.012	0.976–1.050	0.33
CO (mg/m³)				
0	id	1.012	0.977–1.049	0.31
0	log	1.016	0.962–1.073	0.34
1	id	1.004	0.969–1.040	0.39
1	log	1.027	0.973–1.083	0.25
2	id	1.020	0.984–1.057	0.22
2	log	1.024	0.970–1.081	0.28
3	id	1.019	0.984–1.055	0.23
3	log	1.037	0.984–1.093	0.16
4	id	1.029	0.995–1.063	0.10
4	log	1.055	1.003–1.110	0.04
5	id	0.997	0.965–1.031	0.39
5	log	1.014	0.966–1.065	0.34

^a For interquartile ranges see Table 18.

Table 20. Weights for Distributed Polynomial Lag Models in Table 18^a

Pollutants	Lag 0	Lag 1	Lag 2	Lag 3	Lag 4	Lag 5
Particle Number Concentration						
NC _{0.01–0.03}	1.35	–0.78	–0.90	–0.03	0.80	0.56
NC _{0.03–0.05}	0.14	0.42	–0.13	–0.35	0.92	
NC _{0.05–0.1}	0.39	0.16	0.05	0.03	0.11	0.26
NC _{0.01–0.1}	0.44	0.07	–0.33	–0.19	1.02	
NC _{0.01–2.5}	2.56	–0.69	–2.08	–1.19	2.50	
Particle Mass Concentration						
MC _{0.1–0.5}	0.56	0.37	–0.02	–0.30	–0.20	0.59
MC _{0.5–1.0}	0.57	0.39	–0.10	–0.48	–0.29	0.91
MC _{1.0–2.5}	0.45	2.29	0.12	–2.67	–2.68	3.49
MC _{0.01–1.0}	0.72	0.24	–0.13	–0.29	–0.10	0.55
MC _{0.01–2.5}	0.72	0.20	–0.17	–0.30	–0.07	0.62
Other Particle Mass						
PM _{2.5}	0.16	0.84				
PM ₁₀	3.66	1.53	–1.60	–2.93	0.12	
TSP	–0.08	1.08				
Gaseous Pollutants						
SO ₂	0.82	–0.02	–0.17	0.37		
NO ₂		0.48	–0.19	–0.09	0.80	
CO		0.19	–0.10	0.10	0.81	

^a Data are included here only if the corresponding lag was used in the model.

Parametric Fits Compared with Nonparametric Fits The following plots each showed the best single-day parametric fit of some selected pollutants together with the corresponding LOESS fit. In the areas of low data density (low or high pollution levels, but especially high pollution levels), agreement was quite naturally not as good as indicated by considerably widening CIs of the LOESS fit. As long as the models did not disagree too much in the inner part, the parametric model was a good representation of the overall dose response curve. The parametric curve should not be extrapolated to those upper levels, and the LOESS curve should never be interpreted without its CI.

Figure 23 shows the fit for ultrafine particles. The relative increase from the 25th to the 75th percentile was slightly larger based on the LOESS model, but the flattening of the association above this range was also more pronounced. It was obvious why a log-transformed model fits better than an untransformed one for this variable. The curious drop of the curve happened above the 95th percentile, and any other behavior of the curve after this point would also fit between the CI borders. The LOESS curve did actually seem to indicate the presence of a threshold up to about 15,000 particles/cm³. It was very difficult to verify such an impression as this happened at a level where the signal-to-noise ratio in the data was unfavorable.

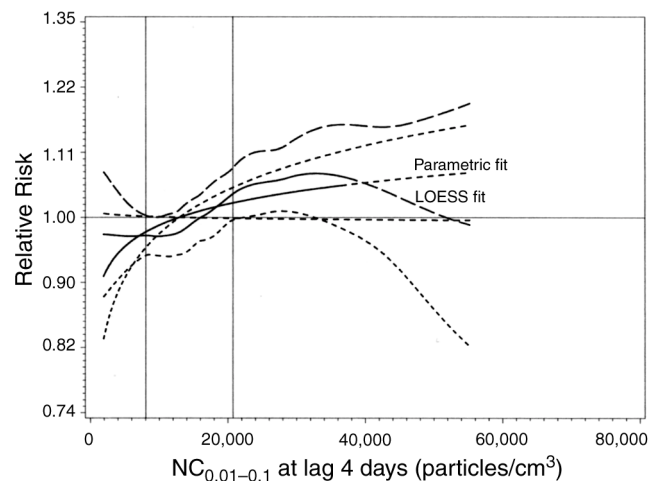


Figure 23. Dose response curves of NC_{0.01–0.1} with parametric fit and non-parametric fit overlaid. Partial fit (corrected for confounders) for NC_{0.01–0.1}. The log-shaped curve is the parametric fit. The more bent curve is a LOESS fit with span = 0.7. Both curves are dotted beyond the 95th percentile. The four outer dashed lines are the respective 95% confidence limits. The y-axis leads to the sum of all effects across the pollution range being zero. For the parametric fit, this implies that it crosses the null line (RR = 1.00) at about the mean of the pollution. The two vertical lines include the interquartile range.

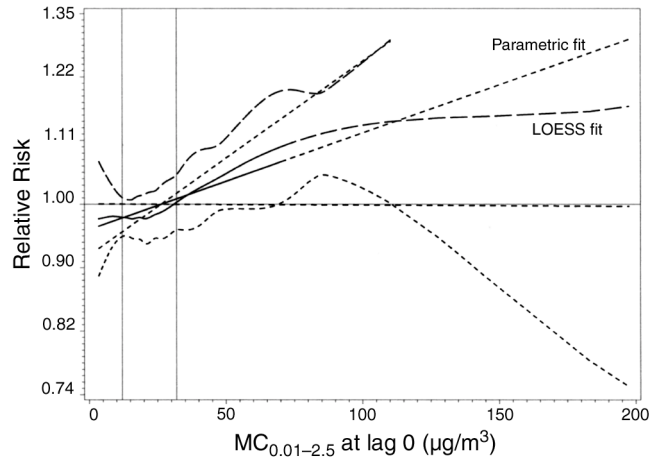


Figure 24. Dose response curves of $MC_{0.01-2.5}$ with parametric fit and nonparametric fit overlaid. Partial fit (corrected for confounders) for $MC_{0.01-2.5}$. The straight line is the parametric fit. The more bent curve is a LOESS fit with span = 0.7. Both curves are dotted beyond the 95th percentile. The four outer dashed lines are the respective 95% confidence limits. The y-axis leads to the sum of all effects across the pollution range being zero. For the parametric fit, this implies that it crosses the null line ($RR = 1.00$) at about the mean of the pollution. The two vertical lines include the interquartile range.

Figure 24 shows the corresponding fit for $MC_{0.01-2.5}$. Here, the parametric fit should definitely not be extrapolated much beyond the 95th percentile (roughly $70 \mu\text{g}/\text{m}^3$) because this would be extremely misleading. Note that the skewness of the data led to the inner 50% of the data being found in a very narrow range. Again, there may have been a threshold below approximately roughly $25 \mu\text{g}/\text{m}^3$, although this interpretation is problematic given the CIs.

The parametric and nonparametric fits for PM_{10} are given in Figure 25. The ongoing steep relation beyond the 95th percentile (roughly $100 \mu\text{g}/\text{m}^3$) was hard to believe, but it has been observed in other studies (see Schwartz 1994a). Note, however, how wide the CI became after that point: The curve might take any shape there. One might see a threshold at about 20 to $30 \mu\text{g}/\text{m}^3$, but again the CIs would need to be considered.

The dose response curves for SO_2 showed good agreement between the nonparametric fit and the parametric fit below the 95th percentile (Figure 26). The skew of the distribution made the 75th percentile correspond to a very low value in the range of values. Why the logarithmic transformation fit so much better than the untransformed curve was clearly visible: The dose-response curve is very steep below roughly $15 \mu\text{g}/\text{m}^3$ and much flatter above that point. In fact, most of the association leading to the relatively large relative risk was seen below $15 \mu\text{g}/\text{m}^3$.

The fits for NO_2 are shown in Figure 27. The nonparametric dose response curve suggested the possibility of a

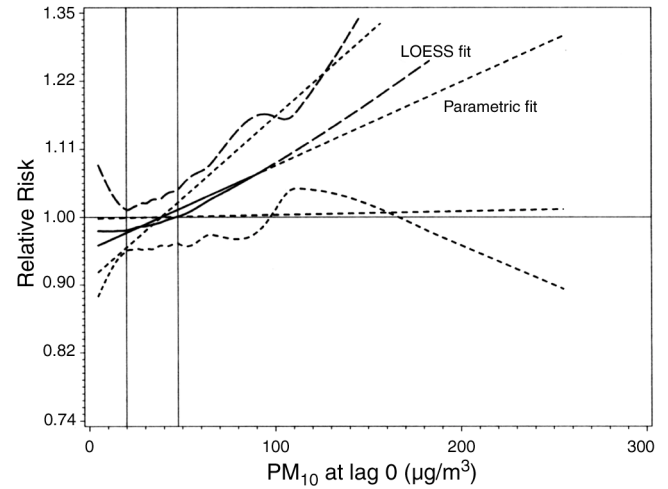


Figure 25. Dose response curves of PM_{10} with parametric fit and nonparametric fit overlaid. Partial fit (corrected for confounders) for PM_{10} . The straight line is the parametric fit. The more bent curve is a LOESS fit with span = 0.7. Both curves are dotted beyond the 95th percentile. The four outer dashed lines are the respective 95% confidence limits. The y-axis leads to the sum of all effects across the pollution range being zero. For the parametric fit, this implies that it crosses the null line ($RR = 1.00$) at about the mean of the pollution. The two vertical lines include the interquartile range.

threshold below the range of 35 to $40 \mu\text{g}/\text{m}^3$. There was no strong flattening of the relation as the level got higher, which was adequately described by the parametric fit (using untransformed data). However, the highest levels

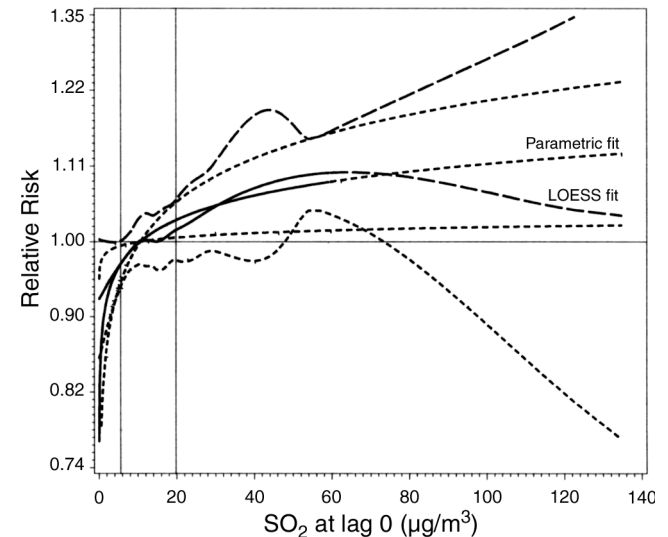


Figure 26. Dose response curves of SO_2 with parametric fit and nonparametric fit overlaid. Partial fit (corrected for confounders) for SO_2 . The log-shaped curve is the parametric fit. The more bent curve is a LOESS fit with span = 0.7. Both curves are dotted beyond the 95th percentile. The four outer dashed lines are the respective 95% confidence limits. The y-axis leads to the sum of all effects across the pollution range being zero. For the parametric fit, this implies that it crosses the null line ($RR = 1.00$) at about the mean of the pollution. The two vertical lines include the interquartile range.

were not very high in absolute terms, and what happened beyond this point was unknown.

Finally, Figure 28 shows the dose response curves for CO. The parametric fit was in rather good agreement with the nonparametric fit until about the 95th percentile; after this point, no additional association was seen. The later decline of the curve should be evaluated in light of the very wide CI. No threshold was indicated.

Sensitivity Against Variations of Confounder Model We checked a large number of deviations from the standard confounder model. The day-of-week pattern found in the data did not follow the usual shape, most likely because Erfurt is small and the pattern was overlaid by randomness. We chose a standard model setting off Monday–Thursday from Friday–Sunday. Inclusion of day-of-week indicators changed the association very little. If there were any changes at all, they mostly became slightly larger. There was no indication of results being spurious due to unaccounted day-of-week patterns (see Table 21).

When building the confounder model, there was a choice between a model where the delayed effect of cold weather might be fitted by temperature with a 3-day lag or by the mean of days 1 to 3. Although the latter version reduced the loss of data, the former fit slightly better. The question arose, Would it change the conclusions preferring one lag over the other? There was no indication of a bias in a specific direction by this change in the meteorology cor-

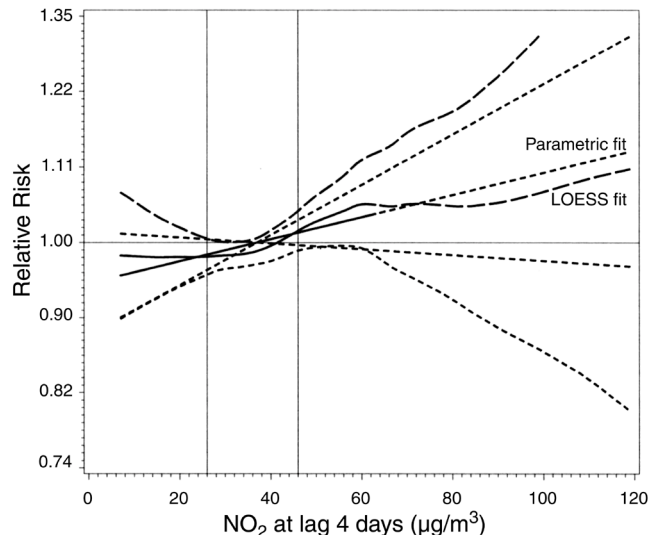


Figure 27. Dose response curves of NO₂ with parametric fit and nonparametric fit overlaid. Partial fit (corrected for confounders) for NO₂. The straight line is the parametric fit. The more bent curve is a LOESS fit with span = 0.7. Both curves are dotted beyond the 95th percentile. The four outer dashed lines are the respective 95% confidence limits. The y-axis leads to the sum of all effects across the pollution range being zero. For the parametric fit, this implies that it crosses the null line (RR = 1.00) at about the mean of the pollution. The two vertical lines include the interquartile range.

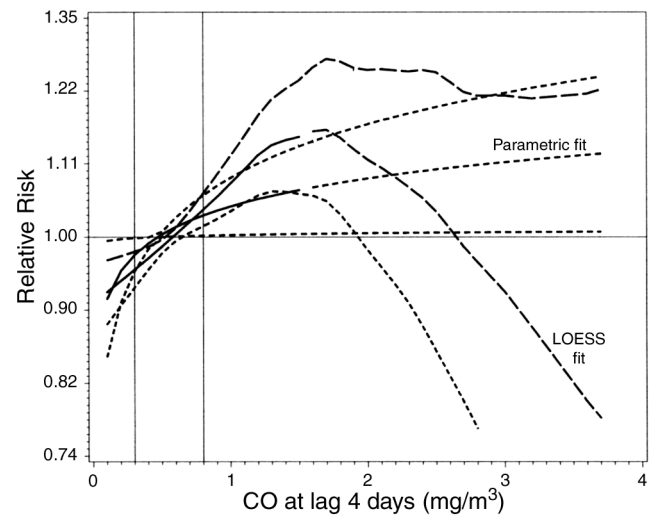


Figure 28. Dose response curves of CO with parametric fit and nonparametric fit overlaid. Partial fit (corrected for confounders) for CO. The log-shaped curve is the parametric fit. The more bent curve is a LOESS fit with span = 0.7. Both curves are dotted beyond the 95th percentile. The four outer dashed lines are the respective 95% confidence limits. The y-axis leads to the sum of all effects across the pollution range being zero. For the parametric fit, this implies that it crosses the null line (RR = 1.00) at about the mean of the pollution. The two vertical lines include the interquartile range.

rection. Because of different missing value patterns, the data basis for this model (mean of lags 1 to 3 days) was slightly different from the basis for the alternative model (see Table 21).

There have been suggestions that including influenza epidemics in the model might present an overcorrection, especially because they tended to appear concurrently with high pollution levels in winter. In the standard model, we corrected for the two-wave epidemic in the first winter (1995–1996). Table 21 includes results if the model had left out the influenza epidemic. Note that some of the influenza effect was picked up by the seasonality term, but it was too smooth to correct for all of it. Almost all air pollution variables, especially the mass indicators, were reduced in a major way. It is not quite clear why there was such a strong deviation in that direction, but certainly we were not overcorrecting by including the epidemic data in the model.

The seasonality smooth for the standard model was deliberately chosen to be rather smooth (eg, 14 *df* in 3.5 years), so that it picked up only season and not any additional, shorter patterns. Other researchers have chosen to fit a seasonal curve with many more ripples, with the effect of correcting for patterns that make up only a few weeks. This approach is intended to correct for epidemics too, when no extraneous data are available. To check how much effect this would have, we allowed the seasonal smooth to have

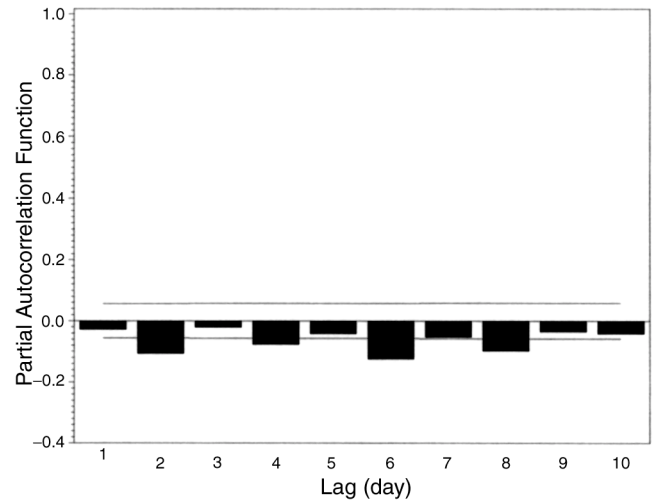
Table 21. Regression Results for Different Confounder Models^a

	Lag	TR	RR	CI	P	Change
Day-of-Week Indicators for Each Day						
NC _{0.01-0.1} (particles/cm ³)	4	log	1.049	0.997–1.104	0.06	>
MC _{0.01-2.5} (µg/m ³)	0	id	1.034	1.003–1.067	0.03	>
PM ₁₀ (µg/m ³)	0	id	1.036	1.003–1.071	0.03	–
SO ₂ (µg/m ³)	0	log	1.065	1.015–1.117	0.01	–
NO ₂ (µg/m ³)	4	id	1.036	0.995–1.078	0.09	–
CO (mg/m ³)	4	log	1.058	1.005–1.113	0.04	–
Temperature Mean of Lags 1 to 3						
NC _{0.01-0.1} (particles/cm ³)	4	log	1.045	0.997–1.095	0.07	–
MC _{0.01-2.5} (µg/m ³)	0	id	1.028	0.997–1.059	0.08	<
PM ₁₀ (µg/m ³)	0	id	1.035	1.002–1.069	0.04	–
SO ₂ (µg/m ³)	0	log	1.052	1.004–1.103	0.04	<
NO ₂ (µg/m ³)	4	id	1.034	0.997–1.073	0.08	–
CO (mg/m ³)	4	log	1.062	1.011–1.115	0.02	–
Leaving Out Influenza Models						
NC _{0.01-0.1} (particles/cm ³)	4	log	1.041	0.992–1.092	0.11	<
MC _{0.01-2.5} (µg/m ³)	0	id	1.017	0.986–1.048	0.29	<<
PM ₁₀ (µg/m ³)	0	id	1.016	0.984–1.050	0.32	<<
SO ₂ (µg/m ³)	0	log	1.054	1.005–1.106	0.04	<
NO ₂ (µg/m ³)	4	id	1.021	0.985–1.059	0.21	<<
CO (mg/m ³)	4	log	1.037	0.987–1.091	0.14	<<
Seasonality with Many More Degrees of Freedom						
NC _{0.01-0.1} (particles/cm ³)	4	log	1.044	0.995–1.095	0.08	<
MC _{0.01-2.5} (µg/m ³)	0	id	1.031	1.000–1.063	0.05	–
PM ₁₀ (µg/m ³)	0	id	1.039	1.006–1.073	0.02	>>
SO ₂ (µg/m ³)	0	log	1.064	1.015–1.116	0.01	–
NO ₂ (µg/m ³)	4	id	1.036	0.995–1.078	0.07	–
CO (mg/m ³)	4	log	1.056	1.004–1.111	0.04	–

^a For interquartile ranges, see Table 18.

45 *df*. We considered this an overcorrection. The overdispersion after this step was 0.98, and we had expected it to decrease more. The PACF confirmed the assumption of severe overcorrection because at least the first ten lags were consistently below zero (Figure 29). The fitted curve with this heavy overcorrection for season, and much shorter temporal patterns in the data, had remarkably little influence on the associations, except for that of PM₁₀, which actually increased (Figure 30; Table 21).

Results by Season and Study Winters In performing the analysis, we wanted to know if certain groups of days drove the overall observed association. If so, and if we could identify such groups of days, we could investigate whether the differences were in the population or the pollution mix of those days. Table 22 shows the results when the question was addressed for the seasons. For NC_{0.01-0.1}, MC_{0.01-2.5},

**Figure 29.** Partial autocorrelation function of mortality Pearson residuals after overfitting season. Horizontal lines indicate 95% confidence limits.

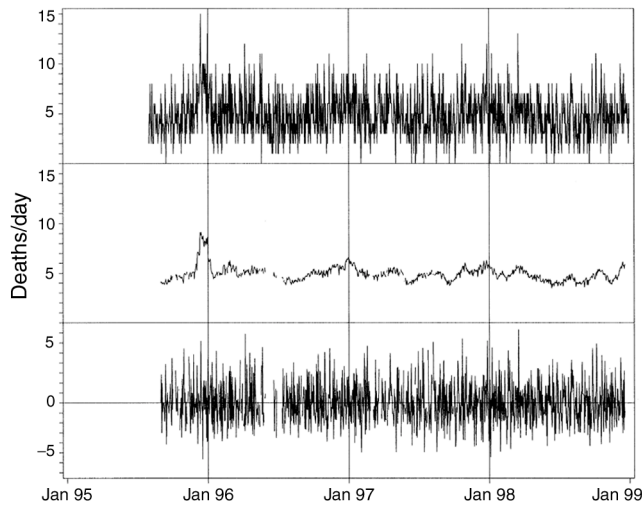


Figure 30. Mortality after overfitting seasonality correction. From top to bottom: raw data, fitted data, residuals.

Table 22. Regression Results for Effects by Season^{a,b}

Component by Season ^c	Lag	TR	RR/IQR	CI	P
NC_{0.01-0.1} (particles/cm³): Best Single-Day Lag					
Winter (22,211)	4	log	1.050	1.001–1.101	0.05
Spring (15,175)	4	log	1.049	0.999–1.101	0.05
Summer (10,218)	4	log	1.036	0.986–1.088	0.16
Fall (15,262)	4	log	1.043	0.993–1.095	0.09
NC_{0.01-0.1} (particles/cm³): Polynomial Distributed Lag^d					
Winter	0–4	id	1.048	1.002–1.097	0.05
Spring	0–4	id	1.052	0.992–1.114	0.09
Summer	0–4	id	0.927	0.836–1.029	0.14
Fall	0–4	id	1.059	1.011–1.110	0.02
MC_{0.01-2.5} (µg/m³): Best Single-Day Lag					
Winter (40.4)	0	id	1.035	1.000–1.071	0.05
Spring (25.7)	0	id	1.008	0.960–1.059	0.72
Summer (15.3)	0	id	0.974	0.879–1.081	0.62
Fall (22.7)	0	id	1.044	0.994–1.095	0.08
MC_{0.01-2.5} (µg/m³): Polynomial Distributed Lag^d					
Winter	0–5	id	1.067	1.022–1.114	0.00
Spring	0–5	id	1.038	0.985–1.093	0.15
Summer	0–5	id	0.965	0.858–1.085	0.33
Fall	0–5	id	1.071	1.014–1.131	0.02
PM₁₀ (µg/m³): Best Single-Day Lag					
Winter (51.4)	0	id	1.057	1.017–1.099	0.01
Spring (40.0)	0	id	1.025	0.979–1.073	0.30
Summer (28.2)	0	id	0.925	0.849–1.009	0.08
Fall (34.3)	0	id	1.022	0.973–1.074	0.39

Table continues next column

PM₁₀, SO₂, and NO₂ the association was always weakest or not observable at all in summer (when pollution levels were low); the association was strongest in winter, and occasionally also strong in fall or spring. CO was an exception: it showed the strongest association in summer and fall.

The difference in the timing of associations had 4 possible causes:

1. The risk groups were different. This seems unlikely. If excess risk was confined to those who would have lived only a few days longer if unexposed, we would have expected smaller associations in winter or spring.
2. The pollution mixes that the measurements represented were different. This was quite possible. In winter, a larger fraction of air pollution would be due to home heating than in summer, and there were bound to be other differences, too.
3. There was an effect of errors in variables. Because the pollutant levels were different in different seasons, the signal-to-noise ratio (ie, measurement error, measurement accuracy) was less favorable in summer compared with the ratio in winter, which biased the association downward in summer.

Table 22 (continued).

Component by Season ^b	Lag	TR	RR/IQR	CI	P
PM₁₀ (µg/m³): Polynomial Distributed Lag^d					
Winter	0–4	id	1.048	0.995–1.104	0.08
Spring	0–4	id	1.043	0.984–1.106	0.14
Summer	0–4	id	0.977	0.866–1.103	0.37
Fall	0–4	id	1.037	0.983–1.094	0.17
SO₂ (µg/m³): Best Single-Day Lag					
Winter (29.9)	0	log	1.074	1.016–1.135	0.02
Spring (13.7)	0	log	1.072	1.011–1.136	0.03
Summer (9.3)	0	log	0.994	0.931–1.062	0.39
Fall (13.9)	0	log	1.057	1.002–1.115	0.05
NO₂ (µg/m³): Best Single-Day Lag					
Winter (44.1)	4	id	1.040	0.999–1.083	0.07
Spring (33.4)	4	id	1.029	0.978–1.083	0.22
Summer (28.5)	4	id	0.996	0.930–1.068	0.40
Fall (39.3)	4	id	1.020	0.976–1.067	0.27
CO (mg/m³): Best Single-Day Lag					
Winter (1.0)	4	log	1.002	0.922–1.088	0.40
Spring (0.5)	4	log	1.019	0.942–1.102	0.36
Summer (0.3)	4	log	1.085	1.018–1.156	0.02
Fall (0.6)	4	log	1.111	1.039–1.188	0.00

^a Winter: Dec–Feb; Spring: Mar–May; Summer: Jun–Aug; Fall: Sep–Nov.

^b Interquartile ranges see Table 18.

Table 23. Effects by Study Winters Based on Mean of All Winters

Component ^a	Interquartile Range	Lag	TR	RR/IQR	CI	P
NC_{0.01-0.1} (particles/cm³): Best Single-Day Lag^b						
10/95–3/96 (23,453)	10,593–27,311	4	log	1.041	0.984–1.100	0.16
10/96–3/97 (16,308)	10,593–27,311	4	log	1.044	0.993–1.098	0.09
10/97–3/98 (19,193)	10,593–27,311	4	log	1.050	1.000–1.102	0.05
NC_{0.01-0.1} (particles/cm³): Polynomial Distributed Lag^c						
10/95–3/96		0–4	id	0.988	0.908–1.076	0.38
10/96–3/97		0–4	id	1.100	1.007–1.202	0.04
10/97–3/98		0–4	id	1.104	1.033–1.179	0.01
MC_{0.01-2.5} (µg/m³): Best Single-Day Lag						
10/95–3/96 (47.3)	15.0–45.7	0	id	1.021	0.956–1.091	0.53
10/96–3/97 (29.7)	15.0–45.7	0	id	1.070	0.988–1.160	0.10
10/97–3/98 (27.7)	15.0–45.7	0	id	1.086	0.994–1.186	0.07
MC_{0.01-2.5} (µg/m³): Polynomial Distributed Lag^c						
10/95–3/96		0–5	id	1.042	0.952–1.141	0.27
10/96–3/97		0–5	id	1.091	0.994–1.120	0.28
10/97–3/98		0–5	id	1.186	1.065–1.321	0.00
PM₁₀ (µg/m³): Best Single-Day Lag						
10/95–3/96 (65.7)	19.8–59.1	0	id	1.034	0.958–1.116	0.39
10/96–3/97 (45.3)	19.8–59.1	0	id	1.063	0.994–1.138	0.08
10/97–3/98 (31.6)	19.8–59.1	0	id	1.025	0.933–1.126	0.61
PM₁₀ (µg/m³): Polynomial Distributed Lag^c						
10/95–3/96		0–4	id	1.073	0.977–1.178	0.13
10/96–3/97		0–4	id	1.026	0.946–1.114	0.33
10/97–3/98		0–4	id	1.003	0.909–1.106	0.40
SO₂ (µg/m³): Best Single-Day Lag						
10/95–3/96 (37.8)	7.4–25.5	0	log	1.037	0.942–1.141	0.30
10/96–3/97 (24.0)	7.4–25.5	0	log	1.077	1.016–1.141	0.02
10/97–3/98 (11.7)	7.4–25.5	0	log	1.059	1.000–1.122	0.06
NO₂ (µg/m³): Best Single-Day Lag						
10/95–3/96 (42.8)	31–51	4	id	1.057	0.976–1.145	0.16
10/96–3/97 (46.1)	31–51	4	id	1.052	1.006–1.101	0.03
10/97–3/98 (38.7)	31–51	4	id	1.027	0.976–1.080	0.24
CO (mg/m³): Best Single-Day Lag						
10/95–3/96 (1.1)	0.5–1	4	log	1.046	0.949–1.153	0.26
10/96–3/97 (0.9)	0.5–1	4	log	1.091	0.998–1.193	0.06
10/97–3/98 (0.6)	0.5–1	4	log	1.028	0.966–1.095	0.27

^a The number in parentheses is the mean pollution level for the winter (October–March).

^b The smallest size fraction NC_{0.01-0.03} contributed 64% to NC_{0.01-0.1} (UP) in 10/95–3/96, 61% in 10/96–3/97, and 68% in 10/97–3/98 which corresponds to 15,010, 9,948 and 13,051 particles/cm³.

^c The weights are approximately the same as in Table 20.

4. There was a threshold of the association, and more days in summer were below this threshold than in the other seasons, especially winter. The existence of a threshold is hard to prove. The possibility of its existence was at least hinted in the nonparametric fits, so this might have contributed to the other explanations.

The next analysis looked for time trends over the study period (Table 23). The relation among $NC_{0.01-0.1}$, $MC_{0.01-2.5}$, gaseous pollutants, and mortality shifted over the three study winters. We included an interaction in the model with a factor that had the following levels: All April–September periods, October 1995–March 1996, October 1996–March 1997, October 1997–March 1998, and October 1998–December 1998. We report the slopes for the middle three levels (eg, the three fully observed study winters).

With the exception of PM_{10} , all parameters indicated that the association was weakest in the first winter. This may have been due to the influenza epidemic of the first winter, which coincided more or less with high air pollution episodes and left little visible association to other influences. Among the pollutants, ultrafine and fine particles especially had larger associations in the second and third winters. It did not make a difference for this gradient when we omitted the first winter influenza correction.

Two-Pollutant Models When the results for the best single-day lag were compared (see Tables 18 and 19), SO_2 , $MC_{0.01-2.5}$, and PM_{10} had immediate associations, whereas $NC_{0.01-0.1}$, NO_2 , and CO had delayed associations. SO_2 had the strongest immediate association, and CO had the strongest delayed association. Furthermore, SO_2 had the strongest overall association. If one considered distributed lag models (see Table 18), comparable results were found as for the best single-day lag models. We then investigated whether two-pollutant models could give further insight about the relative importance of the individual pollutants.

The results of two-pollutant models without interaction are shown in Table 24 along with the comparable results for the standard one-pollutant models. In the one-pollutant models, SO_2 , $MC_{0.01-2.5}$, and PM_{10} showed immediate associations with lag 0 (ie, without delay) and $NC_{0.01-0.1}$, NO_2 , and CO showed delayed associations (lag 4 days) on mortality. When SO_2 and the particle masses were considered in parallel in the two-pollutant models, the association of SO_2 was stronger, and when $NC_{0.01-0.1}$ was compared with NO_2 and CO, $NC_{0.01-0.1}$ was stronger. If $NC_{0.01-0.1}$ was compared with SO_2 and $MC_{0.01-2.5}$, the association of SO_2 was bigger and of $MC_{0.01-2.5}$ smaller than the association of $NC_{0.01-0.1}$.

For results of two-pollutant models with interaction and associations without delay (lag 0), SO_2 , $MC_{0.01-2.5}$, and PM_{10} had to be compared. Table 25 shows this comparison. First, the association of SO_2 was calculated for the interquartile range (25th to 75th percentile) while $MC_{0.01-2.5}$ was kept low (at the 25th percentile). This led to $RR = 1.078$. Then the opposite was considered: the association of $MC_{0.01-2.5}$ for the interquartile range while SO_2 was kept low (at the 25th percentile). This led to $RR = 1.016$. Finally, the simultaneous association of SO_2 and $MC_{0.01-2.5}$ for their interquartile ranges was calculated (noted as “both” in Table 25). The result was $RR = 1.095$. This result was interpreted in the following manner. When SO_2 and $MC_{0.01-2.5}$ were analyzed in a two-pollutant model with interaction, SO_2 showed a strong association, $MC_{0.01-2.5}$ had a weak association, and the combined association was higher than the individual associations. When we considered SO_2 and PM_{10} in the same model, a clear association of SO_2 was apparent and no association of PM_{10} was found, and the combined relative risk was larger than the individual relative risks.

The same consideration was possible for delayed associations. In this setting, $NC_{0.01-0.1}$, NO_2 , and CO had to be compared. If $NC_{0.01-0.1}$ and NO_2 were in the same model, the $NC_{0.01-0.1}$ showed an association, but NO_2 showed no association. Similarly, when $NC_{0.01-0.1}$ and CO were compared, there was a small effect of $NC_{0.01-0.1}$, no association of CO, and a strong interaction. This suggested that ultrafine particles, represented by $NC_{0.01-0.1}$, was more relevant for delayed effects than NO_2 and CO.

Immediate and delayed associations were considered simultaneously for SO_2 and $NC_{0.01-0.1}$ and for $MC_{0.01-2.5}$ and $NC_{0.01-0.1}$. For these analyses, clear and strong interactions were found. The combined relative risk was higher than the individual relative risks. These findings suggest that the immediate and delayed associations were independent from each other and that the risk was enhanced if both associations occurred at the same time.

Although these considerations look quite suggestive, one has to keep in mind that the findings nevertheless might be spurious. The reason for this caveat is that the power of the study might be too small for a thorough analysis using two-pollutant models.

Summarizing Size-Specific Associations A method analogous to distributed lags can be used to sum the association of all sizes of particles. This analysis was very exploratory and descriptive in nature. Not only the total association, but also the weights of the different size fractions, were of interest. It was necessary to keep in mind that the general shape of the weight curve was given. Thus, the weights at the respective ends should not be overinterpreted. For up

Table 24. Standard One-Pollutant and Two-Pollutant Models Without Interaction for Best Single-Day Lags^a

	Lag	TR	RR/IQR	CI	P	Change ^b
One-Pollutant Model						
NC _{0.01–0.1} (particles/cm ³)	4	log	1.046	0.997–1.097	0.07	
MC _{0.01–2.5} (µg/m ³)	0	id	1.031	1.000–1.063	0.05	
PM ₁₀ (µg/m ³)	0	id	1.035	1.001–1.069	0.04	
SO ₂ (µg/m ³)	0	log	1.060	1.011–1.112	0.04	
NO ₂ (µg/m ³)	4	id	1.029	0.992–1.067	0.12	
CO (mg/m ³)	4	log	1.055	1.003–1.110	0.04	
Two-Pollutant Model Without Interaction						
SO ₂ (µg/m ³)	0	log	1.078	1.014–1.147	0.02	>>
MC _{0.01–2.5} (µg/m ³)	0	id	1.016	0.982–1.052	0.25	<<
SO ₂ (µg/m ³)	0	log	1.052	0.995–1.112	0.08	<
PM ₁₀ (µg/m ³)	0	id	1.023	0.986–1.061	0.20	<<
SO ₂ (µg/m ³)	0	log	1.064	1.013–1.118	0.02	>
NC _{0.01–0.1} (particles/cm ³)	4	log	1.045	0.996–1.097	0.07	–
NC _{0.01–0.1} (particles/cm ³)	4	log	1.039	0.986–1.094	0.14	<
MC _{0.01–2.5} (µg/m ³)	0	id	1.034	1.000–1.068	0.05	–
NC _{0.01–0.1} (particles/cm ³)	4	log	1.040	0.984–1.100	0.15	<
NO ₂ (µg/m ³)	4	id	1.007	0.963–1.054	0.38	<<
NC _{0.01–0.1} (particles/cm ³)	4	log	1.034	0.978–1.093	0.20	<<
CO (mg/m ³)	4	log	1.031	0.970–1.095	0.25	<<

^a For interquartile range (IQR), see Table 18.^b Compared to one-pollutant model.

to 3 lags we used a cubic polynomial, for 2 lags a quadratic one, and for 1 lag a linear one.

Several versions were tested with numbers for the three size categories from 0.01 to 0.1 µm and with masses for 0.1 to 2.5 µm. Each was tested with raw data and with log transformed data, with the transformation applied to all sizes. Here, the log transformed data always fitted better. This may have occurred because of the variance-stabilizing nature of log transformation and because the ranges of the independent variables became less dissimilar. Another possibility was that the numbers in the small particle sizes, whose associations were larger than those of the mass measures, generally fit better with a log transformation. The results are shown in Table 26.

The comments for the *P* values of distributed lags applied here similarly. The pattern that emerged was one of more or less equal importance of lagged associations below 0.05 µm and of immediate associations at 0.05 to 0.5 µm, with no additional contribution from particles

above 0.5 µm. Note that only 0.1% of the count and less than 20% of the mass were found above 0.5 µm in size.

Summing the associations over the particle sizes, with each size class given its preferred lag, showed two things: First, after taking into account associations from all smaller sizes, there was no more association observable for particles with diameter above 0.5 µm. Secondly, although highly correlated, the particle classes below 0.5 µm did not only act as proxies for each other. In combination, they had a stronger association than each of them had alone.

Subgroup Analyses

The working hypothesis was that some subgroups of the population may be more sensitive toward air pollution and that effects would be more strongly visible in those subgroups: Older persons and persons with cardiovascular or respiratory diseases may have been such subgroups. Also, we wanted to see if the difference in sensitivity differed by particle size classes and whether there may be indications of different mechanisms.

Table 25. Two-Pollutant Models with Interaction

	Lag	TR	RR/IQR ^{b,c}
Immediate Effects Only (Lag 0)			
SO ₂ (µg/m ³) at MC _{0.01–2.5} low ^a	0	log	1.078
MC _{0.01–2.5} (µg/m ³) at SO ₂ low	0	id	1.016
both			1.095
SO ₂ (µg/m ³) at PM ₁₀ low	0	log	1.051
PM ₁₀ (µg/m ³) at SO ₂ low	0	id	0.994
both			1.068
Delayed Effects Only (Lag 4)			
NC _{0.01–0.1} (particles/cm ³) at NO ₂ low	4	log	1.028
NO ₂ (µg/m ³) at NC _{0.01–0.1} low	4	id	0.980
both			1.040
NC _{0.01–0.1} (particles/cm ³) at CO low	4	log	1.017
CO (mg/m ³) at NC _{0.01–0.1} low	4	log	1.006
both			1.060
Immediate and Delayed Effects (Lag 0, Lag 4)			
SO ₂ (µg/m ³) at NC _{0.01–0.1} low	0	log	1.047
NC _{0.01–0.1} (particles/cm ³) at SO ₂ low	4	log	1.031
both			1.109
MC _{0.01–2.5} (µg/m ³) at NC _{0.01–0.1} low	0	id	1.069
NC _{0.01–0.1} (particles/cm ³) at MC _{0.01–2.5} low	4	log	1.071
both			1.101

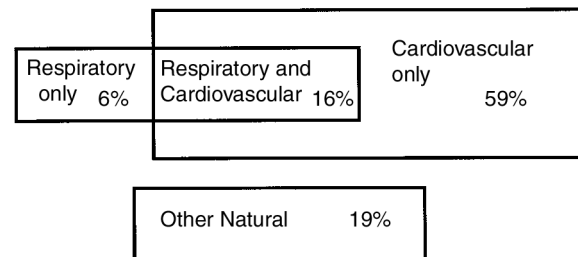
^a The second pollutant is kept low (at the 25th percentile).

^b No confidence interval is given because the covariance could not be obtained.

^c For interquartile range (IQR), see Table 18.

We considered both subgroups by age and prevalent diseases. Subgroups were defined in Methods (see Selection of Subgroups for Analysis). Results for underlying disease are presented in Appendix F. The possible additional subgroups “respiratory but not cardiovascular” and “respiratory and cardiovascular” were too small for meaningful analysis, as demonstrated in Figure 31 and Table 27.

Confounder Modeling As a basis, we used the confounder model determined from the total deaths time series. Major deviations of the elements of this model were not planned to be tested. However, we considered that the relation of one of the predetermined model elements and mortality might differ in the subgroups if there were different parameter estimates between the subgroups. To retain the maximum stability of the confounder model, we used identical confounder correction across subgroups unless the interaction with the subgroup indicator increased the model fit more than the cost in degrees of freedom (ie, improved AIC). Although this procedure increased the stability of the model, especially for small subgroups, it could lead to rather inappropriate confounder models, especially for small subgroups. We resolved

**Figure 31.** Distribution of prevalent diseases.**Table 26.** Accumulation of Effects Over All Size Ranges

NC _{0.01–0.03}	NC _{0.03–0.05}	NC _{0.05–0.1}	MC _{0.1–0.5}	MC _{0.5–1.0}	MC _{1.0–2.5}	Lag	TR	RR/IQR ^a	CI	P
1	0	0	0	0	0	4	log	1.048	1.000–1.099	0.05
0	1	0	0	0	0	4	log ^a	1.040	0.994–1.089	0.09
0	0	1	0	0	0	1	log	1.043	0.999–1.089	0.06
0	0	0	1	0	0	0	id	1.026	0.995–1.058	0.10
0	0	0	0	1	0	0	id	1.015	0.996–1.034	0.13
0	0	0	0	0	1	0 ^b	id	1.019	0.997–1.042	0.10
0.76	0.24	0	0	0	0	4,4	log	1.051	1.001–1.103	0.04
0.13	0.25	0.61	0	0	0	4,4,1	log	1.074	1.020–1.131	0.01
0.36	0.15	0.32	0.16	0	0	4,4,1,0	log	1.086	1.028–1.147	0.00
0.22	0.22	0.32	0.31	–0.06	0	4,4,1,0,0	log	1.086	1.025–1.150	0.01
0.14	0.32	0.34	0.25	0.08	–0.13	4,4,1,0,0,0	log	1.088	1.024–1.155	0.01

^a For interquartile ranges (IQR), see Table 18.

^b These are the respective second best fitting transformation-delay combinations as indicated in Table 17. They fit better into the pattern. The overall conclusions are not affected by this choice.

Table 27. Overview of Subgroups for Analysis

Subgroup	Deaths/Day	% of Total
Age		
<70 Years	1.5	30
70–79 Years	1.3	26
≥80 Years	2.2	44
Prevalent Condition		
Cardiovascular or Respiratory	4.0	81
Cardiovascular Only	2.9	59
Respiratory	1.1	22
Other Natural	0.9	19
Total	4.9	100

this conflict by allowing each subgroup different parameters in the context of the sensitivity analysis.

When modeling by age groups, the subgroup parameters differed only for the trend and season correction. This was then considered the standard subgroup model for this aggregation. When modeling by two prevalent disease categories, the model was improved by differing parameters for the day-of-week and for the seasonal pattern. Differing parameters for influenza epidemics and meteorology almost improved the model, so we expected at least some difference between the associations given in the standard and extended confounder models. When prevalent disease categories were split further, only the differing treatment of the first influenza epidemic improved the fit. When modeling by underlying cause categories, only the parameters for the first influenza epidemic were clearly different between the groups but no other confounder model elements.

Standard Analyses for Selected Pollutants The lags of the standard single-day lag models were chosen based on the total deaths analysis. There was no difference between the age at death groups for $MC_{0.01-2.5}$ and PM_{10} . For $NC_{0.01-0.1}$, the younger subjects (age at death up to 70 years) seemed to be more affected. If polynomial distributed lag models were considered for particle number and mass, the strongest association was observed in the youngest age group (see Table 28).

Table 29 presents the results for deaths in four categories of prevalent disease (cardiovascular or respiratory, cardiovascular but not respiratory, respiratory, and other natural deaths). In the single-day lag models, $NC_{0.01-0.1}$ showed delayed associations, and $MC_{0.01-2.5}$ and PM_{10} showed immediate associations, and these were strongest for cardiovascular and/or respiratory diseases. The “other natural” disease group does not show a clear association

Table 28. Regression Results by Age (years) at Death

	Lag	TR	RR/IQR ^a	CI	P
$NC_{0.01-0.1}$ (particles/cm³): Best Single-Day Lag					
<70	4	log	1.070	0.989–1.158	0.09
70–79			1.037	0.953–1.129	0.39
≥80			1.034	0.967–1.105	0.33
$NC_{0.01-0.1}$ (particles/cm³): Polynomial Distributed Lag^b					
<70	0–4	log	1.106	1.025–1.194	0.01
70–79	0–4	log	1.041	0.958–1.131	0.25
≥80	0–4	log	1.037	0.973–1.105	0.22
$MC_{0.01-2.5}$ (μg/m³): Best Single-Day Lag					
<70	0	id	1.034	0.984–1.086	0.19
70–79			1.038	0.984–1.094	0.17
≥80			1.024	0.982–1.068	0.27
$MC_{0.01-2.5}$ (μg/m³): Polynomial Distributed Lag^b					
<70	0–5	id	1.075	1.013–1.141	0.02
70–79	0–5	id	1.030	0.964–1.100	0.27
≥80	0–5	id	1.057	1.005–1.112	0.04
PM_{10} (μg/m³): Best Single-Day Lag					
<70	0	id	1.033	0.978–1.092	0.24
70–79			1.038	0.978–1.102	0.22
≥80			1.033	0.986–1.082	0.17
PM_{10} (μg/m³): Polynomial Distributed Lag					
<70	0–4	id	1.078	1.018–1.136	0.01
70–79	0–4	id	1.058	0.996–1.124	0.08
≥80	0–4	id	1.004	0.959–1.053	0.39

^a For interquartile ranges (IQR), see Table 18.

^b The weights are approximately the same as in Table 20.

for either of these pollutants. In the polynomial distributed lag models, it was especially clear that “respiratory” diseases were more strongly affected than “cardiovascular but not respiratory” diseases. Categorization by underlying causes of death did not lead to notable differences between the cause groups (see Appendix F). Clearly, the categorization by prevalent diseases provided more information.

Sensitivity Analyses As shown in Appendix F, alternatively different confounder models per subgroup were allowed, which may be more appropriate—especially for small subgroups—but are less stable. For regression by age, differing confounder models did not change the results (Table F.1 versus Table 28): The larger effect of $NC_{0.01-0.1}$ on the youngest group was still there although somewhat attenuated. Under differing confounder models, the associations for prevalent diseases were confirmed and become even clearer (Table F.2).

Table 29. Regression Results by Prevalent Disease

Disease Group	Lag	TR	RR/IQR ^a	CI	P
NC_{0.01–0.1} (particles/cm³): Best Single-Day Lag					
Cardiovascular or Respiratory ^b	4	log	1.055	1.001–1.111	0.04
Cardiovascular but Not Respiratory			1.051	0.990–1.115	0.10
Respiratory			1.048	0.956–1.149	0.31
Other Natural			1.029	0.932–1.136	0.57
NC_{0.01–0.1} (particles/cm³): Polynomial Distributed Lag^c					
Cardiovascular or Respiratory ^b	0–4	log	1.063	1.013–1.116	0.02
Cardiovascular but Not Respiratory	0–4	log	1.058	1.001–1.119	0.05
Respiratory	0–4	log	1.083	0.994–1.180	0.07
Other Natural	0–4	log	1.030	0.938–1.130	0.33
MC_{0.01–2.5} (µg/m³): Best Single-Day Lag					
Cardiovascular or Respiratory ^b	0	id	1.033	0.999–1.068	0.05
Cardiovascular but Not Respiratory			1.007	0.969–1.047	0.72
Respiratory			1.098	1.040–1.160	0.00
Other Natural			1.019	0.955–1.087	0.57
MC_{0.01–2.5} (µg/m³): Polynomial Distributed Lag^c					
Cardiovascular or Respiratory ^b	0–4	id	1.047	1.014–1.081	0.01
Cardiovascular but Not Respiratory	0–5	id	1.051	1.004–1.099	0.04
Respiratory	0–5	id	1.098	1.029–1.172	0.01
Other Natural	0–5	id	1.029	0.957–1.106	0.30
PM₁₀ (µg/m³): Best Single-Day Lag					
Cardiovascular or Respiratory ^b	0	id	1.036	1.001–1.074	0.05
Cardiovascular but Not Respiratory			1.022	0.981–1.065	0.29
Respiratory			1.083	1.017–1.152	0.01
Other Natural			1.016	0.946–1.090	0.67
PM₁₀ (µg/m³): Polynomial Distributed Lag					
Cardiovascular or Respiratory ^b	0–4	id	1.042	1.007–1.079	0.03
Cardiovascular but Not Respiratory	0–4	id	1.038	0.998–1.081	0.07
Respiratory	0–4	id	1.062	0.997–1.133	0.07
Other Natural	0–4	id	1.016	0.947–1.090	0.36

^a For interquartile ranges (IQR), see Table 18.^b Results were obtained on the basis of a slightly different confounder model.^c The weights are approximately the same as in Table 20.

The observation of different patterns seen under particle class, delay, and disease group is summarized in a different way in Table 30: The “cardiovascular but not respiratory” group mainly showed delayed associations (4-day lag, 0–4 days, or 5-day lag, 0–5 days). On the other hand, the respiratory group showed immediate associations (lag 0 or 1 day) which were stronger than delayed associations (4-day or 5-day lag) or distributed lags (0–4 days or 0–5 days).

SUMMARY OF THE REGRESSION RESULTS

Particles

In the following, the most important results are summarized. Only size classes that gave a relevant contribution to particle number (three size classes below 0.1 µm) or particle mass (three size classes above 0.1 µm) are considered.

For the best single-day lag model, the association of the smaller size fractions was more pronounced compared with that for the larger size fractions (Figure 32), but this was not seen for distributed lags (Figure 33). The associations of

Table 30. Regression Results by Cardiovascular and Respiratory Diseases Under Respective Best Immediate (0 or 1 Day) or Delayed (4 or 5 Days) Model per Disease Group.^a

	Lag	TR	RR/IQR	CI	P
Cardiovascular (But Not Respiratory)^b					
NC _{0.01–0.1} (particles/cm ³)	0	id	1.004	0.955–1.056	0.43
	4	log	1.051	0.990–1.115	0.10
	0–4	log	1.058	1.001–1.119	0.05
MC _{0.01–2.5} (µg/m ³)	0	id	1.007	0.969–1.047	0.72
	5	log	1.037	0.978–1.099	0.22
	0–5	id	1.051	1.004–1.099	0.04
PM ₁₀ (µg/m ³)	0	id	1.022	0.981–1.065	0.29
	5	log	0.992	0.941–1.046	0.76
	0–4	id	1.038	0.998–1.081	0.07
Respiratory^b					
NC _{0.01–0.1} (particles/cm ³)	1	log	1.155	1.055–1.264	0.00
	4	log	1.048 ^c	0.956–1.149	0.31
	0–4	log	1.083	0.994–1.180	0.07
MC _{0.01–2.5} (µg/m ³)	0	id	1.098	1.040–1.160	0.00
	5	log	1.030	0.940–1.130	0.52
	0–5	id	1.098	1.029–1.172	0.01
PM ₁₀ (µg/m ³)	0	id	1.083	1.017–1.152	0.01
	5	log	1.041	0.956–1.134	0.35
	0–4	id	1.062	0.997–1.133	0.07

^a The effect sizes are based on models in which all subgroups were forced to have the same delay.

^b For interquartile ranges (IQR), see Table 18.

^c This effect went away when confounder models were different per subgroup.

particle number were usually delayed by 4 days, and the associations of mass indicators were immediate if single-day lags were considered. However, the distributed lags showed comparable relative risks. The difference in strength of association among NC_{0.01–0.1}, MC_{0.01–2.5}, and PM₁₀ was only slight as indicated by the wide overlap of the CIs.

The associations of combining particle number and mass are shown in Figure 34: The combination of number and mass led to a clearly higher total relative risk, almost 1.09. If the combination was built such that the contribution of the different size fractions was in increasing sequence, up to 0.5 µm in each additional size fraction led to a larger total association. Larger particle sizes (> 0.5 µm) did not contribute.

The associations of the particles varied by season. During summer, the associations were weaker compared with the other seasons of the year (Figure 35). Between age categories, the strongest association seems to occur in the youngest age group (below 70 years), especially if distributed lags are considered (Figure 36).

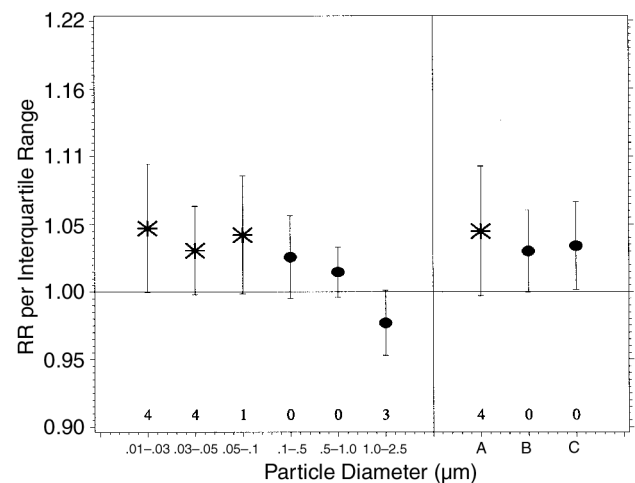


Figure 32. Standard best single-day regression results. The stars (particle number) or dots (particle mass) give the relative risk per interquartile range; the lines denote the 95% CI. In the bottom, the lag (days) is given above the abscissa. Below the abscissa are the size ranges. For NC_{0.03–0.05}, the log transformed model yielded a slightly larger effect with a slightly worse fit. For MC_{0.1–2.5}, choosing lag 0, which fits better into the pattern, yields a small, positive, nonsignificant effect (see Table 16). A = NC_{0.01–0.1}, B = MC_{0.01–2.5}, C = PM₁₀.

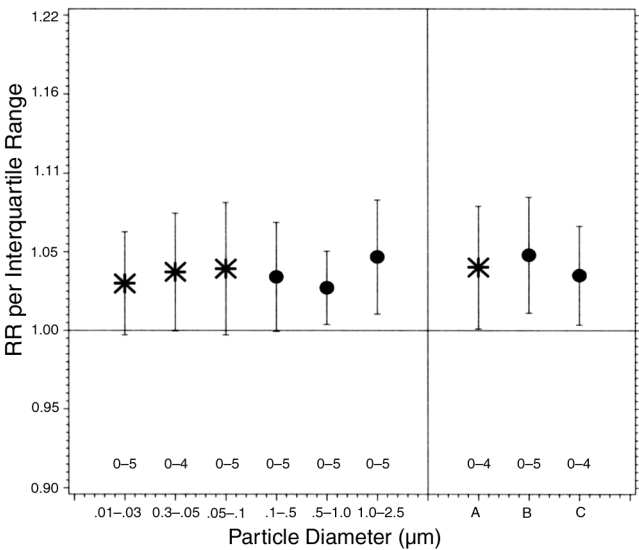


Figure 33. Polynomial distributed lag, regression results. The stars (particle number) or dots (particle mass) give the relative risk per interquartile range; lines denote the 95% CI. In the bottom, above the abscissa, is the delay range (days). Below the abscissa are the size ranges. A = $NC_{0.01-0.1}$, B = $MC_{0.01-2.5}$, C = PM_{10} .

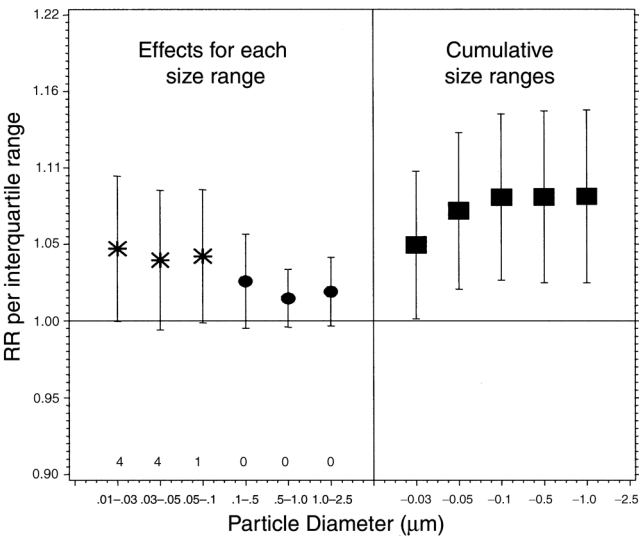


Figure 34. Combining single-day effects across particle sizes. The stars (particle number), dots (particle mass), or rectangles (cumulative effects) give the relative risk per interquartile range; the lines denote the 95% CI. In the bottom, above the abscissa, are the delays (days). Below the abscissa are the size ranges. On the left side are the second best fitting effects for 0.05–0.1 and 1.0–2.5 μg chosen because they fit better into the pattern (see also Table 32 and text).

Regarding the prevalent disease subgroups, comparison of the standard analyses and the sensitivity analyses showed that there might be differences with respect to the associations for the different subgroups. There seemed to be the strongest association in respiratory subjects by all size particles, whereas cardiovascular subjects were less affected and “other natural causes” showed the weakest effects (Figure 37). Cardiovascular subjects (cardiovascular but no respiratory disease) were the largest subgroup (2.9 deaths/day), whereas respiratory subjects were a small subgroup (1.1 deaths/day). Roughly 73% of the respiratory subjects also had cardiovascular disease. When one considered the

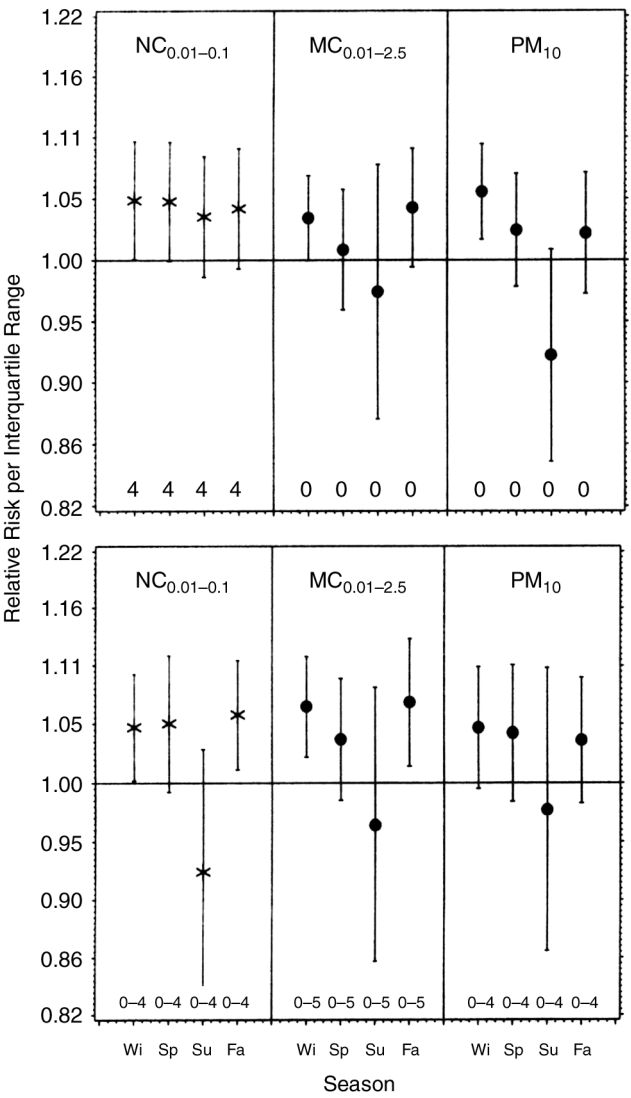


Figure 35. Regression results by season for best single-day (top) and polynomial distributed models (bottom). The stars (particle number) and dots (particle mass) give the relative risk per interquartile range. The lines denote the respective 95% CI. Above the abscissa are the delays (days). Abbreviations: Wi, winter; Sp, spring; Su, summer; Fa, fall.

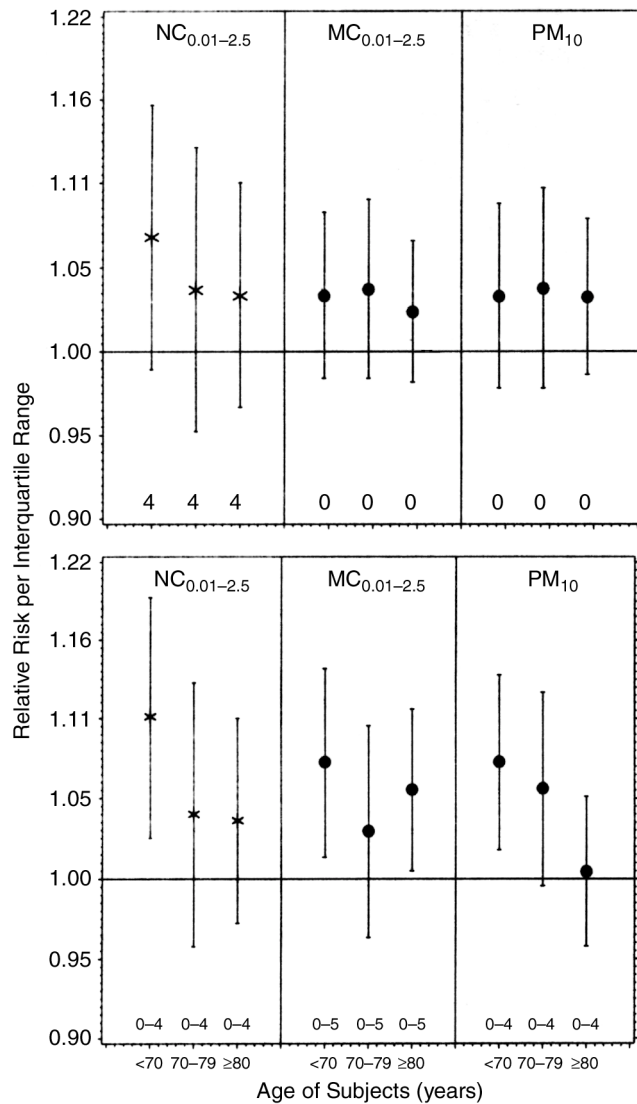


Figure 36. Regression results by age for best single-day (top) and polynomial distributed models (bottom). The stars (particle number) or dots (particle mass) give the relative risk per interquartile range. The lines denote the respective 95% CI. On top the pollution variable is given. Below the abscissa are the subgroups (age at death).

cardiovascular and respiratory subjects separately and in detail with respect to delay, persons with cardiovascular disease but not respiratory disease showed mainly delayed associations, but persons with (additional) respiratory disease showed strong or immediate associations (Figure 38).

Gaseous Pollutants

In the best single-day lag models, SO_2 showed a same-day association as did $\text{MC}_{0.01-2.5}$ and PM_{10} . In contrast, NO_2 and CO showed associations after a 4-day lag similar to the pattern for $\text{NC}_{0.01-0.1}$. When gases and particles

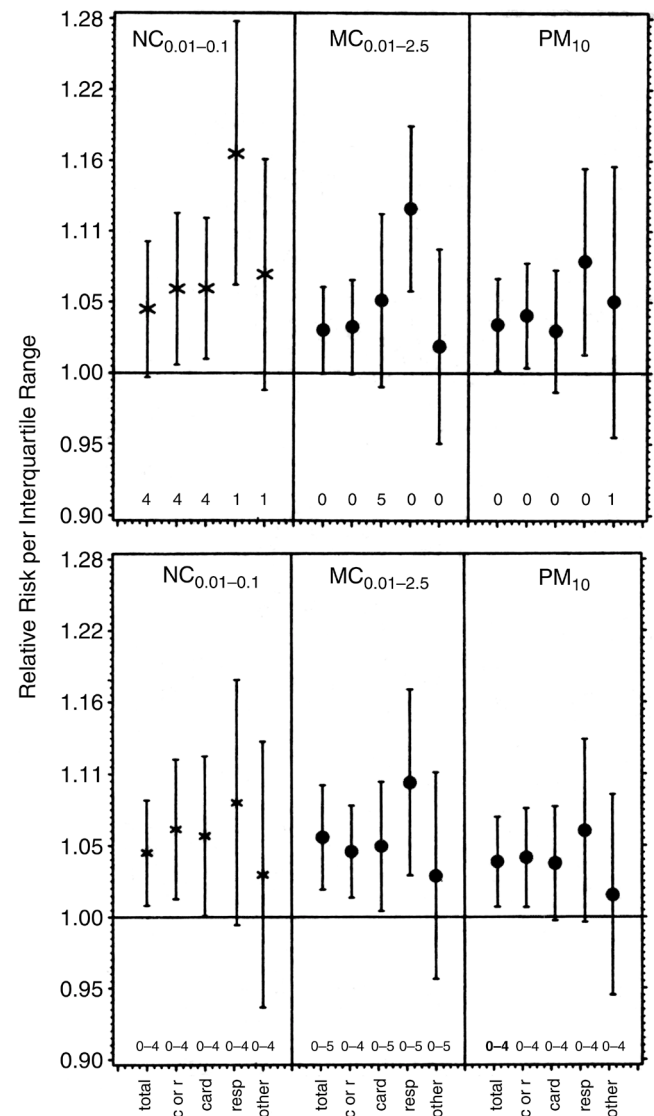


Figure 37. Regression results by disease group (prevalent diseases) for best single-day (top) and polynomial distributed models (bottom). The stars (particle number) or dots (particle mass) give the relative risk per interquartile range; the lines denote the 95% CI. In the bottom, above the abscissa, are the delays. On top are the pollution variables. Below the abscissa the subgroups are indicated: total, all natural cases; c or r, cardiovascular or respiratory; card, cardiovascular only; resp, respiratory; other, other natural causes. Note that the “c or r” results were obtained on the basis of a slightly different confounder model.

were compared, the immediate association was strongest for SO_2 , whereas the delayed association was strongest for $\text{NC}_{0.01-0.1}$. This finding was irrespective of the two-pollutant model used (Tables 24 and 25). Furthermore, the immediate and the delayed associations seemed to be independent of each other. This is also found in the model summing associations over all size ranges in which the delayed (ultrafine particles) and immediate (fine particles)

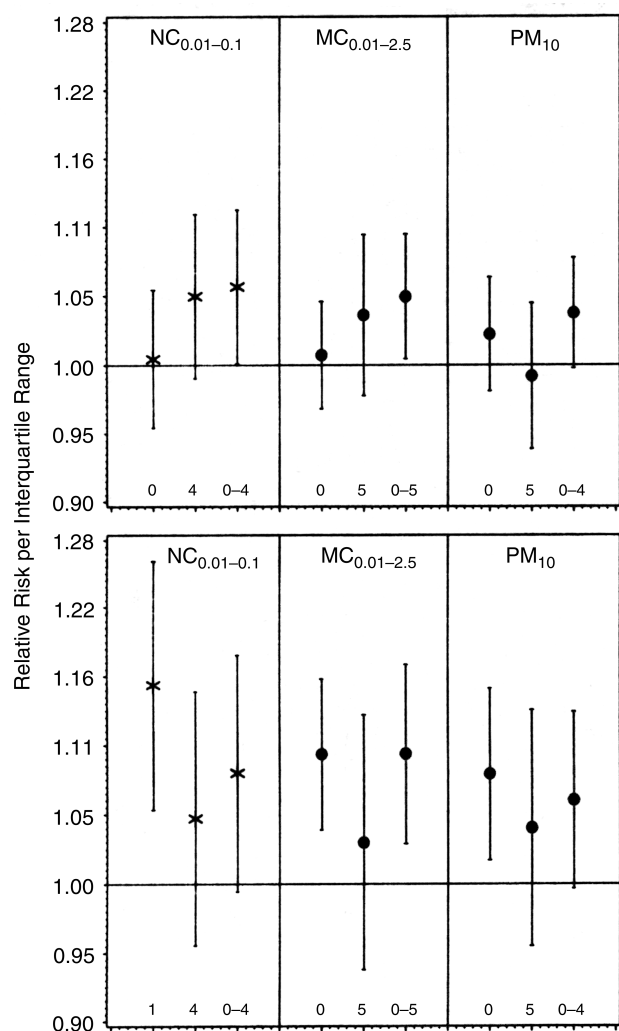


Figure 38. Regression results by prevalent diseases and delay. (Top) cardiovascular deaths only; (bottom) respiratory deaths. The stars (particle number) and dots (particle mass) give the relative risk per interquartile range. The lines denote the respective 95% CI. Numbers above the abscissa indicate the delay (days).

associations together were stronger than each alone (see Figure 34).

The surprisingly strong association of SO_2 needs further analysis. Firstly, it is remarkable that in contrast to all other variables the difference in strength of association between the log transformed dose response curve and the untransformed curve for SO_2 was rather large (Table 19). This corresponded with the fact that the smoothed dose response curve showed most of the association at the left end, below $15 \mu\text{g}/\text{m}^3$, a level at which effects were considered biologically implausible (see Figure 26). SO_2 is discussed below in the contexts of historical data from Erfurt and of source apportionment in Part II of this report.

DISCUSSION AND SYNTHESIS

AMBIENT AIR POLLUTION IN ERFURT

Most particles in ambient air were found to be ultrafine particles (diameters smaller than $0.1 \mu\text{m}$, 88% of all particles below $2.5 \mu\text{m}$). The largest mass fraction was made up of fine particles in the size range 0.1 to $0.5 \mu\text{m}$, namely, 78% of the mass of particles below $2.5 \mu\text{m}$. The low correlation between fine particle mass and ultrafine particle number showed that it was not possible to obtain information on the particle number from conventional mass-based air pollution parameters.

The MAS instrumentation was successfully deployed in a 40-month measuring campaign (September 1995 to December 1998) without significant losses in data acquisition time. It reliably recorded spectral number distributions at 6-minute cycle times. It needs to be noted that intensive maintenance was necessary to operate the MAS for this long time period. The sizing capabilities of the MAS were tested several times during the study. These intercomparisons (see Appendix G for details) showed good sizing stability of the instrument. Both testable endpoints of the size distribution, the daily average total particle number (obtained by CPC) and the daily average mass concentration of fine particles ($\text{PM}_{2.5}$ from the impactor) were highly correlated with MAS-derived parameters, which indicated that instrument function was stable throughout the study.

The time series of particle number and mass obtained during this study showed a clear seasonal pattern. All particulate air pollution concentration parameters were higher during winters than during summers. This seasonality was primarily driven by domestic heating habits induced by low temperatures and high relative humidity during the winter. The frequent occurrence of temperature inversions over the city in winter enhanced this seasonal effect. There was virtually no domestic air conditioning in Erfurt during summer due to moderate temperatures.

The pronounced day-of-week pattern of ultrafine particle number pointed to automobile traffic as the major source. Ultrafine particle concentrations were high from Monday through Friday (on Friday, it decreased) and low on the weekends. Because there was little long-range ultrafine particle transport due to rather fast coagulation kinetics of ultrafine particles in the atmosphere, these particles appeared to originate from local sources. There was no major industrial production in Erfurt with lower emissions on weekends, and domestic heating habits would (if at all) have increased emissions on weekends. Therefore, the day-of-week ultrafine particle pattern could not be

attributed to these sources. On the other hand, there was significantly less car and truck traffic on weekends (with most truck traffic even prohibited on Sundays by law). Furthermore, the day-of-week pattern did not look different when corrected for seasonality. This finding pointed to the same source because use of cars and trucks in Erfurt was almost unaffected by season. Consequently, automobile sources could be identified as the major source of ambient ultrafine particles causing the day-of-week pattern.

The day-of-week pattern of a representative measure of fine particle mass ($MC_{0.01-2.5}$) was different from that for ultrafine particles. Particles with diameters larger than $0.1\ \mu\text{m}$ are more persistent in the atmosphere. Therefore, these particles were subject to long-range transport to and from Erfurt. Long-range transport of aerosol particles should not have exhibited a very distinct day-of-week pattern because aerosol transport would have blurred any pattern of release from the source. Examination of the remaining day-of-week pattern showed that measures were higher than average from Tuesday to Friday, and lower than average on the weekend and on Monday. This delay represented the time constants of aerosol dynamics in removing ultrafine particles by coagulation and of the air chemistry for particles 0.1 to $0.5\ \mu\text{m}$ in size, which contributed most to $MC_{0.01-2.5}$. The pattern did not look different after correction for seasonality. It could therefore be assumed that the day-of-week $MC_{0.01-2.5}$ pattern reflected the influence of locally coagulated ultrafine particles from automobile sources on Erfurt's ambient aerosol mass.

In the 1980s, the concentrations of ambient SO_2 and TSP in Erfurt were extremely high (average SO_2 in 1980, $456\ \mu\text{g}/\text{m}^3$; average TSP in 1989, $119\ \mu\text{g}/\text{m}^3$; see Figure 42; Spix et al 1993a; Wichmann and Heinrich 1995; Wichmann et al 2000). After German reunification in 1990, levels of ambient SO_2 and TSP declined drastically (to average SO_2 of $6\ \mu\text{g}/\text{m}^3$ and average TSP of $44\ \mu\text{g}/\text{m}^3$ in 1998; see Figure 42; Brauer et al 1995; Cyrus et al 1995; Wichmann et al 2000) due to industrial breakdown and reduction in emissions of SO_2 and TSP caused by the replacement of sulfur-rich surface coal as a fuel. Comparing MAS-derived data at the same location from October 1991 to March 1992 (Tuch et al 1997a) with data for the average of the four winters in this study (October to March, 1995 to 1999), significant changes in ambient aerosol were observed. The fine particle mass was reduced from $82\ \mu\text{g}/\text{m}^3$ in winter 1991/1992 to a winter average of $33\ \mu\text{g}/\text{m}^3$ observed during this study. Particle reduction affected primarily particles 0.1 to $0.5\ \mu\text{m}$ in size (1991/1992, $68\ \mu\text{g}/\text{m}^3$; 1995 to 1999, $25\ \mu\text{g}/\text{m}^3$). In contrast, the average winter particle number increased from $18,767/\text{cm}^3$ in 1991/1992 to an average winter particle number of

$22,050/\text{cm}^3$ during this study. This increase was driven only by the increase in $NC_{0.01-0.1}$ (1991/1992, $13,110/\text{cm}^3$; 1995 to 1999, $19,410/\text{cm}^3$). The average particle number in the size range 0.1 to $0.5\ \mu\text{m}$ was reduced from $5,594/\text{cm}^3$ in winter 1991/1992 to $2,581/\text{cm}^3$ during this study. Even more pronounced was the shift in particle number for the smallest size fraction, 0.01 to $0.03\ \mu\text{m}$, from 46% in 1991/1992 to 55% in 1995 to 1999 (Figures 39 and 40).

The observed shift of the particle size distribution toward ultrafine particles, along with an increased total particle number, may have been caused by the rebuilding of domestic heating systems and the renewal of car fleets in eastern Germany. Domestic heating systems have been rebuilt primarily from systems fired by surface coal to central heating systems using natural gas. During the last few years, the car fleet has been partly replaced by vehicles equipped with catalysts (gasoline) or soot filters (diesel). In 1993, only 30% of cars in Thüringen were equipped with a catalyst. In 1998, 91% of cars had catalysts. More details on source apportionment are investigated in Part II of this report.

The ambient aerosol is a dynamic system that may change its concentration and size distribution due to coagulation and chemical reactions. Because of their high diffusivity, ultrafine particles coagulate with other aerosol particles depending on the ambient aerosol conditions such as concentration, size distribution, and thermodynamic parameters (Fuchs 1964; Willeke and Baron 1993). For example, ultrafine particles of $0.01\ \mu\text{m}$ diameter coagulate with fine particles (polydispersed coagulation) at a rate 10 to 100 times faster than with ultrafine particles of their size (monodispersed coagulation); that means that ultrafine particles are scavenged in the presence of fine particles. However, this is only true if fine particles are present at the same concentration as ultrafine particles.

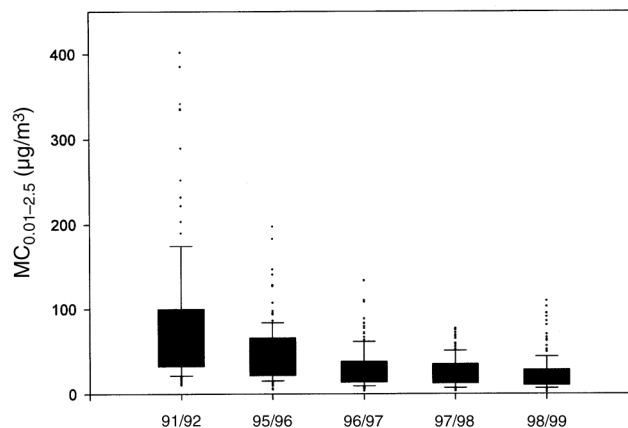


Figure 39. Seven-year trend of $MC_{0.01-2.5}$ in Erfurt, from winter 1991/1992 to winter 1998/1999. (See also Part II of this report and Tuch et al 2000a.)

For example, a polydispersed aerosol of $2 \times 10^4 \text{ cm}^{-3}$ concentration with a count median diameter of 45 nm and a geometric standard deviation (GSD) of 3.5 coagulates with a half-time of 28 minutes, whereas an aerosol with a count median diameter of 14 nm and a GSD of 2.1 has a half-time of 100 minutes.

The first example corresponds to the situation in Erfurt 1991/92, the second example to 1998/99 (T Tuch et al, unpublished data, 2000). If one does not consider the half-time but the residence time of ultrafine particles (that is, how long ultrafines remain ultrafine even after coagulation with other ultrafines), a residence time of about 5 hours (3 half-times of 100 minutes) is predicted during which the size distribution of the aerosol only slightly changes. This long time interval provides the basis for ultrafine particle dispersion within the urban atmosphere resulting in a less source-dependent ultrafine particle concentration pattern and a rather uniform exposure of the population. In total, the size distribution of the aerosol plays an important role, and coagulation dynamics increase with increasing number concentration, decreasing count median diameter, and increasing width of the aerosol distribution.

According to regulatory demands based on toxicologic and epidemiologic studies associating particle masses with adverse health effects in humans, high efficiency engines (ie, those performing more complete combustion and equipped with filters and catalysts in the exhaust pipe) have been developed to reduce particle emission. These measures have resulted in a drastically reduced number of freshly generated ultrafine condensation particles, which were then again reduced in the filter/catalyst system, and have thereby prevented rapid coagulation into the accumulation mode. In this manner the system led to the required reduction in particle mass of the exhaust aerosol. As a matter of fact, these measures also led to coagulation of freshly generated ultrafine condensation

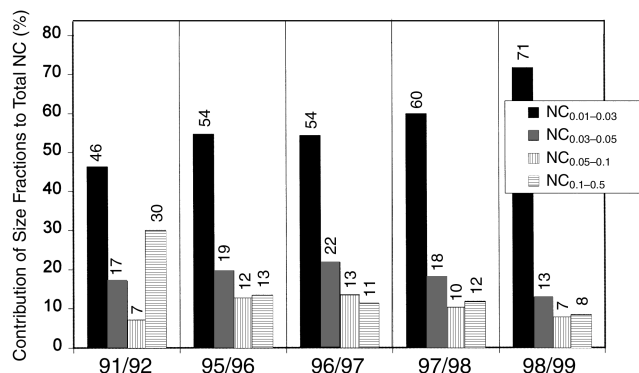


Figure 40. Seven-year trend of percentage of total particles in different size ranges in Erfurt, from winter 1991/1992 to winter 1998/1999. (See also Part II of this report and Tuch et al 2000a.)

particles into smaller particle agglomerates, namely ultrafine particles, such that ultrafine particle number may have risen in the exhaust aerosol.

The observed change in ambient urban particle number distribution and concentration was predominantly caused by more complete combustion in burners and engines, especially those equipped with filter/catalyst systems, not only in cars but also in burners of power plants and domestic heating. In total, the drastic reduction of larger particles in the last 20 years in Erfurt may have reduced the scavenging of ultrafine particles and thus prolonged their half life in the atmosphere. As a result, even if no more ultrafine particles were emitted, ambient concentration nevertheless may have increased. This is schematically shown in Figure 41.

We conclude that the shift of size distribution to smaller particles has been caused by the reaction of industry to regulatory demands focused on reduction of ambient particle mass. We hypothesize that automobile sources will increasingly contribute to ambient urban ultrafine particle number due to advancements in engine and burner technologies unless it is recognized that ultrafine particle number is of similar concern as the fine particle aerosol mass.

In addition to Erfurt, only a limited number of European locations such as Helgoland Island (Brand et al 1991) and several sites in Sachsen-Anhalt Germany (M Pitz et al 2000, unpublished data) have ultrafine particle measurements available. In addition, there is the ULTRA study in Germany, Finland, and The Netherlands (Pekkanen et al

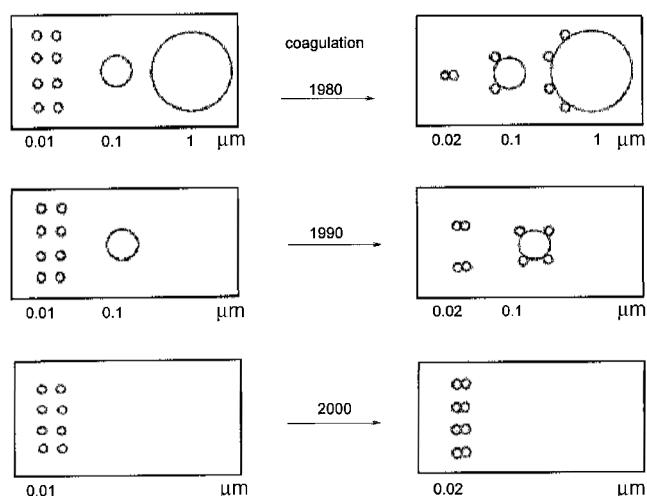


Figure 41. Coagulation dynamics in Erfurt from 1980 to 2000. In 1980, large particles effectively scavenged ultrafines, shortening their half-life (right panel). In 2000, the predominant small particles coagulate much more slowly, and the coagulation products are still small. In total, in the year 2000, the half-life of ultrafines is clearly longer than in the year 1980 (that is, if the same number of ultrafines is generated, the measured ambient concentration of ultrafines has increased).

Table 31. Relative Risks for Daily Mortality for 10 µg/m³ Increase in PM₁₀ and PM_{2.5}

Study	PM ₁₀		PM _{2.5}	
	RR	CI	RR	CI
Dockery et al 1992	1.016	0.999–1.033	1.017	0.998–1.037
	1.017	0.988–1.057	1.023	0.986–1.061
Schwartz et al 1996			1.022	1.015–1.029
	1.012	1.007–1.017		1.002–1.026
	1.009	1.001–1.018	1.014	1.004–1.017
	1.006	1.001–1.010	1.011	0.999–1.021
	1.009	1.001–1.016	1.010	0.997–1.028
	1.007	0.996–1.107	1.012	0.980–1.036
Our Study, MAS ^a	0.995	0.980–1.009	1.008	
			1.015 ^b	1.000–1.031
Our Study, Impactor ^a	1.012	1.001–1.024	1.010 ^c	0.995–1.026

^a Immediate effects based on Table 18.^b MC_{0.01–2.5}^c PM_{2.5}; the second best fit was lag = 0, TR = id, RR = 1.019, CI = 0.991–1.049, *P* = 0.19

1999; Mirme et al 2000; Tuch et al 2000; J Ruuskanen et al, unpublished data, 2000).

HEALTH EFFECTS OF PARTICLES

Fine particles and mortality

With respect to fine particles and total mortality, our findings were consistent with the literature. As shown in Table 31, the associations in our study (1.2% per 10 µg/m³ PM₁₀ and 1–1.5% per 10 µg/m³ PM_{2.5}) are comparable to those summarized by Dockery and colleagues (1992) and Schwartz and coworkers (1996). They are higher than the average associations in the APHEA project and the National Morbidity, Mortality, and Air Pollution Study (NMMAPS) (0.4–0.6% per 10 µg/m³ PM₁₀) and correspond to the results for the Northeast cities of NMMAPS (1.2% per 10 µg/m³ PM₁₀) (Katsouyanni et al 1997; Samet et al 2000). Our findings are also compatible with the recent review of more than 60 studies worldwide by Pope (2000). He found that changes in mortality associated with particulate air pollution were typically estimated at approximately 0.5 to 1.5% per 10 µg/m³ PM₁₀ or at about 1 to 3% per 10 µg/m³ PM_{2.5}.

This review also allows a direct comparison with our data for cause-specific mortality. Both show the strongest associations for respiratory diseases, followed by cardiovascular diseases. The weakest associations were found for other causes (Table 32).

In our study, the highest effect estimate for fine particles was observed without delay (that is, the increased mortality

occurred concurrently). This was also found in other studies where the strongest effect of particle mass was seen on the same day or with a lag of 1 day (Katsouyanni et al 1996; Samet et al 2000). However, often the increased mortality occurred within 0–5 days following an increase in air pollution (Pope 2000). For those cities of the NMMAPS study for which daily measurements were available, the effect of a single-day exposure also manifested across several days (Samet et al 2000; Schwartz 2000). The overall effect on total mortality of an increase in exposure was 1.4% per 10 µg/m³ PM₁₀ using a polynomial distributed lag model. The effect was spread over several days and did not reach zero until 5 days of exposure. In contrast, constraining the model to assume the effect occurs all in one day resulted in an estimate of only 0.65%. In our study we did not find a comparable influence of lagged days for PM₁₀. For MC_{0.01–2.5}, however, the effect on daily mortality was 2.5% per 10 µg/m³ MC_{0.01–2.5} for a polynomial

Table 32. Comparison of Relative Risk for Daily Mortality for 10 µg/m³ Increase in PM_{2.5}

	Pope (2000)	Our Study ^a
Total	1.014	1.015
Respiratory	1.050	1.049
Cardiovascular	1.021	1.017
Other	1.001	1.010

^a Immediate effects (lag = 0, not transformed).

distributed lag model considering lags of 0 to 5 days, whereas it was 1.5% per 10 $\mu\text{g}/\text{m}^3$ $\text{MC}_{0.01-2.5}$ if the model was constrained to a single day (see Table 18).

Ultrafine Particles and Mortality

Ultrafine particles showed effect estimates similar to fine particles or total mortality in our study. For the interquartile range of the $\text{NC}_{0.01-0.1}$ and $\text{MC}_{0.01-2.5}$ concentrations, an increase of 4.6% (95% CI: -0.3% to 9.7%) and 3.1% (0% to 6.3%) was observed if the model was constrained to a single day and 4.1% (0.1% to 8.2%) and 4.9% (1.1% to 8.8%), respectively, if lags from 0 to 5 days were allowed (Table 18). Looking in more detail at the lag structure, $\text{NC}_{0.01-0.1}$ showed the highest effect estimate after 4 days, whereas $\text{MC}_{0.01-2.5}$ showed the strongest immediate association (lag = 0) (Table 19). For cause-specific mortality, ultrafine particles showed a somewhat stronger association with respiratory diseases compared to cardiovascular diseases and other causes, as was observed for fine particles (Table 29).

Because this is the first mortality study on ultrafine particle effects, no external comparison can be made.

Ultrafine Particles and Morbidity

As summarized in Wichmann and Peters (2000), the following studies have investigated morbidity effects of ultrafine particles.

In Erfurt, 27 nonsmoking persons with asthma recorded peak expiratory flow (PEF) and respiratory symptoms daily during the winter season 1991/92 (Peters et al 1997). Both ultrafine and fine particle fractions were associated with a decrease of PEF and an increase in cough and feeling ill during the day. Health effects of the number of ultrafine particles were larger than those of the mass of fine particles. The effects were strongest for the five day mean of the particle number concentrations.

Daily medication use was reported in 58 adults with asthma in Erfurt from October 1996 to March 1997 (von Klot 2000, personal communication). Overall prevalence of bronchodilator use and inhaled corticosteroids were analyzed with a logistic regression model controlling for trend, temperature, weekend, holidays, and autocorrelation. Corticosteroid use and bronchodilator use both increased in association with cumulative exposure over 5 days of ultrafine and fine particles. The data suggest that asthma medication use increases with particulate air pollution. The effect might be more delayed but stronger on anti-inflammatory medication than on bronchodilators.

The effects of daily variations in particles of different sizes on PEF were investigated during a 57-day study of

39 children with asthma aged 7 through 12 years in 1994 in Koupio, Finland (Pekkanen et al 1997). In addition to measuring PM_{10} and black smoke, the electric aerosol spectrometer was used to measure particle number concentrations in the size range of 0.01 to 10 μm . All pollutants tended to be associated with declines in morning PEF. In this study, the concentration of ultrafine particles was less strongly associated with variations in PEF than PM_{10} or black smoke.

A group of 78 adults with asthma were followed with PEF measurements and symptoms and medication diaries for six months in the winter and spring season 1996/97 in Helsinki, Finland (Penttinen et al 1998, 2000). The associations between daily health endpoints and indicators of air pollution were examined by multivariate autoregressive linear regression. Daily mean number concentration but not particle mass ($\text{PM}_{2.5}$, PM_{10}) was negatively associated with daily PEF deviations. The strongest association was seen for particles in the ultrafine range. No significant association of particulate pollution on symptoms or bronchodilator use was seen.

In total, the data available from diary studies suggest that associations were observed in adults with asthma. While the associations of ultrafine particles were slightly stronger, associations of both ultrafine and fine particles were observed generally. The associations cumulated over 5 days. In two-pollutant models, the association of the same day was stronger for fine particles, whereas the cumulative effect was stronger for ultrafine particles (Peters et al 1997).

Selected Results on Toxicology of Ultrafine Particles

Published knowledge about toxicology of ultrafine particles has been summarized by Donaldson and colleagues (1999), Salvi and Holgate (1999), and Seaton (1999).

Ultrafine particles deposit with high efficiency in the respiratory tract. Large amounts pose a substantial burden for the macrophage phagocytic system and result in increased numbers of particles coming in contact with the epithelium.

For a range of nontoxic particles lung burden expressed as surface area predicts the ability to induce inflammation (Oberdörster 1995). Even low concentrations (1 $\mu\text{g}/\text{m}^3$) of ultrafine carbon black particles (14 nm diameter) caused severe inflammation effects in rats, whereas fine carbon black particles (260 nm diameter) showed no effects (MacNee et al 2000). After instillation of 125 μg of carbon black, the particles induced more inflammation the smaller they were (for 14, 50 and 260 nm particles, 40, 14 and 4% of neutrophils were found in the bronchoalveolar lavage) (Li et al 1999).

Seaton and coworkers (1995) have suggested that low-grade inflammation caused by ultrafine particles deposited in the alveoli might increase coagulation and that the altered blood rheology might be a part of the pathological mechanism linking particulate pollution with cardiovascular mortality and morbidity. Instillation of ultrafine carbon black in the lungs of rats has been demonstrated to increase the levels of coagulation factor VII (Li et al 1999).

A 1-hour exposure to diesel exhaust particles in healthy human volunteers in chamber studies has demonstrated an increase in circulating platelets and neutrophils in the peripheral blood along with an acute cellular and mediator inflammatory response in the airways (Salvi and Holgate 1999). An increase in the number of leukocytes and platelets in the systemic circulation may impair the flow of blood cells through the microcirculation and increase the hemodynamic resistance to flow in many organs. There is increasing evidence to suggest that neutrophils play a key role in reducing myocardial function as part of the systemic response to inflammation. Release of interleukin-6 (IL-6) from macrophages following particle phagocytosis could increase blood viscosity (Salvi and Holgate 1999).

Another, completely different hypothesis proposes that a neural reflex may be initiated by the irritant effects of air pollutants in the lung that lead to changes in heart rate and, by implication, increases liability to fatal changes in its rhythm. Support for this hypothesis comes from studies of heart rate changes related to exposure to particulate pollution (Peters et al 1999c; Pope et al 1999).

Godleski and coworkers (2000) investigated pathophysiologic mechanisms that result from exposure to concentrated ambient particles (CAPs) in dogs with and without cardio-pulmonary compromise. While fine particles were concentrated up to 30 times their level in ambient air, ultrafine particles were not concentrated and were at ambient levels. The most important finding was that dogs with coronary occlusion exposed to CAPs showed more rapid elevation of the ST segment of their electrocardiogram (ECG) traces than controls. This suggests that in susceptible individuals (ie, those with ischemic heart disease) particle pollution may lead to increased prevalence of fatal arrhythmia. The study, however, did not suggest that PM exposure has large effects on cardiopulmonary parameters, including heart rate variability, in normal dogs.

In conclusion (Donaldson et al 1999):

- Studies in rats with different types and sizes of ultrafine particles suggest that some ultrafine particles (eg, carbon black) have extra toxicity compared to the same material as respirable but not ultrafine particles when they are present in the lung at the same mass dose.
- This effect may be explained by the greater surface area of the ultrafine material, which could deliver oxidative stress because of a greater surface for release of transition metals, for generation of free radicals, or for other activity.
- Some ultrafine particles appear to have less or no pathogenic (eg, amorphous silica, magnesium oxide).
- The toxicologic data suggest that smallness, free radical activity, release of transition metals, and insolubility may be the most important factors for the ability to induce inflammation.
- Experimental studies with rats suggest that increases in procoagulants such as factor VII, an independent risk factor for heart attack and stroke, may occur in individuals exposed to ultrafine particles at low level for quite short times. Thus they show clearly that low exposure to ultrafine particles can cause systemic and local pulmonary effects that could impact heart attacks and strokes.
- The role of ultrafine particles in the adverse health effects of PM₁₀ remains unresolved.
- If surface area is an important metric that drives inflammatory response of particles, then exposure to a given airborne mass concentration of ultrafine particles carries significantly more risk than exposure to the same material as fine particles.

Plausible Pathomechanisms of Fine and Ultrafine Particles

Based on the described toxicologic knowledge, the following mechanisms are plausible.

Exposure Fine particles are rather uniformly distributed in the urban atmosphere (as shown earlier in other studies), and ultrafine particles are assumed to be similar—unless next to an ultrafine particle source—because of the ultrafine particle residence times of hours under the ambient aerosol conditions of Erfurt.

Deposition Like ultrafine particles, fine particles deposit on the alveolar and airway epithelium as ultrafine particles, but the deposition probability of particles is minimal at 0.5 μm and increases towards smaller and larger particles (International Commission on Radiological Protection 1994). Therefore, the deposition probability of ultrafine particles in the respiratory tract is higher than that of fine particles in the ambient aerosol.

Soluble Fraction If ultrafine particles are rather soluble, the dissolved mass is so small that adverse effects are unlikely. However, fine particles provide the dominating mass fraction of the ambient aerosol. In case of rather soluble

fractions of fine particles, the dissolved mass concentration of compounds may be sufficient to initiate inflammatory processes, lead to acute local inflammation in the lung, and thereby eventually contribute to exacerbation of preexisting diseases (Bates 1992).

Insoluble Fraction For the insoluble fraction, the particle surface area is the interface to the cells, tissues, and fluids of the lungs. Since the surface area of the large number of ultrafine particles is much greater than that of the few fine particles, insoluble ultrafine particles are more likely to cause adverse health effects than insoluble fine particles.

Kinetics Ultrafine particles are less likely to be phagocytized by alveolar macrophages and are found not only in the epithelium but also in interstitium (Ferin et al 1991; Stearns et al 1994). Translocation of ultrafine particles through the epithelium into the interstitium is likely to be a slow process. Therefore, the initiation of a chain of pathophysiologic reactions is delayed. At the same time, up-regulation of inflammatory indicators suggests that increased access of ultrafine particles to the interstitial space may trigger an inflammatory response. In addition, ultrafine particles may have access to the circulation, which is not the case for fine particles under physiologic conditions. In other words, ultrafine particles may be translocated to reactive sites in and beyond the epithelium, which may activate epithelial and interstitial cells as well as circulating leukocytes and endothelial adhesion molecules in the blood and eventually alter blood coagulability. This process may also need some time to become effective after some delay. Hence, these events could exacerbate preexisting cardiovascular disease.

This hypothesis leads to the following expectation of health effects of fine and ultrafine particles:

1. Effects of fine particles should depend on the amount of toxic material deposited in the lung by respirable particles and should occur immediately.
2. Effects of ultrafine particles should depend on the number of particles (and their surface), which serve as carriers and are able to reach the epithelium, the interstitium and more remote sites and should occur later than the fine particle effect.
3. The respiratory system should be more directly affected than other systems since it is immediately in contact with the inhaled particles.
4. The effects on the cardiovascular system should be delayed since the responsible indirect mechanisms may need more time.

How do the available epidemiologic data fit to this hypothesis? From our earlier study on persons with asthma, there are hints for (1) and (2) because the effect on the same day was stronger for fine particles and the cumulative effect over the final five days was stronger for ultrafine particles (Peters et al 1997e).

In the mortality study of this report, more immediate effects of fine particles and more delayed effects of ultrafine particles were observed for the best single-day lag models, which also support (1) and (2). Even more pronounced, if one looks at individual size classes, the strongest effect is seen after 4 days for particles with a diameter between 0.01 and 0.05 μm , after 1 day for particle diameter between 0.05 and 0.1 μm , and immediately for particle diameter between 0.1 and 2.5 μm (see Table 26 and Figure 34).

Also from the best single-day lag models of this report, more immediate effects were found for prevalent respiratory diseases (lag 0 or 1 day), whereas more delayed effects are observed for prevalent cardiovascular diseases (lag 4 or 5 days). This supports (3) and (4) (see Table 29 and Figures 37 and 38).

Further, support for the effects of fine and ultrafine particles is quite independent, suggesting different underlying mechanisms: If the (single-day) effects over all size classes are combined in a “distributed size model” (in analogy to a distributed lag model), the overall effect is clearly stronger than the contributions of the individual size classes (see Table 26 and Figure 34). Furthermore, in two-pollutant models immediate and delayed effects (represented by ultrafine and fine particles) seem to be independent. That is, the effects are almost unchanged by the presence of the other indicator (see Tables 24 and 25).

However, epidemiologic data have clear limitations with respect to extracting information on pathomechanisms:

- Since ambient fine and ultrafine particle concentrations used in epidemiologic studies are correlated, due to common sources and meteorologic influences, their effects can not be completely separated. The correlation coefficient between $\text{NC}_{0.01-0.1}$ and $\text{MC}_{0.01-2.5}$ is moderate ($r = 0.57$), however, which gives a chance to at least partly separate their effects.
- The information in death certificates on diseases is crude. While the official death statistics rarely cite respiratory disease as the underlying cause of death, the classification that uses all information on diseases of the deceased person, termed *prevalent condition*, might be more appropriate, especially in older persons with multiple diseases. However, this

information is not always complete. With respect to regression results, the effects for prevalent diseases are somewhat clearer than for underlying causes, but the general picture is comparable (see Appendix F).

- We see the described patterns for the best single-day model. If polynomial distributed lag models are used, they indicate that cumulative effects are stronger than single-day effects. The pattern of immediate (lag 0 or 1 day) and delayed effects (lag 4 to 5 days) is seen again, but the finding that fine particles show more immediate effects and ultrafine particles show more delayed effects is only gradual. Also, the observation of more immediate effects on respiratory diseases and more delayed effects on cardiovascular diseases is only gradual and not absolute.
- One might argue that in many studies the spatial distribution of fine particle concentration is quite homogeneous. Therefore, one single measurement station for fine particles might be sufficient for a place like Erfurt. For ultrafine particles, however, no comparable information is available for Erfurt and the spatial distribution may be more heterogeneous, especially since the most important source is automobile traffic. Thus, one measurement station might not be sufficient for good exposure assessment. This argument would mean that measurement error introduces random misclassification, shifting the finding of an epidemiologic study to zero. Since effects of ultrafine particles have been observed, random misclassification of exposure would mean that these were underestimated and that the real effects of ultrafine particles are stronger than the observed effects.

In addition, our estimates of the ultrafine particle residence times under the ambient aerosol condition in Erfurt yielded several hours providing sufficient time for ultrafine particle dispersion—unless right next to an ultrafine particle source. This in turn suggests that our single monitoring station might well sample representatively the overall ultrafine particle concentration of the urban aerosol of Erfurt.

This argument is supported by a study from Helsinki, in which the spatial variation of urban aerosol number concentration was investigated (Buzorius et al 1999). During the winter 1996/97, in addition to continuous daily measurements at the central site, simultaneous measurements were performed at 3 further sites for 14 days. The correlation coefficients of 24-hour averages were between 0.59 and 0.94. The distance between the downtown sites was below 2 km, and the remote site was 22 km northwest of Helsinki. These correlation

coefficients are comparable to those found for PM_{10} in Erfurt (between 0.69 and 0.94) (Cyrys et al 1998).

Overall, the results of this study agree with the formulated hypothesis on pathomechanisms and the expectations (1) to (4). The study alone would not have generated exactly this hypothesis. Therefore, the study results should not be overinterpreted with respect to the timing of the effects or the mode of action of fine and ultrafine particles on the respiratory and cardiovascular system.

In other epidemiologic studies, the mixture of ultrafine and fine particles have been found to affect lung function, respiratory symptoms, blood plasma viscosity, blood pressure, heart rate, heart rate variability, ECG, and fibrillator discharge to prevent the induction of arrhythmia in cardiovascular patients with an implanted defibrillator (Peters et al 1997, 1999, 2000; Pope et al 1999; Ibaldo-Mulli et al 2000). In these studies, only particulate mass concentrations have been measured ($PM_{2.5}$, PM_{10} , or TSP), which did not allow for differentiation between the effects of ultrafine and fine particles.

While other studies indicate that older persons are at higher risk of death in association with particulate air pollution (Schwartz 1994), the data presented here also suggest that the effects of air pollution might not be limited to the very old and frail.

The effect estimates also varied by season. Potential explanations are different composition of particles per season, measurement error (as the summer levels are much lower, the noise in the data would be relatively larger), and the possible existence of a threshold. With respect to trends over the three winter seasons, no clear pattern emerged. The effects due to particles during the first winter may have been slightly weaker than during the later winters. However, during the first winter, two influenza epidemics were present, which may have diminished (Spix 1995) the susceptible population to such an extent that the smaller effects of particles was not longer as well detectable.

GASEOUS POLLUTANT EFFECTS

The effects of gaseous pollutants in our study were comparable with those for particles. (The effect of SO_2 was even higher than particle effects.) To understand whether this was causal or probably explained by collinearity with particles, one should first consider the chance of seeing effect based on knowledge about threshold values and guidelines for the relevant gases. The 95th percentiles of concentrations of all three gases (SO_2 , NO_2 , and CO) reached less than 50% of value of the World Health Organization (WHO) guidelines (WHO 1996) (see Table 33).

Table 33. Concentrations of Gaseous Pollutants in Erfurt (1995 to 1998) and WHO Air Quality Guidelines for Europe (1996)

	Erfurt (24 hr) ^a		WHO Guideline	
	Mean	95th percentile	Original ^b	Recalculated ^c
SO ₂ (µg/m ³)	16.8	59.2	125 (24 hr)	125 (24 hr)
NO ₂ (µg/m ³)	36.4	63.0	200 (1 hr)	160 (24 hr)
CO (mg/m ³)	0.6	1.5	10 (8 hr)	8.1 (24 hr)

^a Data from this report.^b Guideline values from WHO (1996).^c WHO guideline values recalculated according to the method in Köppe et al (1996).

Because these are threshold substances, one would not expect causal effect at the concentrations found in Erfurt.

One might argue that these interpretations are also valid for particles. Mean (95th percentile) concentrations were 26 (69) µg/m³ for PM_{2.5} and 38 (93) µg/m³ for PM₁₀. WHO (1996) evaluated the literature on particle effects and came to the conclusion that no threshold concentration can be identified. Therefore, a linear exposure response relationship for PM₁₀ (and PM_{2.5}) was suggested. This view is supported by the results of NMMAPS (Samet et al 2000), where a log linear model without threshold was the most appropriate model. If a threshold was used, it appeared to be at low concentrations (around 15 µg/m³ for total mortality). Furthermore, there is increasing toxicologic evidence for relevant effects of fine and ultrafine particles.

Thus, the situation for particles is completely different from the situation for SO₂, NO₂, and CO. These gases clearly have thresholds, and no new data has questioned

the epidemiologic and toxicologic basis of the WHO guidelines from 1996.

A second consideration was consistency of effects. Information existed on ambient concentrations of SO₂ and TSP in earlier years in Erfurt. A mortality study was performed for the years 1980 to 1989 (Spix et al 1993a) (see Table 34). Measurements of SO₂ were available for the whole period, whereas measurements of suspended particles (similar to TSP) were only available for 1988–1989. In that study, a multivariate model was fitted including corrections for long-term fluctuations, influenza epidemics, and weather that was similar to our standard model. The best fit was obtained for log-transformed variables with a lag of 2 days for SO₂ and no lag for suspended particles. Daily mortality increased by 10% for SO₂ and by 22% for suspended particles for the 5th to 95th percentile range.

These results can be compared with the findings of our study. They are surprisingly consistent for suspended

Table 34. Daily Mortality in Erfurt in This Study and in Spix et al (1993)

	Mean Calculation (µg/m ³)	Period	Range (µg/m ³)	Lag	TR	RR per Range	RR per 10 µg/m ³	Source
Suspended particulates		1988–89	15–331 ^b	0	log	1.22 ^a	1.007 ^a	Spix et al ^b
TSP	50	1995–98	29–62 ^c	1	log	1.023	1.006	Table 18 ^c
SO ₂		1980–89	23–929 ^b	2	log	1.10 ^d	1.001 ^d	Spix et al ^b
SO ₂	17	1995–98	6–20 ^c	0	log	1.060 ^a	1.043 ^a	Table 23 ^c
SO ₂	38	10/95–3/96	7–26 ^e	0	log	1.037	1.019	Table 23 ^e
SO ₂	24	10/96–3/97	7–26 ^e	0	log	1.077 ^a	1.041 ^a	Table 23 ^e
SO ₂	12	10/97–3/98	7–26 ^e	0	log	1.059	1.026	Table 23 ^e

^a $P < 0.05$.^b Spix et al (1993): range = 5–95th percentile.^c This study, Table 18: range = 25th–75th percentile.^d $P < 0.01$.^e This study, Table 23: range = 25th–75th percentile of all 3 winters.

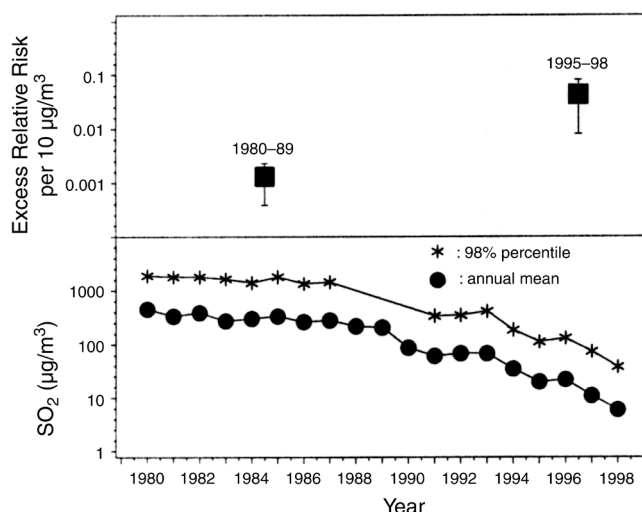


Figure 42. Historical inconsistencies of SO₂ effects in Erfurt (note log scales). (Top) The annual mean SO₂ dropped from 456 µg/m³ in 1980 to 6 µg/m³ in 1998. (Bottom) In the same period the excess relative risk (ERR = RR - 1) for daily mortality per 10 µg/m³ SO₂ increased 43 fold from 0.001 in 1980–89 to 0.043 in 1995–98. This suggests that SO₂ is not the causal agent.

particles and TSP: In 1988–1989, an increase in suspended particles of 316 µg/m³ led to a 22% increase in mortality. In 1995–1998, concentrations were lower by a factor of 10, and an increase in TSP of 33 µg/m³ led to a 2% increase of mortality. When one calculated the relative risk per 10 µg/m³ suspended particles–TSP, it was 1.007 in the earlier study and 1.006 in this study.

On the other hand, SO₂ results were not at all consistent (Figure 42): In 1980–1989, an increase by 926 µg/m³ led to a 10% increase of mortality. In 1995–1998, concentrations were lower by nearly a factor of 100, but nevertheless an increase by 14 µg/m³ still leads to a 6% increase of mortality. Considering the relative risk per 10 µg/m³ SO₂, it was 1.001 in the 1980s and 1.043 in 1995–1998 (that is, the excess relative risk was 43-fold). Also, despite a decrease of SO₂ over the three study winters, the relative risk increased (Table 34). These inconsistent results for SO₂ strongly suggested that SO₂ was not the causal agent but an indicator for something else. This view was supported by the dose response curve for SO₂ shown in Figure 22: The curve is very steep below 15 µg/m³ and much flatter above that point. Most of the effect leading to the large relative risk happened below 15 µg/m³, which makes no sense biologically.

Interestingly, Buringh and associates (2000) reported a similar problem for our neighbor country, The Netherlands. Based on nationwide data on SO₂ and daily mortality covering the period 1986–1994, they found an increase in total mortality of 0.6% per 10 µg/m³. If they

Table 35. Influence of Excluding High SO₂ Concentrations on Total Mortality Increase per 10 µg/m³. Study in the Netherlands 1986–94 from Buringh et al (2000)

SO ₂ weekly average (µg/m ³)	RR per 10 µg/m ³ SO ₂
All	1.007 ^a
<100	1.008 ^a
<50	1.014 ^a
<25	1.021 ^a
<10	1.043 ^a

^a $P < 0.05$.

successively excluded the highest concentrations, the risk increased with decreasing concentrations (see Table 35). Furthermore, when considering the years 1986–1988, 1989–1991, and 1992–1994 separately, they found the excess mortality risk increased by a factor of 4 over this time period. The authors conclude that SO₂ is probably not causally linked with the health effects and that a factor correlated with SO₂ might explain the observed association with total mortality.

Given the much lower SO₂ concentrations in The Netherlands during the 1980s, this looks very similar to the results for Erfurt in Table 34. In this report, SO₂, MC_{0.01–2.5}, PM₁₀, and also TSP showed mainly immediate effects. They may have represented a similar source because they also were similar with respect to their seasonal fluctuation (much higher in winter compared with summer) and they showed no pronounced difference between the weekend and the rest of the week.

In addition, there was lengthy experience with short-term effects of air pollution featuring high concentrations of TSP and SO₂ in western Germany (mainly from the industrialized Rhine-Ruhr district). Smog episodes with effects on mortality and morbidity occurred in 1962 (Steiger and Brockhaus 1971), in 1979 (Steiger 1980), in 1985 (Kuelske et al 1985; Perkuhn et al 1985; Schmitt 1986; Wichmann et al 1986, 1987, 1989, 1990, 1991; Peters et al 1997d, 1999; A Peters et al, unpublished data, 2000), and in 1987 (Wichmann et al 1988a,b). Furthermore, mortality and panel studies over several years in the 1980s were performed (Schwartz et al 1991; Franke et al 1992; Spix and Wichmann 1996). Not all of these studies tried to separate the effects of different pollutants. Wherever separation was done, however, TSP showed stronger effects than SO₂, although SO₂ was present in much higher concentrations then than during the study in Erfurt. Thus, studies from western Germany strongly supported particulate air pollution as more relevant than SO₂.

This was consistent with findings from eastern Germany, both for mortality studies during 1980–1989 in Erfurt (Spix et al 1993a, 1996; Wichmann et al 1995) and 1985–1989 and 1991–1995 in Thuringia (Spix et al 1993b, 1998) and for panel studies with children and adults with asthma in Erfurt, Weimar, Sokolov, Hettstedt and Zerbst (Wichmann et al 1996; Peters et al 1996, 1997a,b,c; Beyer et al 1998; A Peters et al, unpublished data, 2000). Again, in these studies, TSP, PM₁₀, and MC_{0.01–2.5} showed stronger effects than those for SO₂.

Ultrafine particles, NO₂, and CO formed a second group of pollutants. They had a less pronounced difference between winter and summer, but they had a very strong day-of-week pattern with much lower concentrations during the weekend, especially on Sundays. This strongly pointed to automobile traffic as common source. These pollutants showed an effect on mortality delayed by 4 days.

The two-pollutant model analyses suggested that immediate and delayed effects were independent. For the delayed effects, ultrafines gave a stronger signal than NO₂ and CO. This made sense because the concentrations of these gases were so low that one would not have expected to see health effects given knowledge from epidemiology, exposure chamber studies, and animal experiments (WHO 1996). On the other hand, there are studies showing ultrafine particle-related health effects at concentrations similar to those of our study (Peters et al 1997d; Penttinen et al 1998).

For immediate effects, the situation was more confusing. On one hand, SO₂ showed a stronger effect than particle masses in two-pollutant models. On the other hand, the risk estimates found for SO₂ made no sense when compared with the available knowledge. (WHO 1996). In addition, the SO₂ effects in this study were not at all compatible with those of an earlier mortality study in Erfurt. Thus, we conclude that the observed effect for SO₂ was artificial and probably came from a compound that had a similar time pattern.

In summary, an immediate effect of particle mass coincided with an effect represented by SO₂ as an indicator substance, but the latter is not yet understood. Also, a delayed effect coming from automobile exhausts was most clearly correlated to ultrafine particle number.

LIMITATIONS

A relatively short observation period in a relatively small city was the natural limitation of this study. Many results were only borderline significant. However, the amount of data was sufficient. The results were stable internally and formed a consistent pattern seen from many

different angles. A study like this must be seen clearly as what it is: an observational study (not experimental) with very little information on individuals. The associations we observed are statistical in nature and depend on data quality and details of the modeling process. However, modeling was based on hypotheses generated from earlier epidemiologic studies and animal experiments.

The use of Poisson regression is standard procedure for this type of data because they are always Poisson distributed (with overdispersion). The corrections for overdispersion and serially correlated errors are equally standard, but we could show in our case that they were not required to prevent biased variance estimates. In recent years, the use of GAM has also become something of a standard, at least when a nonlinear relation seems possible.

Even when following these general principles of modeling, decisions still had to be made at each point of the model building process. These decisions were not entirely objective and could not be automated; they required a certain degree of experience and judgement. To make sure that we did not thus produce biased results, we performed extended sensitivity analyses looking at almost every element of the confounder model from a different angle that someone else might have adopted. As the results seemed remarkably stable against this, we are quite confident of our results.

Single-day lags have been used in mortality studies of short-term effects for over a decade. They have the advantages of being easier to implement and easier to compare. To assess the effect over several days, we first attempted to assess the unweighted mean over 5 days. As the single-day lag results over days 0–5 already indicated, this approach was not very successful. At the time of these investigations no software for distributed lag models in a Poisson data situation using GAM was available. We thus adapted a semi-manual approach that leads to a new pollution variable and a point estimate, which is valid conditional on the choices that led to the weights. The standard deviation of this estimate was necessarily slightly underestimated, and the confidence intervals are somewhat too small. This approach was intended to give some additional insights to the single-day lag models, but we felt it was too experimental to replace them.

Note that whenever one of those alternative models required including a large number of additional (mostly far from significant) elements, the CIs grew larger. A similar effect was of course produced when looking at subgroups (of days, such as by season, or of persons, such as by cause of death). Given the relatively sparse database, we needed to be rather careful about randomness and degrees of freedom.

When presenting the results, we finally chose the interquartile range. This was the innermost, most stable range of the data. Because of the skewness of the pollution distribution, it was also very narrow compared with the bandwidth of actually observed data. The LOESS-smoothed plots suggested that outside this narrow range the parametric fit could deviate quite considerably from what the data suggested. Thus, extrapolation much beyond this range using the parametric fitted function should be avoided. At most, one could extrapolate up to the 95th percentile.

When interpreting the cumulative results, we should be aware that the interquartile range to which this related was something of a weighted geometric mean of the number and mass variables involved. Such a parameter is meaningless outside of the calculation of relative risk at this point. Note that the properties of this parameter might have contributed to the impression of a joint effect larger than each effect alone.

Parallel time courses of all pollutants and meteorologic conditions due to seasonality and shorter meteorologic variations complicated the separation of effects. We chose a conservative approach, preferring to underestimate the effects of air pollution by controlling for epidemics, season, and weather rather than to overestimate. Only one measurement site (GSF) was used, but comparison with the city sites for some pollutants showed very good agreement. There were arguments that the most relevant parameter is not particle number or particle mass, but particle surface area. However, no additional measurement of the surface area—such as $PM_{2.5}$ for mass—was available to allow an approach similar to the mass calibration of the MAS for estimation of surface concentrations. An additional complication in estimating the entire particle surface area arose from the fact that a major fraction of particles in the size range 0.05 to 0.5 μm was made of agglomerates of smaller ultrafine particles ($< 0.05 \mu m$). Hence, the surface area of this agglomerated particle fraction could only be estimated if the number and size of the primary particles were known. The investigation of this question should be the topic for further studies.

CONCLUSIONS

The study shows that particles did have an effect on daily mortality in Erfurt. These effects were evident for both ultrafine and fine particles:

- The effects of ultrafine and fine particles were comparable in strength.
- They were distributed over several days and were stronger when the pollution of more than a single day

was considered to influence the mortality on a given day.

- The effect was stronger if the contributions of all size classes were added up.
- The effects were strongest for respiratory diseases, followed by cardiovascular diseases.
- The observed correlations of gaseous pollutants and mortality were explained by collinearity of the gases to particles rather than by independent causal effects.
- The results match observations in other studies on fine particles and mortality and on ultrafine particles and morbidity.

Based on the available toxicologic knowledge, the following expectations can be formulated with respect to health effects of fine and ultrafine particles.

1. Effects of fine particles should depend on the amount of toxic material deposited in the lung by respirable particles and should occur more immediately.
2. Effects of ultrafine particles should depend on the number of particles (and their surface area) that reaches the epithelium, the interstitium and more remote sites, and the effects should be more delayed.
3. The respiratory system should be more directly affected since it is immediately in contact with the inhaled particles.
4. The cardiovascular response should be more delayed because the responsible indirect mechanisms need more time.

These toxicologic expectations cannot be statistically verified by our study. However, there are indications from our data that effects of fine particles occur more immediately (lag days 0–1) and that effects of ultrafine particles occur more delayed (lag days 4–5). Furthermore, there are clues that mortality in patients with respiratory diseases occurs more immediately whereas mortality in patients with cardiovascular diseases occur more delayed. However, these observations should not be overinterpreted and need sound confirmation in other—preferentially toxicologic—investigations.

IMPLICATIONS OF FINDINGS

This study carries regulatory implications. Given the indications that ultrafine particles may be relevant for human health, it is insufficient to study only fine particle mass (Wichmann and Peters 1999a,b; T Tuch et al, unpublished data, 2000). This is illustrated by Figures 39 and 40. Since 1991/1992, fine particle mass was clearly reduced.

However, ultrafine particle number was not decreased during the same period, and the fraction of very small particles (0.01 to 0.03 μm) increased steadily over 7 years of observation. Regarding regulation, this makes clear that reduction of fine particle mass does not automatically mean that ultrafine particle number is also reduced. Therefore, identification of relevant particle fractions with respect to human health is crucial for sound regulatory activities.

The ambient aerosol is a dynamic system that may change its concentration and size distribution due both to sources and to coagulation and chemical reactions. Hence, specific pollution control measures to reduce fine particle mass, which effectively reduce fine particle concentration, may paradoxically increase ultrafine particle persistence and number.

In the United States and Europe, standards for particulate air pollution currently consider particle mass exclusively. Early regulations sought to reduce TSP, but epidemiologic research using PM_{10} and, more recently, $\text{PM}_{2.5}$ has shown clearer effects for those indicators of fine rather than coarse particle mass. $\text{PM}_{2.5}$ is regulated in the United States (EPA 1997). A net of monitoring stations for $\text{PM}_{2.5}$ (and PM_{10}) is currently implemented for regulatory purposes. Technically, instruments are being developed to measure $\text{PM}_{1.0}$ in the future. If particle number or surface are—independently from particle mass—relevant for health effects, however, additional measurements of particle number are needed.

Furthermore, improvement of car engines and efforts to reduce particle mass (filters, catalysts) have shifted the ambient particle size distribution toward the smaller sizes. There are indications that, even if ultrafine particle emission did not increase, mass reduction by cleaning coarse and fine particles from the air provides fewer chances for ultrafines to accumulate after production. Thus, ultrafine particles may be more persistent in air and have a longer half life before they accumulate.

It is important to realize that technologies different from the ones currently used to reduce mass emission are needed to reduce particle number emission. Further implications with respect to sources are discussed in Part II of this report.

ACKNOWLEDGMENTS

We would like to acknowledge the assistance of this study by many persons and institutions:

Gesundheitsamt Erfurt (Frau Dr Cöllen) for her assistance in extracting the death certificates;

Landesamt für Umweltschutz, Erfurt (Herr Schmidt, Herr Häfner, Herr Preiss) and Umweltministerium Thüringen (Herr Schwinkowski), for providing data on emission and daily TSP, SO_2 , NO_2 , and CO;

Arbeitsgemeinschaft Influenza (Herr Uphoff) for the Influenza data;

GSF collaborators Drs Christa Roth, Peter Brand, and Erwin Karg for their help with aerosol spectrometry;

Drs Jonathan Samet, Frank Speizer, Glen Cass, Gerald van Belle, Aaron Cohen, Alison Geyh, George Allen for valuable input during their numerous site visits; and

GSF–National Research Center for Environment and Health for additional support.

REFERENCES

- Abshagen J, Rudolf W, Stahl H. 1984. Massnahmen zur Sicherstellung einer bundeseinheitlichen Praxis bei der Überwachung der Immissionen (Steps for safeguarding a uniform federal praxis of control of ambient air quality). *Staub-Reinhalte Luft* 43:107–112.
- Arbeitsgemeinschaft Influenza Hrsg. 1996. Ergebnisse der Meldephase 1995–1996. Arbeitsgemeinschaft Influenza Institute, Marburg, Germany.
- Arbeitsgemeinschaft Influenza Hrsg. 1997. Ergebnisse der Meldephase 1996–1997. Arbeitsgemeinschaft Influenza Institute, Marburg, Germany.
- Arbeitsgemeinschaft Influenza Hrsg. 1998. Ergebnisse der Meldephase 1997–1998. Arbeitsgemeinschaft Influenza Institute, Marburg, Germany.
- Bascom R, Bromberg PA, Costa DA, Devlin R, Dockery DW, Frampton MW, Lambert W, Samet JM, Speizer FE, Utell M. 1996. Health effects of outdoor air pollution. *Amer J Respir Crit Care Med* 153:3–50.
- Bates DV. 1992. Health indices of the adverse effects of air pollution. The question of coherence. *Environ Res* 59:336–349.
- Beyer U, Franke K, Cyrys J, Peters A, Heinrich J, Wichmann HE, Brunekreef B. 1998. Air pollution and respiratory health of children: The PEACE panel study in Hettstedt and Zerbst, Eastern Germany. *Eur Respir Rev* 8:61–69.
- Brand P. 1989. Forschungs- und Entwicklungsarbeiten zum Aufbau eines mobilen Messtandes zur Charakterisierung von Umweltaerosolen, PHD Thesis, Johann-Wolfgang Goethe University, Frankfurt, Germany.

- Brand P, Gebhart J, Below M, Georgi B, Heyder J. 1991. Characterization of environmental aerosol on Helgoland Island. *Atmos Environ* 25A:581–585.
- Brand P, Ruoss K, Gebhart J. 1992. Technical note: Performance of a mobile aerosol spectrometer for in situ characterization of an environmental aerosol in Frankfurt city. *Atmos Environ* 26A:2451–2457.
- Brauer M, Dumyahn TS, Spengler JD, Gutschmidt K, Heinrich J, Wichmann HE. 1995. Measurement of acid aerosol species in Eastern Europe: Implications for air pollution epidemiology. *Environ Health Perspect* 103:482–488.
- Buringh E, Fischer P, Hoek G. 2000. Is SO₂ a causative factor for the PM-associated mortality risks in The Netherlands? *Inhalation Toxicol* 12 (Suppl):55–60.
- Buzorius G, Hämeri K, Pekkanen J, Kulmala M. 1999. Spatial variation of aerosol number concentration in Helsinki city. *Atmos Environ* 33:553–565.
- Chow J. 1995. Measurement methods to determine compliance with ambient air quality standards for suspended particles. *J Air Waste Manage Assoc* 45:320–382.
- Cyrys J, Gutschmidt K, Brauer M, Dumyahn T, Heinrich J, Spengler JD, Wichmann HE. 1995. Determination of acid sulfate aerosols in urban atmospheres in Erfurt, FRG and Sokolov, former CSSR. *Atmos Environ* 29:3545–3557.
- Cyrys J, Heinrich J, Brauer M, Wichmann HE. 1998. Spatial variability of acid aerosols, sulfate and PM₁₀ in Erfurt, Eastern Germany. *J Expo Anal Environ Epidemiol* 8:447–464.
- Dockery DW, Pope CA. 1994. Acute respiratory effects of particulate air pollution. *Annu Rev Public Health* 15:107–132.
- Dockery DW, Schwartz J, Spengler JD. 1992. Air pollution and daily mortality: Association with particulates and acid aerosols. *Environ Res* 59:362–373.
- Donaldson K, Stone V, MacNee W. 1999. The toxicology of ultrafine particles. In: *Particulate Matter: Properties and Effects Upon Health* (Maynard RL, Howard CV, eds) pp 115–129. BIOS Scientific Publishers, Oxford, England.
- Eldering A, Cass GR, Moon KC. 1994. An air monitoring network using continuous particle size distribution monitors: connecting pollutant properties to visibility via Mie scattering calculations. *Atmos Environ* 16: 2733–2749.
- European Union. 1991. Guideline on Standards for Sulfur Dioxide and Particulate Matter. Bulletin EU 89/427/EWG, changed 1990 and 1991. European Union, Luxembourg.
- European Union. 1994. Guideline on Standards for Nitrogen Dioxide. Bulletin EU 85/203/EWG, changed 1990 and 1994. European Union, Luxembourg.
- Federal Focus. 1996. Principals for Evaluating Epidemiologic Data in Regulatory Risk Assessment. Federal Focus, Washington DC.
- Ferin J, Oberdörster G, Soderholm SC, Gelein R. 1991. Pulmonary tissue access of ultrafine particles. *J Aerosol Med* 4:57–68.
- Franke K, Boeriu A, Spix C, Wichmann HE et al 1992. A 3-year cohort study on short-term effects of air pollution in Germany. 1. Influences of medication and season. *Sci Total Environ* 127:69–78.
- Fuchs NA. 1964. *The Mechanic of Aerosols*, pp 288–302. Pergamon Press, Oxford, England.
- Gebhart J, Brand P, Roth C. 1989. High resolution size analysis of submicron particles in liquid suspensions via aerosolization. In: *Proceedings of the IV European Symposium on Particle Characterization*, April 19–21, 1989; Nürnberg, Germany.
- Godleski JJ. 1999. Systemic effects of inhaled environmental particles (abstract). *J Aerosol Med* 12:104.
- Godleski JJ, Verrier RL, Koutrakis P, Catalano P. 2000. Mechanisms of Mortality and Morbidity from Exposure to Ambient Air Particles. Research Report 91. Health Effects Institute, Cambridge MA.
- Hänel G, Thudium J. 1977. Mean bulk densities of samples of dry atmospheric particles: summary of measured data. *Pure Appl Geophys* 115:799–803.
- Hering SV, McMurry PH. 1991. Optical counter response to monodispersed atmospheric aerosols. *Atmos Environ* 25A:461–468.
- Hinds WC, Kraske G. 1986. Performance of PMS model LAS-X optical particle counter. *J Aerosol Sci* 17:67–72.
- Ibald-Mulli A, Stieber J, Wichmann HE, Koenig W, Peters A. 2000. Effects of air pollution on blood pressure: A population-based approach. *Am J Public Health* (in press).
- International Commission on Radiological Protection. 1994. Human respiratory tract model for radiological protection. *Ann ICRP* 24:36–52.
- Joshi PV. 1988. Density of atmospheric aerosol particles. In: *Proceedings of the Twelfth International Conference on Atmospheric Aerosols and Nucleation*, August 22–27, 1988. Vienna, Austria. Springer Verlag, Berlin, Germany.

- Katsouyanni K, Schwartz J, Spix C, Touloumi G, Zmirou D, Zanobetti A, Wojtyniak B, Vonk JM, Tobias A, Pönkä A, Medina S, Bacharova L, Anderson HR. 1996. Short-term effects of air pollution on health: A European approach using epidemiologic time series data: The APHEA Protocol. *JECH (Suppl)* 50:12–18.
- Katsouyanni K, Touloumi G, Spix C, Schwartz J, Balducci F, Medina S, Rossi G, Wojtyniak B, Sunyer J, Bacharova L, Schouten JP, Pönkä A, Anderson R. 1997. Short-term effects of ambient sulfur dioxide and particulate matter on mortality in 12 European cities: Results from time series data from the APHEA project. *Br Med J* 314:1658–1663.
- Knutson EO. 1976. Extended electric mobility method for measuring aerosol particle size. In: *Fine Particles* (Liu BYH, ed). Academic Press, New York NY.
- Koenig W, Sund M, Filipiak B, Döring A, Löwel H, Ernst E. 1998. Plasma viscosity and the risk of coronary heart disease: Results from the MONICA-Augsburg cohort study, 1984 to 1992. *Arterioscler Thromb Vasc Biol* 18:768–772.
- Kuelske S, Giebel J, Pfeiffer HU, Beier R. 1985. Analysis of the smog episode from January 16 to 21, 1985, in the Rhine-Ruhr District (in German). *LIS-Berichte, Landesanstalt für Immissionsschutz Essen* 55:1–74.
- Li XY, Brown D, Smith S, MacNee W, Donaldson K. 1999. Short-term inflammatory responses following intratracheal instillation of fine and ultrafine carbon black in rats. *Inhalation Toxicol* 11:709–731.
- Liu BYH, Marple VA, Whitby KT, Barsic NJ. 1974. Size distribution measurements of airborne coal dust by optical particle counters. *Am Ind Hyg Assoc J* 35:443–451.
- MacNee W, Li XY, Seaton A, Donaldson K. 2000. Effects of short-term low exposure to carbon black. *Am J Respir Crit Care Med*, in press.
- Marple V, Rubow KL, Turner W, Spengler JD. 1987. Low flow rate sharp cut impactors for indoor sampling: Design and calibration. *J Air Pollut Control Assoc* 37:1303–1307.
- Oberdörster G, Gelein RM, Ferin J, Weiss B. 1995. Association of particulate air pollution and acute mortality: Involvement of ultra-fine particles? *Inhalation Toxicol* 7:111–124.
- Pekkanen J, Brunekreef B, Wichmann HE. 1999. Exposure and risk assessment for fine and ultrafine particles in ambient air (ULTRA). Final Report. European Union Environment Programme Contract ENV4-CT95-0205. European Union, Brussels, Belgium.
- Pekkanen J, Timonen KL, Ruuskanen J, Reponen A, Mirme A. 1997. Effects of ultrafine and fine particles in an urban air on peak expiratory flow among children with asthmatic symptoms. *Environ Res* 74:24–33.
- Penttinen P, Timonen KL, Tiittanen P, Mirme A, Ruuskanen J, Pekkanen J. 1998. Fine and ultrafine particulate matter in ambient air are associated with peak flow decreases in adult asthmatic subjects. *Am J Respir Crit Care Med* 157:A878.
- Penttinen P, Timonen KL, Tiittanen P, Mirme A, Ruuskanen J, Pekkanen J. 2000. Ultrafine particles in urban air and respiratory health among adult asthmatics. *Eur Respir J* (in press).
- Perkühn J, Puls KE, Otte U. 1985. Meteorologic Situation During the Smog Episode in the Ruhr District in January 1985 (in German). Report of the Wetteramt Essen 1–35.
- Peters A, Dockery DW, Heinrich J, Wichmann HE. 1997b. Medication use modifies the health effects of particulate sulfate pollution in children with asthma. *Environ Health Perspect* 105:430–435.
- Peters A, Dockery DW, Heinrich J, Wichmann HE. 1997c. Short-term effects of particulate air pollution on respiratory morbidity in asthmatic children. *Eur Respir J* 10:872–879.
- Peters A, Döring A, Wichmann HE, Koenig W. 1997d. Increased plasma viscosity during the 1985 air pollution episode: A link to mortality? *Lancet* 349:1582–1587.
- Peters A, Goldstein IF, Beyer U, Franke K, Heinrich J, Dockery DW, Spengler JD, Wichmann HE. 1996. Acute health effects of exposure to high levels of air pollutants in Eastern Europe. *Am J Epidemiol* 144:570–581.
- Peters A, Liu E, Verrier RL, Schwartz J, Gold DR, Mittleman M, Baliff J, Oh A, Allen G, Monahan K, Dockery DW. 1999e. Air pollution and incidence of cardiac arrhythmia. In: *The Health Effects of Fine Particles: Key Questions and the 2003 Review*. Report of the Joint Meeting of the EC and HEI, January 14–15, 1999; Brussels, Belgium. Communication 8. Health Effects Institute, Cambridge MA.
- Peters A, Liu E, Verrier RL, Schwartz J, Gold DR, Mittleman M, Baliff J, Oh A, Allen G, Monahan K, Dockery DW. 2000. Air pollution and incidences of cardiac arrhythmia. *Epidemiology* 11:11–17.
- Peters A, Perz S, Döring A, Stieber J, Koenig W, Wichmann HE. 1999b. Activation of the autonomic nervous system and blood coagulation in association with an air pollution episode. In: *Proceedings of the Third Colloquium on*

- Particulate Air Pollution and Human Health, June 6–8, 1999; Durham NC.
- Peters A, Perz S, Döring A, Stieber J, Koenig W, Wichmann HE. 1999c. Increases in heart rate during an air pollution episode. *Am J Epidemiol* 150:1094–1098.
- Peters A, Tuch T, Wichmann HE, Löwel H. 1999a. Particulate air pollution and the onset of nonfatal myocardial infarction—Setting up a case-crossover study (abstract). In: *Air Pollution: Understanding Air Toxics and Particulates, The Fifteenth Health Effects Institute Annual Conference Program*, May 9–12, 1999; San Diego CA. Health Effects Institute, Cambridge MA.
- Peters A, Wichmann HE, Koenig W. 1999d. Air pollution exposure influences cardiovascular risk factors: A link to mortality? In: *Proceedings of the International Inhalation Symposium*, Hannover, Germany.
- Peters A, Wichmann HE, Tuch T, Heinrich J, Heyder J. 1997a. Respiratory effects are associated with the number of ultrafine particles. *Am J Respir Crit Care Med* 155:1376–1383.
- Peters A, Wichmann HE, Tuch T, Heinrich J, Heyder J. 1997e. Comparison of the number of ultrafine particles and the mass of fine particles with respiratory symptoms in asthmatics. *Ann Occup Hyg* 41 (Suppl 1):19–23.
- Pope CA. 2000. Epidemiology of fine particulate air pollution and human health: Biological mechanisms and who's at risk. *Environ Health Perspect* (in press).
- Pope CA, Dockery DW. 1999. Epidemiology of particle effects. In: *Air Pollution and Health* (Holgate ST, Samet JM, Koren HS, Maynard RL, eds) pp 673–705. Academic Press, San Diego CA.
- Pope CA, Dockery DW, Kanner RE, Villegas GM, Schwartz J. 1999. Oxygen saturation, pulse rate, and particulate air pollution. *Am J Respir Crit Care Med* 159:365–372.
- Reineking A, Porstendörfer J. 1984. Measurement of particle losses in a DMA and its influence on the evaluation of size distributions. In: *Aerosols*. Elsevier Science Publishing, New York NY.
- Reineking A, Porstendörfer J. 1986. Measurement of particle losses in a DMA (TSI, 3071) for different flow rates. *Aerosol Sci Technol* 5:483.
- Reisert W, Roth C, Gebhart J, Fischer P, Schäfer R. 1991. Inter-cavity laser light scattering: Experimental verification of theoretical response functions. *J Aerosol Sci* 22:S355–S358.
- Salvi S, Holgate ST. 1999. Mechanisms of particulate matter toxicity. *Clin Exp Allergy* 29:1187–1194.
- Samet JM, Zeger SL, Berhane K. 1995. The Association of Mortality and Particulate Air Pollution. In: *Particulate Air Pollution and Daily Mortality, Replication and Validation of Selected Studies, The Phase I.A Report of the Particle Epidemiology Evaluation Project*. Health Effects Institute, Cambridge MA.
- Samet JM, Zeger SL, Dominici F, Curriero F, Coursac I, Dockery DW, Schwartz J, Zanobetti A. 2000. The National Morbidity, Mortality, and Air Pollution Study, Part II. Morbidity, Mortality, and Air Pollution in the United States. Research Report 94. Health Effects Institute, Cambridge MA.
- Samet JM, Zeger SL, Kelsall JE, Xu J, Kalkstein LS. 1997. Air pollution, Weather, and Mortality in Philadelphia. In: *Particulate Air Pollution and Daily Mortality, Analysis of the Effects of Weather and Multiple Air Pollutants, The Phase I.B Report of the Particle Epidemiology Evaluation Project*. Health Effects Institute, Cambridge MA.
- Schmitt OA. 1986. Smog episodes in the Ruhr District since 1980 (in German). In: *Smog Episodes* (von Nieding G, Jander K, eds) pp 119–128. Fischer Verlag, Stuttgart, Germany.
- Schwartz J. 1994a. Air pollution and daily mortality: A review and meta analysis. *Environ Res* 64:36–52.
- Schwartz J. 1994b. What are people dying of on high air pollution days? *Environ Res* 64:26–35.
- Schwartz J. 2000. The distributed lag between air pollution and daily deaths. *Epidemiology* 11:320–326.
- Schwartz J, Dockery DW, Neas LM. 1996a. Is daily mortality associated specifically with fine particles? *J Air Waste Manage Assoc* 46:927–939.
- Schwartz J, Spix C, Touloumi G, Bacharova L, Barumandzadeh T, LeTertre A, Piekarski T, Ponce de Leon A, Pönkä A, Rossi G, Saez M, Schouten JP. 1996b. Methodological issues in studies of air pollution and daily counts of deaths or hospital admissions. *JECH (Suppl)* 50:3–11.
- Schwartz J, Spix C, Wichmann HE, Malin E. 1991. Air pollution and acute respiratory illness in five German communities. *Environ Res* 56:1–14.
- Seaton A. 1999. Airborne particles and their effects on health. In: *Particulate Matter: Properties and Effects Upon Health* (Maynard RL, Howard CV, eds) pp 9–17. BIOS Scientific Publishers, Oxford, England.
- Seaton A, MacNee W, Donaldson K, Godden D. 1995. Particulate air pollution and acute health effects. *Lancet* 345:176–178.

- Spix C. 1995. Tägliche Zeitreihen von Sterbeziffern—Regressionsmodelle und ein Modell zur Erklärung des Harvestingphänomens (Daily time series of numbers of deaths—Regression models, and a model to explain the harvesting phenomenon). Dissertation. Universität Dortmund.
- Spix, C, Heinrich J, Dockery D, Schwartz J, Völksch G, Schwinkowski K, Cöllen C, Wichmann HE. 1993a. Air Pollution and Daily Mortality in Erfurt, East Germany, from 1980–1989. *Environ Health Perspect* 101:518–526.
- Spix C, Heinrich J, Wichmann HE. 1996. Daily Mortality and Air Pollution in Erfurt 1980–1989 and Thüringen 1985–1989, East Germany. In: Workshop on Air Pollution Epidemiology: Experiences in East and West Europe (Englert N, Seifert B, Wichmann HE, eds). European Commission, Directorate General XII, Science, Research and Development, Air Pollution Epidemiology Reports Series, Report Number 7. European Commission, Brussels, Belgium.
- Spix C, Mey W, Rehm JU, Heinrich J, Wichmann HE. 1998. Untersuchungen zu Kurzzeiteffekten von Luftschadstoffen auf die Mortalität in ausgewählten Regionen des Freistaates Thüringen 1991–1995. (Investigation of short-term effects of air pollutants on mortality in selected regions in Thüringia.) Final Report. Thüringer Landesanstalt für Umwelt, Erfurt.
- Spix C, Wichmann HE. 1996. Daily mortality and air pollutant: Findings from Köln, Germany. *JECH (Suppl)* 50:52–58.
- Spix C, Winkel M, Heinrich J, Wichmann HE. 1993b. Analyse zur akuten Wirkung von Luftschadstoffen auf die Gesundheit in den Jahren 1985–1989 in Thüringen und einem Vergleichsgebiet. (Analysis of acute effects of air pollutants on human health in the years 1985–1989 in Thüringia and a control area). Thüringer Landesanstalt für Umwelt, Erfurt.
- Stearns RC, Murthy GCK, Skornik, Hatch V, Katler M, Godleski JJ. 1994. Detection of ultrafine copper oxide particles in the lungs of hamsters by electron spectroscopic imaging. In: ICEM-13, Proceedings of International Congress of Electron Microscopy, pp 763–764, July 17–22, 1994; Paris, France.
- Steiger H, Brockhaus A. 1971. Investigations on mortality in Northrhine Westfalia during the inversion-weather situation in December 1962 (in German). *Staub Reinh Luft* 31:190–192.
- Steiger H. 1980. Investigation on mortality during the smog period in the Western Ruhr District on January 17, 1979 (in German). *Zbl Bact Hyg B* 171:445–744.
- Szymanski WW, Lui BYH. 1986. On the sizing of laser optical particle counters. *Part Charact* 3:1–7.
- TA Luft. 1986. Technische Anleitung zur Reinhaltung der Luft (Technical rules for control of clean air). GMBL.27.2.1986.
- Tuch T, Brand P, Wichmann HE, Heyder J. 1997a. Variation of particle number and mass concentration in various size ranges of ambient aerosols in Eastern Germany. *Atmos Environ* 31:4193–4197.
- Tuch T, Hietel B, Kreyling WG, Schulz F, Spix C, Wichmann HE. 1999. Particulate air pollution and daily mortality in Erfurt, East Germany: Characterization of the aerosol size distribution and elemental composition. In: The Health Effects of Fine Particles: Key Questions and the 2003 Review. Report of the Joint Meeting of the EC and HEI, January 14–15, 1999; Brussels, Belgium. Communications 8. Health Effects Institute, Cambridge MA.
- Tuch T, Mirme A, Tamm E, Heinrich J, Heyder J, Brand P, Roth C, Wichmann HE, Pekkanen J, Kreyling WG. 2000. Comparison of two particle size spectrometers for ambient aerosol measurements. *Atmos Environ* 34:139–149.
- Tuch T, Spix C, Roth C, Kreyling WG, Heyder J, Wichmann HE. 1997b. Particulate air pollution and daily mortality in Erfurt, East Germany (abstract). In: The Health Effects Institute Thirteenth Annual Conference Program, May 4–7, 1997; Annapolis MD. Health Effects Institute, Cambridge MA.
- US Environmental Protection Agency. 1996. Air Quality Criteria for Particulate Matter. Document EPA/600/P-95/001. Office of Research and Development, Washington DC.
- US Environmental Protection Agency. 1997. National Ambient Air Quality Standard for Particulate Matter: Final Rule. *Fed Regist* 62:1–54.
- Utell MJ, Frampton MW. 1999. Clinical relevance of particle related effects (abstract). *J Aerosol Med* 12:104.
- Wichmann HE. 1997. Particulate Air Pollution and Daily Mortality in Erfurt, East Germany (1) Site visit 12/95 (2) Audit 4/97 (3) Annual Report 6/97. GSF Institute of Epidemiology Internal Report GSF-EP S 10/97. GSF Institute of Epidemiology, Neuherberg, Germany.
- Wichmann HE, Brockhaus A, Schlipkötter HW. 1991. Smogepisoden in NordrheinWestfalen und ihre gesundheitlichen Auswirkungen (Smog episodes in Northrhine Westfalia and their health effects). In: Public Health Gesundheitssystemforschung. (Schwartz FW, Badura B,

Brecht JG, Hofmann W, Jöckel KH, Trojan A, eds) pp 245–255. Springer Verlag, Berlin, Germany.

Wichmann HE, Heinrich J. 1995. Health effects of high level exposure to traditional pollutants in East Germany: Review and ongoing research. *Environ Health Perspect* (Suppl 2) 103:29–35.

Wichmann HE, Müller W, Allhoff P, Beckmann M, Bocter N, Csicsaky MJ, Jung M, Molik B, Schöneberg G. 1986. Untersuchungen der gesundheitlichen Auswirkungen der Smogsituation im Januar 1985 in NRW-Abschlussbericht (Investigations of the health effects of the smog episode in January 1985 in Northrhine Westfalia. Final Report. ISBN 3-925840-04-4:1–273. Ministry of Labor, Health and Social Affairs, Düsseldorf, Germany.

Wichmann HE, Müller W, Allhoff P, Beckmann M, Bocter N, Csicsaky MJ, Jung M, Molik B, Schöneberg G. 1989. Health effects during a smog episode in West Germany in 1985. *Environ Health Perspect* 79:89–99.

Wichmann HE, Peters A. 1999a. The role of particles of different sizes in humans—Epidemiological studies on effects of fine and ultrafine particles (abstract). In: *Air Pollution: Understanding Air Toxics and Particulates, The Fifteenth Health Effects Institute Annual Conference Program*, May 9–12, 1999; San Diego CA. Health Effects Institute, Cambridge MA.

Wichmann HE, Peters A. 1999b. Epidemiological studies on health effects of fine and ultrafine particles in Germany. In: *The Health Effects of Fine Particles: Key Questions and the 2003 Review. Report of the Joint Meeting of the EC and HEI*, January 14–15, 1999; Brussels, Belgium. Communications 8. Health Effects Institute, Cambridge MA.

Wichmann HE, Peters A. 2000. Epidemiological evidence of the effects of ultrafine particle exposure. *Philos R Soc B Biol Sci* (in press).

Wichmann HE, Peters A, Franke K, Heinrich J. 1996. Investigations of short-term effects on asthmatics in Sokolov/Erfurt/Weimar. Practical aspects and preliminary results. In: *Proceedings of the Workshop on Air Pollution Epidemiology: Experiences in East and West Europe* (Englert N, Seifert B, Wichmann HE, eds) pp 199–212. European Commission, Directorate General XII, Brussels, Belgium.

Wichmann HE, Spix C. 1990. Ergänzende Betrachtungen zu den gesundheitlichen Auswirkungen der Smogepisode 1985 (Complementary considerations to the health effects of the smog episode 1985). *Öff Ges Wesen* 52:260–266.

Wichmann HE, Spix C, Mücke G. 1987. Kleinräumige Analyse der Smogepisode des Januar 1985 unter Berücksichtigung meteorologischer Einflüsse (Small area analysis of the smog episode of January 1985 considering meteorological influences). ISBN 3-925840-08-7:1B231. Ministry of Labor, Health and Social Affairs, Düsseldorf, Germany.

Wichmann HE, Spix C, Tuch T. 1995. Particulate Air Pollution and Daily Mortality in Erfurt, East Germany. GSF Report 1-89. GSF Institute of Epidemiology, Neuherberg, Germany.

Wichmann HE, Spix C, Tuch T, Wittmaack K, Cyrus J, Wölke G, Peters A, Heinrich J, Kreyling WG, Heyder J. 2000. Daily Mortality and Fine and Ultrafine Particles in Erfurt, Germany. Part II. Role of Sources, Elemental Composition, and Other Pollutants. Research Report 98. Health Effects Institute, Cambridge MA (in press).

Wichmann HE, Sugiri D, Herold G, Knülle E. 1988b. Measurement of resistance in healthy persons during the winter 1985–1986 in January and February 1987. *Zbl Bakt Hyg B* 185:509–519.

Wichmann HE, Sugiri D, Islam MS, Haake D, Roscovanu A. 1988a. Lungenfunktion und Carboxyhämoglobin in der Smogsituation des Januar 1987 (Lung function and carboxyhemoglobin in the smog episode of January 1987). *Zbl Bakt Hyg B* 187:31–43.

Willeke K, Baron PA, eds. 1993. *Aerosol Measurements: Principles, Techniques and Applications*. Van Nostrand Reinhold, New York NY.

World Health Organization. 1996. Update and Revision of the WHO Air Quality Guidelines for Europe, Vol 6 Classical. European Centre for Environmental and Health, Bilthoven, The Netherlands.

Zhang Z, Liu BYH. 1991. Performance of TSI 3760 condensation nuclei counter at reduced pressures and flow rates. *Aerosol Sci Technol* 15:228–238.

APPENDIX A. Assigning the Causes of Death to Categories

Table A.1. Assigning Causes of Death to Categories

ICD-9 Code	ICD-10 Code	Description
Cardiovascular or Respiratory		
162	C34	lung cancer
391, 393–398	I01, I05–I09	rheumatic, valves
401, 402	I10, I11	hypertension
410–414	I20–I25	ischemic heart disease, myocardial infarction
415–417	I27–I28	pulmonary heart disease
420–429	I30–I52	various other heart diseases including arrhythmias and congestive heart disease
430–440	I60–I70	cerebrovascular, atherosclerosis
460–465, 472–478	J00–J06, J30–J32, J37, J39	upper airways: acute and chronic
480–487	J10–J18	influenza and pneumonia
466, 490–496	J20–J22, J40–J47	lower airways: acute and chronic, including COPD (490–492, 496, J40, J42–J44) and asthma (493, J45–J46)
500–508	J60–J70	pulmonary diseases through exogenous agents
518, 519	J80–J84, J96–J98	other pulmonary
785	R00, R01, R07, R09	cardiovascular symptoms
786	R04–R09	respiratory symptoms
Other Natural		
001–139	ICD-10: A00–B99	infections and parasites
140–239 (not 162)	C00–D48 (not C34)	tumors and cancers except for lung cancer
270–289	D50–D89	blood generating system and immune diseases
240–269	E00–E90	digestive and glandular, including diabetes mellitus (250, E10–E14)
290–319	F00–F99	mental disorders
320–389	G00–G99, H00–H95	nervous system, senses
390, 392, 441–459	I00, I02, I26, I71–I99	circulatory system, but not included in cardiovascular (rheumatic, lung emboli, blood vessels, unclear diseases)
470–471, 510–517	J33–J36, J38, J85–J94, J95, J99	respiratory system but not included in respiratory (polyps, other tracheal, pleuritic, pneumothorax)
520–579	K00–K93	digestive system
680–709	L00–L99	skin
710–739	M00–M99	muscular and skeletal system
580–629	N00–N99	urogenital tract
630–676	O00–O99	pregnancy and birth related
740–779	P00–P96, Q00–Q99	perinatal and congenital
780–784, 787–799	R02, R03, R10–R99	symptoms not concerning respiratory or cardiovascular, unspecific diseases

APPENDIX B. Comparison of the Distribution of the Underlying Causes of Death

Table B.1. Comparison of Distribution of Underlying Causes of Death

Cause of Death Category (ICD-9)	Cases per 100,000 Inhabitants			
	Germany 1995	Thüringen 1997	Erfurt Study ^a 1996	Erfurt Study ^a 1997
Infections and Parasites (001–139)	9.4	3.3	4.8	2.4
Lung Cancer (162)	42.8	41.2	35.5	36.0
Cancers and Tumors Without Lung Cancer (140–208 / 162)	205.9	205.6	167.2	154.8
Diabetes (250)	26.8	53.1	46.1	43.3
Mental Disorders, Nervous System, Senses (290–389)	30.3	11.4	20.7	30.7
Acute myocardial infarction (410)	101.6	107.1	35.5	28.7
Ischemic Heart Disease (411–414)	105.5	173.7	168.6	172.6
Congestive Heart Disease (428)	59.4	45.9 ^b	68.7	78.9
Cerebrovascular Diseases (430–438)	112.5	144.4	74.5	63.3
Other Circulatory Diseases (390–459 / 410–414, 428, 430–438)	96.6	109.9	139.8	173.4
Pneumonia (480–486)	18.8	12.0 ^b	19.7	14.1
Bronchitis (466, 490, 491)	13.0	22.8	11.0	15.6
Other Respiratory Diseases (460–519 / 466, 480–486, 490, 491)	28.7	16.2	16.4	17.0
Digestive Tract (520–579)	47.6	63.5	61.0	49.2
Urogenital Tract (580–629)	11.2	10.8	13.0	12.2
Pregnancy and Birth Related (630–676)	NA ^c	NA	1.0	0
Congenital and Perinatal (740–779)	NA	3.9	0.5	0.5
Other (780–799)	24.8	NA	12.5	11.7
Injuries and Poisonings (800–999)	46.7	60.2	44.7	44.8
Total	1,001.9	1,117.5	967.4	976.8

^a No official data on Erfurt cause of death distribution is available. For this comparison, we chose the subset Erfurt = last place of residence, indicated as "Erfurt Study".

^b Not quite identical categorization.

^c NA = Not available, mostly because of small numbers and data privacy laws.

APPENDIX C. Comparison of Prevalent Diseases and Underlying Causes of Death

Table C.1. Percentage of Underlying Causes in Categories of Underlying Cause or Prevalent Disease

Underlying Cause of Death	Cardiovascular or Respiratory Underlying	Other Natural Underlying	Cardiovascular or Respiratory Prevalent	Cardiovascular or Respiratory Not Recorded
Chronic Ischemic Heart Disease	23.4	0	17.9	0
Congestive Heart Disease	13.1	0	10.1	0
Atherosclerosis	12.1	0	9.2	0
Stroke	9.4	0	7.2	0
Lung Cancer	6.1	0	4.7	0
Acute Ischemic Heart Disease	5.6	0	4.3	0
Hypertension	5.5	0	4.2	0
Acute Myocardial Infarction	5.2	0	4.0	0
Various Other Heart Diseases	4.3	0	3.3	0
Influenza and Pneumonia	3.4	0	2.6	0
COPD	3.3	0	2.5	0
Pulmonary Heart Disease	2.6	0	2.0	0
Other Cerebrovascular	2.0	0	1.6	0
Other Ischemic Heart Disease, Angina Pectoris	1.5	0	1.2	0
Other Lower Airways Including Asthma	1.3	0	1.0	0
Rheumatic Heart Disease, Valves	0.7	0	0.5	0
Cardiovascular Symptoms	0.2	0	0.1	0
Pulmonary Diseases Through Exogenous Agents	0.1	0	0.1	0
Other Pulmonary Diseases, Respiratory Symptoms	0.1	0	0	0
Upper Airways: Acute and Chronic	0	0	0	0
Tumors and Cancers without Lung Cancer	0	49.1	12.4	65.1
Diabetes Mellitus	0	12.5	3.2	2.8
Digestive Tract Without Liver Cirrhosis and Directly Alcohol-Related Liver Diseases	0	8.8	2.7	6.0
Liver Cirrhosis and Alcohol-Related Liver Diseases	0	6.6	1.0	9.2
Mental Disorders	0	3.8	1.1	3.1
Urogenital Tract	0	3.6	1.3	1.8
Unspecific Symptoms and Diseases	0	3.5	0.6	5.6
Nervous System, Senses	0	2.8	0.8	2.2
Circulatory System, but Not Cardiovascular	0	2.5	0.8	1.5
Blood Generating System and Immune Diseases	0	2.0	0.6	1.4
Digestive and Glandular Without Diabetes Mellitus	0	1.2	0.4	0.7
Muscular and Skeletal System	0	1.1	0.4	0.2
Respiratory System but Not Respiratory Diseases	0	0.8	0.3	0.3
Infections and Parasites	0	0.7	0.2	0.5
Skin	0	0.3	0.2	0
Perinatal and Congenital	0	0.2	0	0.3
Pregnancy and Birth Related	0	0.1	0	0.2
Total	100	100	100	100

Table C.2. Percentage of Prevalent Diseases in Categories of Underlying Cause or Prevalent Disease

Prevalent Cause of Death	Cardiovascular or Respiratory Underlying	Other Natural Underlying	Cardiovascular or Respiratory Prevalent	Cardiovascular or Respiratory Not Recorded
Congestive Heart Disease	40.1	17.2	38.8	0
Chronic Ischemic Heart Disease	36.7	13.2	34.3	0
Diabetes Mellitus	15.9	20.9	19.9	8.7
Stroke	20.4	5.1	18.0	0
Atherosclerosis	16.6	3.9	14.6	0
Tumors and Cancers Without Lung Cancer	5.2	53.8	12.7	70.5
Acute Myocardial Infarction	14.9	2.9	12.7	0
Influenza and Pneumonia	9.8	7.0	10.7	0
Hypertension	10.3	3.3	9.4	0
Acute Ischemic Heart Disease	9.9	2.5	8.9	0
Various Other Heart Diseases	6.5	3.5	6.6	0
Pulmonary Heart Disease	6.3	2.8	6.1	0
Digestive Tract Without Liver Cirrhosis and Alcohol-Related Liver Diseases	3.1	12.2	5.9	9.2
Urogenital Tract	3.8	10.1	5.9	7.4
Lung Cancer	6.9	1.3	5.9	0
COPD	6.3	2.1	5.8	0
Other Cerebrovascular	3.7	1.6	3.6	0
Other Ischemic Heart Diseases, Angina Pectoris	2.9	1.4	2.9	0
Circulatory System, but Not Cardiovascular	1.6	5.1	2.7	4.2
Nervous System, Senses	1.6	4.3	2.5	3.1
Mental Disorders	1.2	5.0	2.2	4.6
Blood Generating System and Immune Diseases	1.2	3.5	2.1	2.2
Liver Cirrhosis and Directly Alcohol-Related Liver Diseases	0.7	9.7	2.0	13.2
Other Lower Airways Including Asthma	1.9	0.7	1.7	0
Unspecific Symptoms and Diseases	0.7	5.8	1.5	7.2
Cardiovascular Symptoms	0.8	1.9	1.5	0
Muscular and Skeletal System	0.9	2.0	1.4	1.0
Digestive and Glandular Without Diabetes Mellitus	0.9	1.8	1.3	1.0
Respiratory System but Not Respiratory Diseases	0.1	1.9	1.2	1.2
Rheumatic Heart Disease, Valves	1.0	0.2	0.9	0
Infections and Parasites	0.4	2.4	0.9	2.5
Other Pulmonary Diseases, Respiratory Symptoms	0.6	0.3	0.6	0
Skin	0.3	0.9	0.5	0.5
Pulmonary Diseases Through Exogenous Agents	0.2	0.3	0.3	0
Perinatal and Congenital	0	0.2	0.1	0.3
Upper Airways: Acute and Chronic	0.1	0	0.1	0
Pregnancy and Birth Related	0.1	0.2	0	0.4
Total	>100	>100	>100	>100

Table C.3. Categorization into Groups of Cardiovascular and Respiratory Causes, Based on ICD-9 and ICD-10**Cardiovascular**

ICD-9	391, 393–402, 410–429, 440
ICD-10	I01, I05–I11, I20–I25, I27, I30–I52, I70, R00, R01, R07–R09

Respiratory

ICD-9	162,415–417, 460–466, 472–508, 518, 519
ICD-10	C34, I27, I28, J00–J32, J37, J39–J84, J96–J98, R04–R09

APPENDIX D. Properties of the Particle Data

Table D.1. Correlations Between Daily Average Number Concentrations

Size Range	NC _{0.01–0.03}	NC _{0.03–0.05}	NC _{0.05–0.1}	NC _{0.01–0.1}
Log-Transformed Raw Data				
NC _{0.03–0.05}	0.86	1		
NC _{0.05–0.1}	0.74	0.93	1	
NC _{0.01–0.1}	0.99	0.94	0.85	1
NC _{0.01–2.5}	0.96	0.95	0.88	0.99
Seasonally Corrected Data				
NC _{0.03–0.05}	0.86	1		
NC _{0.05–0.1}	0.69	0.91	1	
NC _{0.01–0.1}	0.98	0.84	0.82	1
NC _{0.01–2.5}	0.95	0.94	0.85	0.99
Confounder Model Corrected Data				
NC _{0.03–0.05}	0.83	1		
NC _{0.05–0.1}	0.65	0.89	1	
NC _{0.01–0.1}	0.97	0.93	0.79	1
NC _{0.01–2.5}	0.94	0.94	0.84	0.99

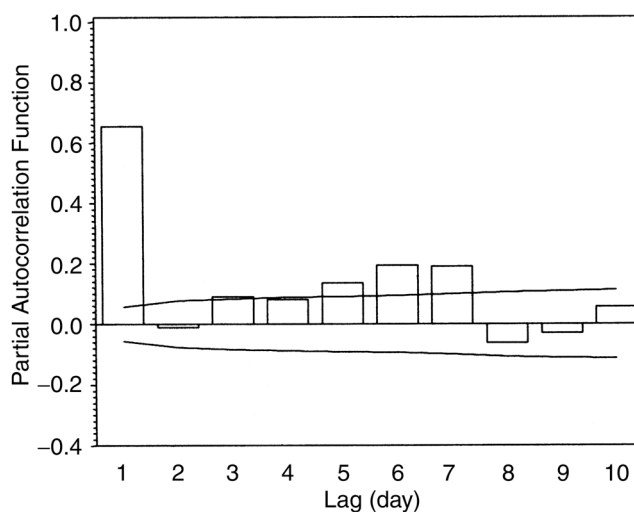
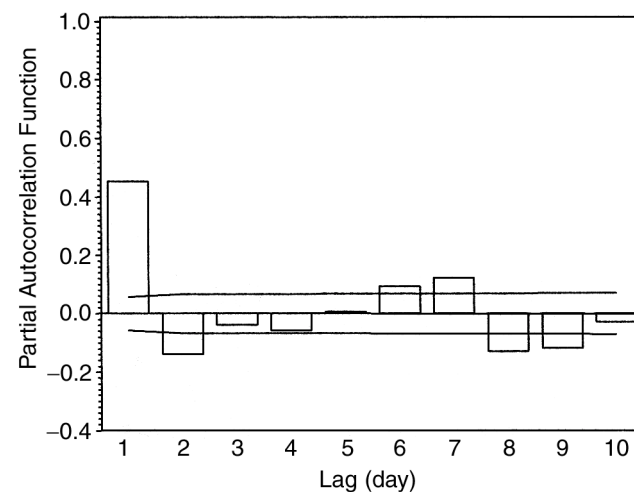
Table D.2. Correlations Between Daily Average Mass Concentrations and Particle Size

Size Range	MC _{0.1–0.5}	MC _{0.5–1.0}	MC _{1.0–2.5}	MC _{0.01–1.0}	MC _{0.01–2.5}
Log-Transformed Raw Data					
MC _{0.5–1.0}	0.84	1			
MC _{1.0–2.5}	0.52	0.68	1		
MC _{0.01–0.1}	0.99	0.89	0.58	1	
MC _{0.01–2.5}	0.99	0.90	0.62	1.00	1
Seasonally Corrected Data					
MC _{0.5–1.0}	0.79	1			
MC _{1.0–2.5}	0.53	0.73	1		
MC _{0.01–0.1}	0.99	0.85	0.59	1	
MC _{0.01–2.5}	0.98	0.87	0.63	1.00	1
Confounder Model Corrected Data					
MC _{0.5–1.0}	0.76	1			
MC _{1.0–2.5}	0.52	0.76	1		
MC _{0.01–0.1}	0.99	0.84	0.60	1	
MC _{0.01–2.5}	0.98	0.85	0.64	1.00	1
Log-Transformed Raw Data					
NC _{0.01–0.03}	0.47	0.41	0.27	0.48	0.48
NC _{0.03–0.05}	0.64	0.51	0.34	0.64	0.64
NC _{0.05–0.1}	0.77	0.58	0.38	0.76	0.76
NC _{0.01–0.1}	0.57	0.47	0.30	0.57	0.57
NC _{0.01–2.5}	0.64	0.53	0.35	0.64	0.64
Seasonally Corrected Data					
NC _{0.01–0.03}	0.32	0.18	0.19	0.31	0.32
NC _{0.03–0.05}	0.51	0.31	0.31	0.50	0.51
NC _{0.05–0.1}	0.69	0.42	0.36	0.67	0.67
NC _{0.01–0.1}	0.43	0.43	0.25	0.42	0.42
NC _{0.01–2.5}	0.52	0.32	0.29	0.52	0.51
Confounder Model Corrected Data					
NC _{0.01–0.03}	0.27	0.15	0.17	0.26	0.27
NC _{0.03–0.05}	0.48	0.29	0.29	0.47	0.47
NC _{0.05–0.1}	0.67	0.41	0.33	0.65	0.64
NC _{0.01–0.1}	0.39	0.22	0.22	0.38	0.38
NC _{0.01–2.5}	0.49	0.30	0.27	0.48	0.48

Table D.3. Correlations Between MAS-Derived Parameters and Other Particle Data

	PM _{2.5} (11:00 am)	PM ₁₀	TSP
Log-Transformed Raw Data			
NC _{0.01–0.03}	0.46	0.45	0.42
NC _{0.03–0.05}	0.64	0.63	0.60
NC _{0.05–0.1}	0.72	0.71	0.69
NC _{0.01–0.1}	0.55	0.54	0.51
NC _{0.01–2.5}	0.61	0.61	0.58
MC _{0.1–0.5}	0.87	0.87	0.85
MC _{0.5–1.0}	0.75	0.74	0.73
MC _{1.0–2.5}	0.55	0.55	0.58
MC _{0.01–1.0}	0.87	0.87	0.85
MC _{0.01–2.5}	0.87 ^a	0.87	0.86
Seasonally Corrected Data			
NC _{0.01–0.03}	0.36	0.36	0.39
NC _{0.03–0.05}	0.54	0.56	0.54
NC _{0.05–0.1}	0.65	0.65	0.64
NC _{0.01–0.1}	0.52	0.56	0.55
NC _{0.01–2.5}	0.52	0.56	0.55
MC _{0.1–0.5}	0.82	0.83	0.82
MC _{0.5–1.0}	0.68	0.71	0.70
MC _{1.0–2.5}	0.46	0.55	0.59
MC _{0.01–1.0}	0.82	0.84	0.83
MC _{0.01–2.5}	0.82	0.84	0.84
Confounder Model Corrected Data			
NC _{0.01–0.03}	0.30	0.34	0.33
NC _{0.03–0.05}	0.49	0.52	0.51
NC _{0.05–0.1}	0.59	0.60	0.60
NC _{0.01–0.1}	0.40	0.43	0.42
NC _{0.01–2.5}	0.47	0.51	0.50
MC _{0.1–0.5}	0.77	0.79	0.80
MC _{0.5–1.0}	0.62	0.65	0.68
MC _{1.0–2.5}	0.44	0.53	0.58
MC _{0.01–1.0}	0.77	0.79	0.82
MC _{0.01–2.5}	0.77	0.80	0.82

^a Based on MC_{0.01–2.5} (11:00 am); the correlation coefficient is 0.93.

**Figure D.1.** Partial autocorrelation function of NC_{0.01–0.1}, raw data (log transformed). The lines indicate the 95% CI.**Figure D.2.** Partial autocorrelation function of deseasonalized NC_{0.01–0.1}, raw data (log transformed). The lines indicate the 95% CI.

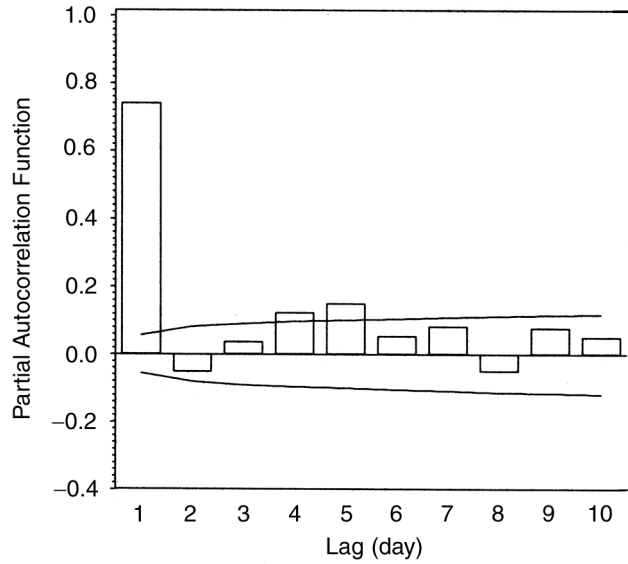


Figure D.3. Partial autocorrelation function of $MC_{0.01-2.5}$, raw data (log transformed). The lines indicate the 95% CI.

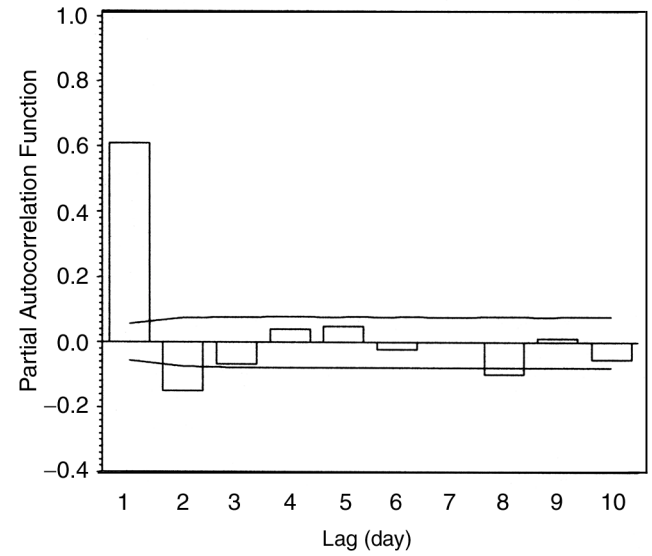


Figure D.4. Partial autocorrelation function of deseasonalized $MC_{0.01-2.5}$, data (log transformed). The lines indicate the 95% CI.

APPENDIX E. Diagnostics of Confounder Model

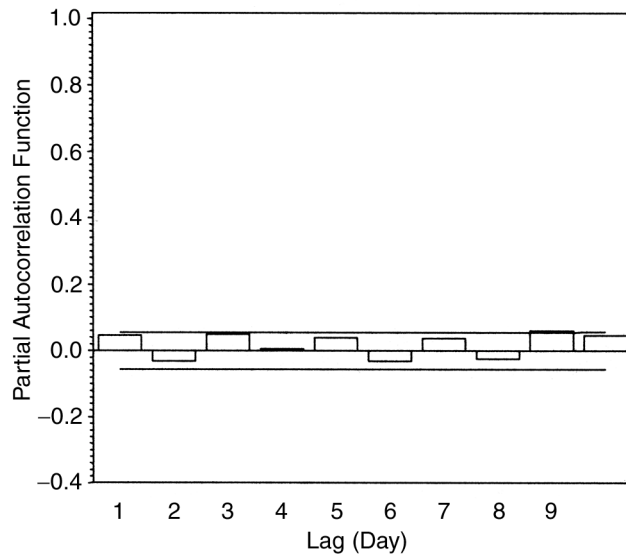


Figure E.1. Partial autocorrelation function of mortality after correcting for influenza epidemics of the first winter (based on Pearson residuals). The lines indicate the 95% CI.

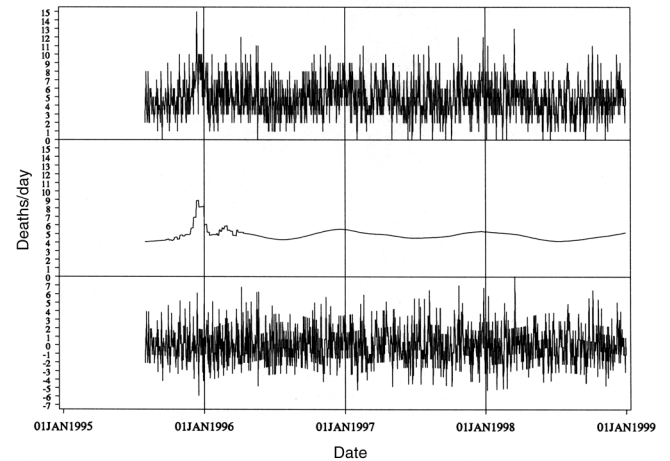


Figure E.2. Mortality time series after fitting epidemics, trend and season. From top to bottom: raw data, fitted, residuals.

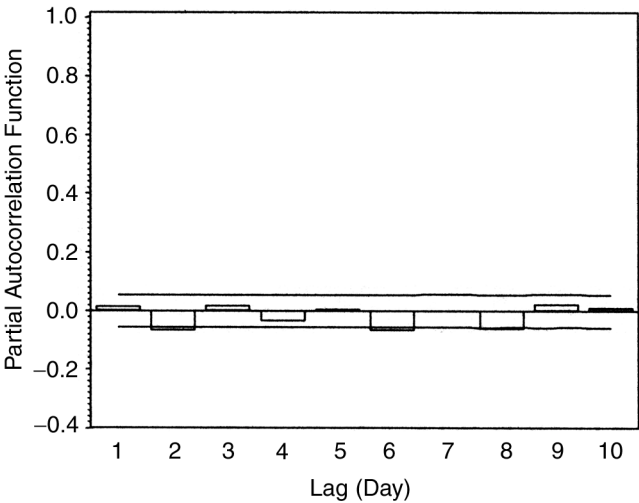


Figure E.3. Partial autocorrelation function of mortality after correcting for influenza epidemics and season (based on Pearson residuals).

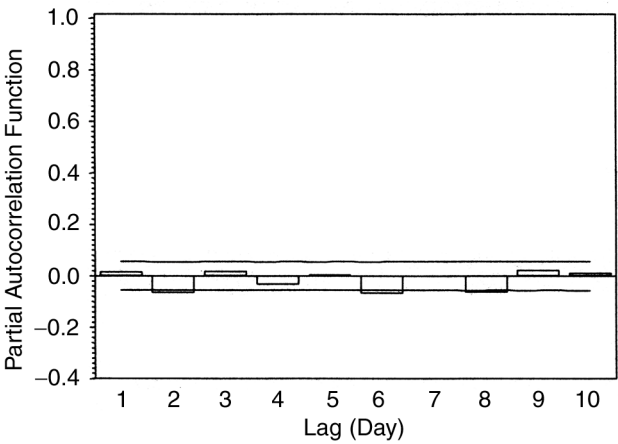


Figure E.4. Partial autocorrelation function of mortality after correcting for influenza epidemics of the first winter, season and day of week (based on Pearson residuals).

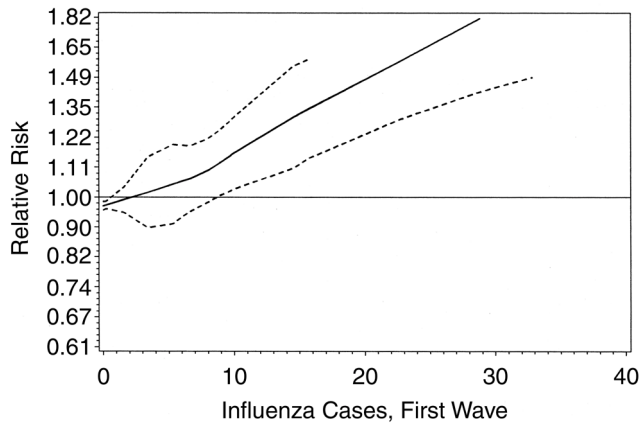


Figure E.5. Dose-response curve (partial fit) of respiratory infection counts used as surrogate measures for first wave of 1995–1996 influenza epidemic.

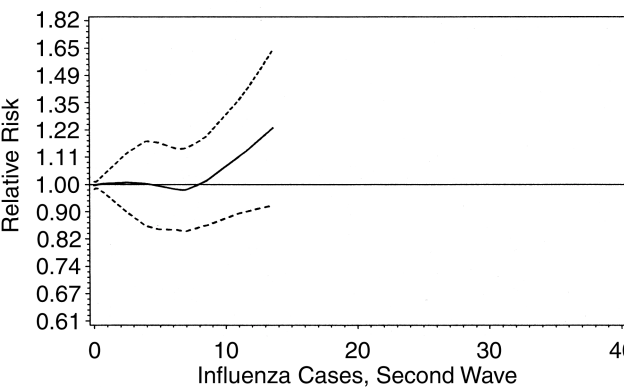


Figure E.6. Dose-response curve (partial fit) of respiratory infection counts used as surrogate measures for second wave of influenza epidemic, early in 1996.

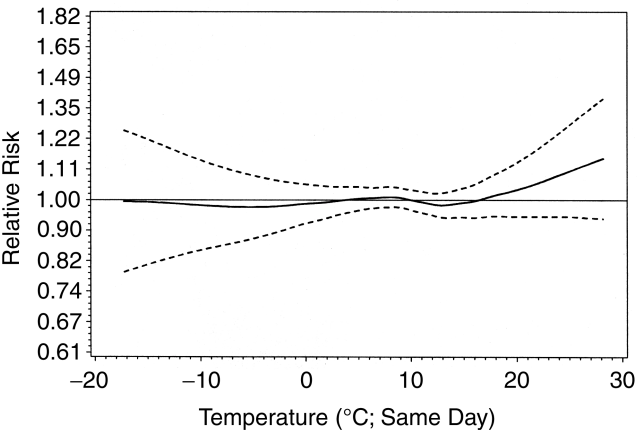


Figure E.7. Dose-response curve (partial fit) of daily mean temperature (corrected for all other elements of confounder model including season

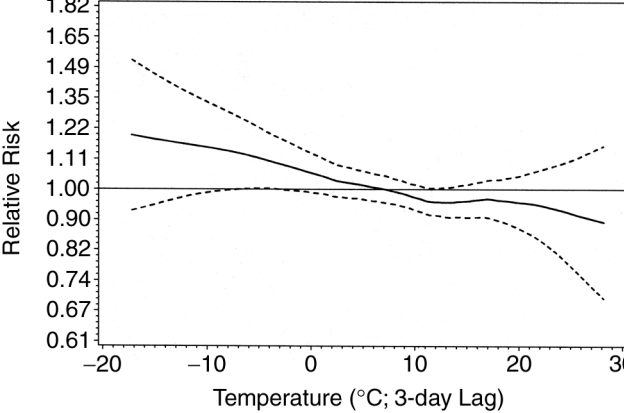


Figure E.8. Dose-response curve (partial fit) of 3-day lagged daily mean temperature (corrected for all other elements of confounder model including season and same day temperature).

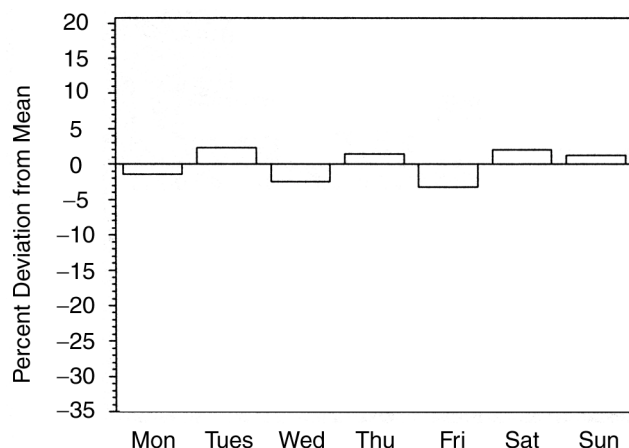


Figure E.9. Day of week pattern of the mortality raw residuals (related to overall mortality mean) after correcting for confounders: deviation (%) of mean raw residuals from raw total mean mortality.

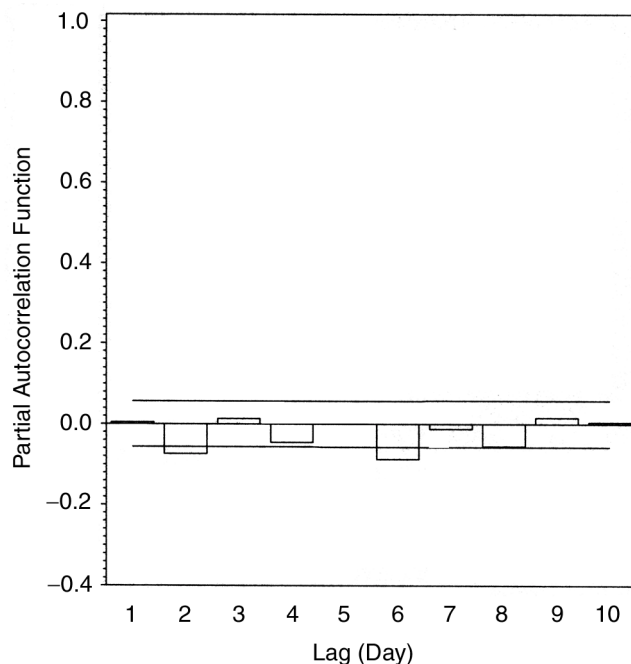


Figure E.10. Partial autocorrelation function of mortality residuals after correcting for confounder model (based on Pearson residuals).

APPENDIX F. Further Subgroup Results

The underlying cause categories (and a slightly different confounder model) show no consistent differences among them; neither does any of them show a preference for a size category different from the one found in the total mortality analysis. About half of the “Other Underlying Cause” subjects did have a cardiovascular disease (mostly congestive heart disease or chronic ischemic heart disease) or

respi-ratory disease (mostly pneumonia) recorded on their certificate besides the underlying cause, which was usually cancer or diabetes.

CONFOUNDER MODELS DIFFER BY SUBGROUP

The results do not look much different from the ones based on a standard parsimonious confounder model. There is still no indication of an age gradient, but there is a slightly larger effect of ultrafine particles on the younger age group (Table F.1). Under differing confounder models, most effects and effect differences seen in the standard model are confirmed. For ultrafine particles, no effect is apparent in the respiratory group (prevalent disease category); clearly, the effect is only on the cardiovascular group here. Based on the underlying cause categorization, the different confounder models cause a few small, inconclusive shifts in the results, possibly due to stronger ultrafine particle effects. None of the data indicate stronger effects by different underlying cause of death.

DELAYS DIFFER BY SUBGROUP

In the total deaths analysis, distinct delay patterns may have been due to different underlying mechanisms. Further, our analyses verify that these patterns are neither caused by inappropriate day-of-week correction nor by lag pattern of the chosen weather model. Different mechanisms may also be at work regarding the effect on subgroups. Investigating this issue for the age groups would be pointless, but the results might prove interesting for the risk groups because different mechanisms would be likely to manifest themselves. Delays worth investigating based on the distributed lag analysis seem to be 0, 1, 4, and 5 days.

The 4-day lag effect of ultrafine particles on the cardiovascular or respiratory group is fully confirmed (Table F.2). Further, a more or less immediate effect on the respiratory risk group (and a smaller one on the “other” group) is evident. The strong immediate effects of $MC_{0.01-2.5}$ and PM_{10} on the respiratory group are confirmed. Here also is a relatively strong 5-day delayed $MC_{0.01-2.5}$ effect on the cardiovascular group. Possibly this effect is at the bottom of the pattern in the distributed lag analyses. Overall, such findings suggest different mechanisms not only for particles of different sizes but also on different risk groups.

Repeating this analysis by underlying disease resulted in the best delay-transformation combination from the total mortality model and in the best for these subgroups, too. Thus, delays also do not differ between risk groups defined by underlying cause of death.

Table F.1. Regression Results with Various Best Single-Day Lag Models

	Lag	TR	RR/IQR ^a	CI	P
By Underlying Cause					
NC _{0.01–0.1} ^b					
Cardiovascular or Respiratory	4	log	1.041	0.983–1.102	0.17
Other			1.054	0.981–1.132	0.15
MC _{0.01–2.5} ^c					
Cardiovascular or Respiratory	0	id	1.028	0.991–1.067	0.14
Other			1.034	0.987–1.082	0.16
PM ₁₀ ^c					
Cardiovascular or Respiratory	0	id	1.041	1.001–1.082	0.05
Other			1.023	0.974–1.076	0.36
By Age in Years (with Different Confounder Models per Subgroup)					
NC _{0.01–0.1} ^b					
<70	4	log	1.061	0.972–1.158	0.19
70–79			1.049	0.954–1.153	0.33
≥80			1.034	0.961–1.112	0.37
MC _{0.01–2.5} ^c					
<70	0	id	1.024	0.968–1.084	0.20
70–79			1.042	0.981–1.108	0.18
≥80			1.028	0.982–1.077	0.24
PM ₁₀ ^c					
<70	0	id	1.036	0.976–1.099	0.24
70–79			1.032	0.982–1.084	0.21
≥80			1.032	0.983–1.083	0.20
By Prevalent Disease (with Different Confounder Models per Subgroup)					
NC _{0.01–0.1} ^b					
Cardiovascular or Respiratory	4	log	1.051	0.996–1.108	0.07
Cardiovascular but Not Respiratory			1.065	1.001–1.134	0.05
Respiratory			1.014	0.916–1.122	0.79
Other Natural			1.026	0.919–1.146	0.65
MC _{0.01–2.5} ^c					
Cardiovascular or Respiratory	0	id	1.027	0.993–1.063	0.12
Cardiovascular but Not Respiratory			1.004	0.963–1.046	0.85
Respiratory			1.084	1.019–1.152	0.01
Other Natural			1.047	0.974–1.125	0.22
PM ₁₀ ^c					
Cardiovascular or Respiratory	0	id	1.040	0.963–1.122	0.09
Cardiovascular but Not Respiratory			1.016	0.974–1.061	0.46
Respiratory			1.073	1.003–1.147	0.04
Other Natural			1.047	0.970–1.130	0.24
By Underlying Causes (with Different Confounder Models per Subgroup)					
NC _{0.01–0.1} ^b					
Cardiovascular or Respiratory	4	log	1.048	0.987–1.112	0.13
Other			1.043	0.965–1.127	0.28
MC _{0.01–2.5} ^c					
Cardiovascular or Respiratory	0	id	1.026	0.987–1.068	0.19
Other			1.037	0.987–1.091	0.15
PM ₁₀ ^c					
Cardiovascular or Respiratory	0	id	1.038	0.996–1.081	0.08
Other			1.029	0.976–1.085	0.29

^a For interquartile range (IQR), see Table 18.^b Particles/cm³.^c µg/m³.

Table F.2. Regression Results by Prevalent Diseases Further Differentiated (Allowing Different Delays by Prevalent Disease)

	Lag	TR	RR/IQR ^a	CI	P
NC_{0.01-0.1} (particles/cm³): Best Single Day Lag					
Cardiovascular or Respiratory ^b	4	log	1.061	1.006–1.119	0.03
Cardiovascular but Not Respiratory	4	id	1.061	1.010–1.115	0.02
Respiratory	1	log	1.168	1.064–1.281	<0.01
Other Natural	1	id	1.072	0.988–1.163	0.09
MC_{0.01-2.5} (µg/m³): Best Single Day Lag					
Cardiovascular or Respiratory ^b	0	id	1.033	0.999–1.068	0.05
Cardiovascular but Not Respiratory	5	log	1.053	0.990–1.119	0.10
Respiratory	0	id	1.123	1.059–1.191	<0.01
Other Natural	0	id	1.019	0.951–1.091	0.59
PM₁₀ (µg/m³): Best Single Day Lag					
Cardiovascular or Respiratory ^b	0	id	1.041	1.004–1.080	0.03
Cardiovascular but Not Respiratory	0	id	1.030	0.987–1.075	0.18
Respiratory	0	id	1.082	1.013–1.156	0.02
Other Natural	1	log	1.052	0.956–1.157	0.30

^a For interquartile range (IQR) see Table 18.^b Results were obtained under a slightly different confounder model.

APPENDICES AVAILABLE ON REQUEST

The following appendices may be obtained by contacting the Health Effects Institute by mail (955 Massachusetts Avenue, Cambridge MA 02139), fax (617-876-6709), or e-mail (pubs@healtheffects.org). Please provide both the Investigators' Report title and the appendix title when requesting appendices.

- G. Quality Control MAS
- H. Standard Operating Procedures Mortality Data
- I. Validation Study for Cause of Death Coding

ABOUT THE AUTHORS

H-Erich Wichmann, born in 1946, studied physics and medicine at the University of Köln. There he also finished his PhD thesis and his MD thesis, as well as his Habilitation. His work in environmental epidemiology began in 1983 at the Medical Institute for Environmental Hygiene in Düsseldorf and continued at the University of Wuppertal, where he received the chair for Labor Safety and Environmental Medicine in 1988. During this period he investigated short-term effects of ambient air pollution on mortality and morbidity, especially during the smog episode 1985. His further interest was in long-term effects of air pollution as well as indoor radon and lung cancer. In 1990, he was appointed director of the GSF Institute of

Epidemiology, Neuherberg, and in 1995, was made a full professor of epidemiology at the University of Munich. Here, he continued and expanded earlier activities and participated in several international projects: Short-term effects were investigated in the framework of the APHEA (Air Pollution and Health: A European Approach) and PEACE (Pollution Effects on Asthmatic Children in Europe) projects. Now his institute is specifically addressing fine and ultrafine particles through the European ULTRA (Exposure and Risk Assessment for Fine and Ultrafine Particles in Ambient Air) study, the HEI-Erfurt study on daily mortality (this report), the HEI-Augsburg study on daily myocardial infarctions (Principal Investigator: Dr Annette Peters), and through research with the EPA–Rochester Particle Center (epidemiologic part in Erfurt). Further activities are cohort studies of newborns, schoolchildren, and adults on risk factors of asthma and allergies; radon (indoors and underground) and lung cancer; cardiovascular studies; genetic and molecular epidemiology.

Claudia Spix, born in 1960, studied statistics at the University in Dortmund. Afterward she began working with Dr Wichmann at the Medical Institute for Environmental Hygiene in Düsseldorf in the field of environmental epidemiology. Among her other projects is the analysis of the 1985 smog episode. After this she continued working with Dr Wichmann in Wuppertal in the Department of Labor Safety and Environmental Medicine, where she predomi-

nantly analyzed data of short-term effects studies of air pollution. During this time she became involved with the APHEA working group. In 1995, she finished her PhD in statistics. Since then, she has worked part time on the analyses for this report for the GSF in Munich. Her other involvement is with the German children's cancer registry at the university clinic in Mainz, where she is specializing in issues of screening for cancer.

Thomas Tuch, born in 1959, studied physics at the University of Heidelberg. Afterward he began to work at the GSF Institute of Inhalation Biology. His main objectives were aerosol characterization of exposure atmospheres in large, whole body exposure chambers for dogs, the development of a new lung function test using inert aerosol particles as a probe, and the design of a mobile lab for ambient aerosol measurements and lung function tests in the context of epidemiologic studies. After five years he joined Dr Wichmann's research group in Wuppertal. He finished his PhD at the University of Wuppertal in the field of environmental epidemiology in 1995. He continued to work in the group of Dr Wichmann at GSF in Munich focusing on the characterization of ambient aerosol in the context of epidemiologic studies.

Gabriele Wölke, born in 1950, studied sociology at the University in Berlin, where she received her degree in 1972. She continued her studies part time to specialize in medical sociology, in which she received her degree in 1985. From 1972 until 1980, she was employed as a sociologist at the Forschungszentrum des Binnenhandels Berlin in Erfurt. From 1980 she worked for the next two years as a scientist at the Institute for Environmental Hygiene in Erfurt. She was involved in projects analyzing the effects of smog and noise. In 1991, she began working with Erich Wichmann at the University of Wuppertal. Among other projects she has been involved in the investigation of short-term effects studies of air pollution. Since 1996, she has been employed at the LMU-IBE Chair of Epidemiology working with Dr Wichmann's group on radon indoor studies and the investigation of short-term effects of ambient air pollution on mortality and morbidity.

Annette Peters, born in 1966, studied biology and mathematics in Konstanz and Tübingen between 1985 and 1992. Her PhD was awarded by the medical faculty of the Ludwig-Maximilians University of Munich in 1996 based on her work on health effects of ambient air pollution on persons with asthma in Central Europe. She began to work at the GSF in 1993 under the supervision of Joachim Heinrich and Erich Wichmann and has broadened the scope of research from respiratory effects of ambient particles to cardiovascular disease outcomes. She worked at Harvard

School of Public Health, Boston Massachusetts, as a visiting scientist under the supervision of Douglas W Dockery for two years during 1993–1994 and 1997–1998. She was awarded an MS in epidemiology from Harvard School of Public Health in 1998. Her main research focus today is the effect of fine and ultrafine particles on respiratory as well as cardiovascular disease outcomes.

Joachim Heinrich, born in 1952, studied mathematics at the University of Jena. He has also had special training in biomathematics. Afterward he began working at the Medical School Erfurt in the fields of cardiovascular and nutritional epidemiology. After this, he worked in the department of labor safety and environmental medicine at the University of Wuppertal, where he established an epidemiologic research unit in eastern Germany including a setup of an ambient particle measurement site. His main research interests are related to air pollution epidemiology (short-term and long-term effects), nutrition and epidemiology of asthma.

Wolfgang G Kreyling, born in 1947, studied physics at Johann-Wolfgang-Goethe University in Frankfurt and received an MSc in physics at Ludwig-Maximilians University in Munich, Germany. After obtaining his PhD from the Technical University of Munich, he joined the GSF–Institute for Radiation Protection. His main research interests are aerosol biophysics, respiratory cell biology, and the interaction of inhaled particles with fluids, cells, and tissues of the respiratory tract of humans and various animal species. In 1987, Dr Kreyling joined the newly founded GSF–Projekt Inhalation, which became the current GSF–Institute for Inhalation Biology in 1994. He broadened his research to include particle-lung interaction during exposure to sulfur-related air pollutants and more recently after exposure to ultrafine surrogate particles. In this study, he supervised the ambient air measurements at Erfurt.

Joachim Heyder, born in 1939, studied physics at the University of Frankfurt, Main, Germany, and received an MSc in physics in 1965 and a PhD in 1968. In 1976, he received the *venia legendi* for biophysics from the university's physics department. In 1965, he joined the Max-Planck Institute for Biophysics in Frankfurt, and in 1968, the GSF–Institute for Biophysical Radiation Research, Frankfurt. Following postdoctoral training at the London School of Hygiene and Tropical Medicine, Dr Heyder initiated a program on biomedical aerosol research at the GSF Institute which became part of an international effort to understand aerosol particle behavior in the respiratory system. In 1984, he was invited to work as a visiting associate professor at the Respiratory Biology Program at the Harvard School of Public Health in Boston. Two years later, he became head of

the GSF-Projekt Inhalation, in which all activities in biomedical aerosol research of the GSF were combined at the main campus of this research center in Neuherberg, Munich. In 1994, Dr Heyder was appointed director of the institute, which was then renamed the GSF-Institute for Inhalation Biology. The research interest of this institute currently focuses on the risk assessment of fine and ultrafine particles and the application of aerosol science in aerosol diagnostics and therapy.

ABBREVIATIONS AND OTHER TERMS

AGI	Arbeitsgemeinschaft Influenza
AIC	Akaike Information Criterion
AP	accumulation mode particles (0.1–1.0 μm) central in context of measuring sites: the site run by the study
APHEA	Air Pollution and Health: A European Approach
CI	confidence interval
CO	carbon monoxide
COPD	chronic obstructive pulmonary disease
CPC	condensation particle counter
cv	cardiovascular
<i>df</i>	degrees of freedom
DMA	differential mobility analyzer
DMPS	differential mobility particle sizer
DWD	Deutscher Wetterdienst
EPA	US Environmental Protection Agency
EU	European Union
GAM	generalized additive modeling
GSD	geometric standard deviation
ICD-9	<i>International Classification of Diseases, Ninth Revision</i>

ICD-10	<i>International Classification of Diseases, Tenth Revision</i>
id	no transformation
IHB	GSF Institute of Inhalation Biology
IQR	interquartile range
ISS	GSF Institute of Radiation Protection
LAS-X	optical laser aerosol spectrophotometer
LOESS	locally weighted smoothing scatterplot
MAS	mobile aerosol spectrometer
MC	mass concentration of particles
MONICA	monitoring of trends and determinants of cardiovascular disease
NC	number concentration of particles
NMMAPS	The National Morbidity, Mortality, and Air Pollution Study
NO	nitric oxide
NO ₂	nitrogen dioxide
PACF	partial autocorrelation function
PEF	peak expiratory flow
PM _{2.5}	particle mass $\leq 2.5 \mu\text{m}$ in diameter
PM ₁₀	particle mass $\leq 10 \mu\text{m}$ in diameter (impactor data)
PSA	particle strong acidity
RR	relative risk
SO ₂	sulfur dioxide
SO ₄ ²⁻	sulfate ions
TR	transformation
TSP	total suspended particles
ULTRA	Exposure and Risk Assessment for Fine and Ultrafine Particles in Ambient Air
WHO	World Health Organization

INTRODUCTION

Evidence from epidemiologic studies supports an association between particulate matter and mortality (Pope and Dockery 1999), but uncertainty persists as to which physical or chemical characteristics of particulate matter underlie the observed associations. On the basis of lung deposition models used by the International Commission on Radiological Protection, the smallest particles, ultrafines, are most efficiently deposited deep in the lungs in the alveolar region. Although ultrafines contribute little to mass, they are present in high numbers and thus may be important in terms of health effects.

At the time the study was funded, no epidemiologic studies had addressed the association of ultrafines and mortality. In the late 1990s, epidemiologic studies that measured number and mass of ultrafines evaluated respiratory disease, not mortality (Pekkanen et al 1997; Peters et al 1997; Tiittanen et al 1999). These studies, like the current study, investigated the association and timing between high air pollution and adverse health outcome in a time-series analysis. When air pollution and health outcomes are linked closely in time, a time-series analysis will show associations on a daily basis. A lagged analysis will show an effect of air pollution that occurs one or more days later. Timing of effects in epidemiologic studies is typically evaluated by examining pollutant levels on the day of adverse health outcome (lag 0), prior day (lag 1), 2 days prior (lag 2), 3 days prior (lag 3), etc. The two approaches to handling lags are a single-day lag or lag averaged over several days. Because each approach requires assumptions regarding which lag is most appropriate, assessment of timing should be based on both types of information.

In July 1994, HEI requested proposals (RFA 94-2) for epidemiologic studies to identify persons at increased risk of death from particles and the conditions of pollutant exposure and other factors associated with increased likelihood of early death. In response to RFA 94-2, a team from the National Research Center for Environment and Health (GSF)* in Neuherberg, Germany, led by H-Erich Wichmann submitted a proposal to study the association of

daily mortality with fine and ultrafine particles in Erfurt, Germany, and were selected by the HEI Research Committee to conduct the study.[†]

EFFECTS OF PARTICLE SIZE

Particles smaller than 2.5 μm in aerodynamic diameter ($\text{PM}_{2.5}$) can be divided into two major fractions: fines (0.1 to 2.5 μm) and ultrafines ($< 0.1 \mu\text{m}$). Ultrafines are less stable than fines: over a period lasting from seconds to minutes to hours, they tend to coagulate to form larger particles. The speed of this conversion depends on the size distribution, concentration of aerosol, and thermodynamic conditions. Because ultrafines are constantly generated from atmospheric processes (such as gas-to-particle conversion) and from combustion sources, however, they are always present in the ambient air at some level. Currently, the composition and concentration of ultrafines in ambient air are not well characterized. One earlier study measured ultrafines in an urban atmosphere at several hundred thousand particles per cubic meter, in sizes from 0.017 to 0.50 μm (Castellani 1993). Ultrafines that may be present in ambient air may be composed of carbon (Willeke and Baron 1993) or metals (such as platinum and its oxides), both of which are believed to be emitted from vehicle tailpipes (Schl  gl et al 1987).

Because different parts of human airways differ in size and structure, particles of different sizes are deposited with varying efficiency at different locations in the respiratory tract and may have distinct biological effects. For example, total deposition of inhaled particles in the respiratory tract is greater for ultrafines than for fines. In addition, 40% to 50% of 0.02- μm particles (ultrafines) inhaled are estimated to be deposited in the critical alveolar region of the human lung (US Environmental Protection Agency [EPA] 1996). In contrast, only 5% to 10% of inhaled 0.3- μm particles (fines) are deposited in this region. Furthermore, the rate of phagocytosis of particles by macrophages reportedly depends on particle size and is lower for ultrafines than for fines (Oberd  rster et al 1992), with the result that ultrafines are cleared from the respiratory tract more slowly. Studies comparing the fate of insoluble particles

* A list of abbreviations and other terms appears at the end of the Investigators' Report.

This document has not been reviewed by public or private party institutions, including those that support the Health Effects Institute; therefore, it may not reflect the views of these parties, and no endorsements by them should be inferred.

† Dr H-Erich Wichmann's 3.5-year study, Daily Mortality and Fine and Ultrafine Particles in Erfurt, Germany, began in August 1995. The total expenditures were \$559,460. This cost includes funding for additional research and a second report, currently in review, in addition to the present report. The Investigators' Report was received for review in August 1999. A revised report, received in December 1999, was accepted for publication in April 2000. During the review process, the HEI Review Committee and the investigators had the opportunity to exchange comments and to clarify issues in the Investigators' Report and in the Review Committee's Commentary.

have indicated that some types of ultrafines are more likely than larger particles to escape phagocytosis and to translocate to the lung's interstitial region and to other organs. This process may provide a mechanism for ultrafines to exert systemic effects (Ferin et al 1990, 1992).

Ultrafine particles constitute only 1% to 8% of the mass of ambient particulate matter, but they are present in very high numbers (Peters et al 1997; Hughes et al 1998). For example, the weight of a single 2.5- μm particle is the same as that of over 2 million 0.02- μm particles (Oberdörster et al 1995). As a consequence of the smaller diameter and increased number of ultrafine particles compared with fine particles in a fixed volume, ultrafines have a larger surface area for biological interactions and the adsorption of toxic agents. Both sizes can act as carriers of adsorbed reactive gases, oxygen free radicals, transition metals, or organic compounds to the deep lung. By virtue of their larger surface areas per amount of mass, however, ultrafines may transport a disproportionate amount of toxic materials adsorbed to their surfaces compared with larger particles and may also have more surface area available for reactions with cellular constituents. All of these factors—higher lung deposition, slower phagocytosis, decreased phagocytosis, and larger surface area for interaction—may contribute to the ability of ultrafines to injure the alveolar epithelium.

EPIDEMIOLOGY

Few studies have investigated the effect of ultrafines on human health. A recent epidemiologic study measured the association between respiratory health and fine and ultrafine particles in Erfurt (Germany) in a panel of subjects with asthma during the winter of 1991/1992 (Peters et al 1997). The investigators found that the 5-day mean number of particles (dominated by ultrafines) was more strongly associated with a decrease in peak expiratory flow in the evening and with the prevalence of cough than the 5-day means of particles up to 10 μm in diameter (PM_{10}). However, the lag 0 mass of PM_{10} was more strongly associated with the prevalence of cough than was the number of particles at lag 0. Both particle sizes showed similar effect estimates for feeling ill during the day. This study points to the need for more specific definition of particulate matter exposure because the findings were not conclusive about a possible role of ultrafines.

Pekkanen and colleagues (1997) compared the associations of black smoke, PM_{10} , and size-fractionated ultrafines (from 0.01 to 10 μm in diameter) with reductions in peak expiratory flow among 39 children with asthma (ages 7 to 12 years) during a 57-day follow-up period in Finland. The results did not show a consistent pattern

across the size ranges from 0-day to 3-day lags or with a 4-day average of lags 0 to 3. Although adjusted models of morning and evening peak expiratory flow showed some associations with ultrafines, no consistent pattern of association emerged across the different lags, and the largest significant coefficient was reported for PM_{10} ($\beta = -2.24$, $P < 0.01$, 4-day average). The results were sensitive to high values, however: exclusion of 5 study days with high particle levels resulted in no significant associations.

Tiitinen and colleagues (1999) studied associations between particles (black carbon [a more analytically rigorous measurement of historically used black smoke], PM_{10} , $\text{PM}_{2.5}$, and number concentration of particles from 0.01 to 10 μm in diameter) and daily chronic respiratory symptoms. Among the 49 asthmatic children (ages 8–13 years) studied for six weeks in spring 1995 in Finland, no consistent effects of ultrafines or fines were found for cough or reduction in peak expiratory flow and possible associations seemed to vary by lag.

TECHNICAL EVALUATION

AIMS AND OBJECTIVES

The overall aims of the current study were to characterize ambient air pollution based on measurements of fines, ultrafines, and gaseous pollutants and to assess the association of ultrafines and fines with mortality. The study had three specific objectives: (1) to identify more precisely which size-fractionated ultrafines or fines were associated with general and cause-specific mortality, (2) to examine whether mortality was more strongly associated with particle mass or number concentrations, and (3) to explore which groups within the population were at greatest risk of death related to air pollution.

STUDY DESIGN

The investigators used a time-series approach to look at short-term changes in particle concentration and mortality over a 3.5-year period in Erfurt, Germany, a geographically self-contained community located in a valley surrounded on three sides by mountains. Erfurt had a population of roughly 200,000 people and about 5 to 6 deaths per day.

Particulate matter was evaluated at a single sampling site (the GSF station) located approximately 50 meters from a major road in a mixed-use area (residences, offices, a school, and a hospital). The mass and number concentration of ultrafines, fines, and larger particles, as well as concentrations of gaseous pollutants and temperature, were continuously recorded each day for 40 months.

Particulate data were gathered using a mobile aerosol spectrometer (MAS), which comprised several different instruments that counted particles. This long monitoring period with daily and hourly measurements of defined quality is unique. Particle mass (PM_{2.5} and PM₁₀), sulfate, and acidity were also measured using the traditional filter-based Harvard impactor without a denuder. Meteorologic data (temperature, relative humidity, wind speed, wind direction) were gathered at the GSF sampling site. Gaseous pollutants (SO₂, NO₂, CO) were measured at the GSF sampling site and two state-run sites. The investigators obtained daily mortality counts in Erfurt from the local health authority and influenza data from a commercial source.

METHODS

Mortality Data

The investigators gathered mortality data from the local, state-run health authority. Anonymous copies of the death certificates included data on immediate, underlying, and contributing causes of death. Based on this information, the investigators identified two main classifications: 1) *underlying* cause of death, or the disease or condition identified by the physician signing the death certificate as being the underlying cause of death; and 2) *prevalent* conditions, or any mention of cardiovascular or respiratory disease on the death certificate. In the main report, the investigators stratified cause-specific mortality based on prevalent conditions; regression results using the traditional underlying cause of death are presented in Appendix F.

PM Data

Mass and number were measured for three size fractions of ultrafines (0.01–0.03, 0.03–0.05, and 0.05–0.1 μm in diameter) and three size fractions of fines (0.1–0.5, 0.5–1.0, and 1.0–2.5 μm in diameter). More traditional particulate matter measurements included larger particles of 2.5–10 μm and 10–40 μm in diameter, based on total suspended particles, PM₁₀, and PM_{2.5}.

Analytic Methods

These particle sizes extend over three orders of magnitude. Because no single instrument was capable of making measurements across this broad range, three different instruments were used; each measured particle size by a different method. The three instruments were combined into a measurement system the investigators called the mobile aerosol spectrometer (MAS).

1. Differential Mobility Analyzer Particles with a diameter of 0.01–0.5 μm were counted using a differential mobility analyzer followed by a condensation particle counter (a combination of instruments termed a *differential mobility particle sizer*). The analyzer separated particles into 13 size bins. To do this, the aerosol was passed through a radioactive bipolar charger (⁸⁵K) that established a bipolar equilibrium charge level on the particles. Nearly all particles from 10 to 300 nm in diameter received either a single positive, single negative, or zero charge. The particles were then separated according to their electrical mobility. The number of particles in each size bin was then counted.

2. Optical Laser Aerosol Spectrometer The number of particles with a diameter of 0.1–2.5 μm was counted with an optical laser aerosol spectrometer (LAS-X) that classified particles according to their light-scattering properties. The extent to which a particle scatters light of a particular wavelength depends on the size of the particle and certain physical characteristics such as density and refractive index.

3. Condensation Particle Counter This counter was used for particles ranging from 0.003 to 3.0 μm . Particles were counted by first condensing alcohol vapor onto particles in the sample flow, creating aerosol droplets large enough to be detected efficiently with a light-scattering technique. Upon entering the counter, the aerosol sample passed through a saturator block where the alcohol evaporated into the sample stream. The sample then passed into a vertical condenser tube cooled by a thermoelectric heat pump. Here, the alcohol vapor supersaturated and condensed onto virtually all particles above the minimum detectable size regardless of chemical composition. As they left the condenser tube, the droplets passed through an optical detector, which either counted single particles up to concentrations of 10⁴/cm³ or determined photometrically the aerosol concentration at higher concentrations.

4. Harvard Impactor

In addition to the particle sizing instruments, Harvard impactors were used to collect integrated particulate matter samples, which then were analyzed for mass (PM_{2.5} and PM₁₀). Data from the more traditional impactors were sampled at least every other day. PM_{2.5} was used for quality control of the MAS-derived data, while PM₁₀ was intended for epidemiologic analysis.

Statistical Methods

The statistical models for daily mortality were developed sequentially, first modeling longer-term trends in

mortality (due to season, influenza epidemics, etc) then adding meteorologic terms (eg, temperature, relative humidity). These adjustments were done separately for total mortality and prevalent conditions of respiratory and/or cardiovascular diseases. The choice of variables and their specification were guided both by prior knowledge of biological plausibility and by statistical criteria (eg, goodness of fit of the model to the data based on Akaike Information Criterion, reduction in overdispersion relative to the Poisson error model, and reduction in serial correlation of the residuals). After fitting the basic model, air pollution variables were added. The relative risk, defined as the relative increase in risk of death per defined change in pollutant concentration (the difference between the 25th to 75th percentiles of their distributions) was calculated.

After fitting the basic model (the best model adjusting for confounding time trends), the next step was to fit the main risk variable of interest (air pollution) to the lag model. In the current study, the best single lag was based on the lowest *P*-value (two-sided). For the effect over multiple days, the investigators fitted a polynomial distributed lag function; as a moving day average, this type of model smoothes random spikes. Polynomial distributed lag weights derived from this function correspond to the individual day lag; the weights allow a comparison of relative effect across the selected series of days. The authors have reported results from both best single-day lag and multiple-day averages.

RESULTS

Health Endpoints

Daily mortality counts from death certificates were collected for a total of 6,793 deaths that occurred between August 1995 and December 1998. Mean deaths from natural causes among Erfurt residents was 4.88 deaths/day. The investigators identified cardiovascular or respiratory disease as a prevalent cause of death on 81% of all death certificates.

PM Data

Number concentration (NC) was measured for each particle size range. Based on the assumption of the sphericity of particles and the apparent mean density, mass concentration (MC) was calculated for each particle size range from the number concentration. The total daily average number was 18,000 particles/cm³; the greatest proportion (88%) of this number represented particles below 0.1 μ m. The authors have discussed the results for the ultrafine fraction in terms of NC_{0.01–0.1}, the number of particles in the size range of 0.01 to 0.1 μ m in diameter. The total daily

average mass was 26 μ g/m³; the greatest proportion (97%) of the mass was contributed by the larger particles (0.1–2.5 μ m in diameter). Note that the authors have discussed the results for fines in terms of MC_{0.01–2.5}, which is analogous to PM_{2.5}, but MC_{0.01–2.5} includes the size range covered by ultrafines (although very little of the mass was contributed by the smaller particles (0.01–0.1 μ m)). The other average concentrations were 38 μ g/m³ for PM₁₀, 17 μ g/m³ for SO₂, 36 μ g/m³ for NO₂, and 600 μ g/m³ for CO.

Ambient air pollution correlated strongly with seasons, with maximum concentrations occurring in the winter. Over the years, however, the mass of fine particles in each winter decreased while the number remained constant. The investigators interpreted this finding to mean that the number of fine particles had diminished while the number of ultrafine particles had increased.

Regression

Both ultrafines and fines were consistently associated with mortality. Results from the best single-day lags suggested relative differences in effect for ultrafines and fines. By comparison, relative risks based on the polynomial distributed lag models were around 1.03 with overlapping confidence intervals for each size-fractionated particle group (see Figure 33). The investigators reported a delayed effect for ultrafines. For example, the size of the weights for NC_{0.01–0.1} increased from lag 0 (0.44) to lag 4 (1.02) (see Table 20), but two of the smaller ultrafines sizes had larger weights on day 0 than day 5 (NC_{0.01–0.03} and NC_{0.05–0.1}). The investigators also found an immediate effect for fines, but for MC_{0.01–2.5}, the polynomial distributed lag weights were similar for lag 0 (0.72) and lag 5 (0.62) (see Table 20). In summary, these findings do not show a consistent pattern regarding relative or temporal differences in effect across the particle sizes.

The authors investigated total mortality grouping by different disease subgroups. When grouping by *prevalent* disease (see Table 29), NC_{0.01–0.1} relative risks of death due to cardiovascular causes were largest for longer lags (lag 4), whereas MC_{0.01–2.5} and PM₁₀ had the highest relative risks for immediate deaths due to respiratory causes (lag 0). Little difference in the pattern of results was observed when classifying disease by *underlying* cause of death (see Appendix F, Table F.1).

Gaseous pollutant results were presented for best single-day lags and models. A strong immediate association between total mortality and SO₂ was followed by a weaker, delayed association (lag 3). These results were in contrast to those for NO₂ and CO, which showed only delayed associations (lag 4).

Sensitivity Analyses

The researchers investigated the sensitivity of their results for air pollutants ($NC_{0.01-0.1}$, $MC_{0.01-2.5}$, PM_{10} , and all gaseous pollutants) to various factors, models, and subgroups. Log-transformed curves often fit the data better than nontransformed curves. Little or no change of effect was observed when the models took into account variations of the correction for day of week, meteorology, or seasonal smooth. After inclusion of indicator variables representing effect modification of the four seasons, however, relative risks for winter were highest for all air pollutants except CO, for which the risks were greater in summer and fall. After the authors included variables for each of the three winters of the study, the strongest effect was observed for the third winter. Exclusion of the independent influenza data reduced all PM effects, which suggests the importance of adjusting for such epidemics in all time-series studies.

In two-pollutant models that included particulate matter, one gaseous pollutant, and interaction terms, $NC_{0.01-0.1}$ relative risks for total mortality were not sensitive to the presence of a gas. They remained about 1.03 regardless of inclusion of SO_2 , NO_2 , or CO (see Table 25), but inclusion of SO_2 reduced the total mortality relative risks of $MC_{0.01-2.5}$ and PM_{10} .

Age at death (< 70, 70 to 79, 80+ years) did not affect the relative risk for either $MC_{0.01-2.5}$ or PM_{10} . However, $NC_{0.01-0.1}$ relative risks were largest (RR = 1.061; 95% confidence interval [CI] 0.972–1.158) for persons whose age at death was less than 70 years.

In Figure 37, the investigators summarize the best lags from the best model results from both standard analyses and sensitivity analyses, according to disease group. Based on these results, they report an immediate association between prevalent respiratory deaths and $NC_{0.01-0.1}$, $MC_{0.01-2.5}$, and PM_{10} . For prevalent cardiovascular deaths, the investigators observed a suggestion of a delayed association for $NC_{0.01-0.1}$ and $MC_{0.01-2.5}$ with an immediate association for PM_{10} .

DISCUSSION

Several issues inherent in epidemiologic time-series studies complicate interpretation of relative effects among air pollutants. Separation of the effects of one pollutant from those of others is extremely difficult due to collinearity of various pollutants; highly correlated particle metrics, copollutants, and other unmeasured pollutants may exist in a mixture with many common sources. Also difficult to separate is the temporal variation

of associations between pollutant and mortality, whether effects are observed on the same day as the exposure indicators or whether the health endpoint lags one, two, three, or more days between recorded concentration and the health endpoint. Estimated effects can be sensitive to different analytic approaches, to inclusion of two or more pollutant variables in the same model, and to sensitive subpopulations. At the same time, multiple testing of many pollutants over several different lags and use of many different models can produce statistically significant associations by chance alone. In addition, the use of one central monitoring site to evaluate exposure of a mobile human population can produce measurement error; that is, error in assuming that exposure of an individual is equal to the level measured by instruments some distance away. Finally, measured values of air pollutants can depend on the sampling techniques used. For example, the sulfate from total suspended particles may have added measurement error when ambient SO_2 reacts with the sampler filter media (glass fiber filter) to form SO_4^{2-} , commonly called sulfur artifact.

LAG PATTERNS

Currently, no biological evidence supports a particular lag. Although many investigators of time-series studies have used the best lag approach, this method can bias the results toward statistically significant associations (positive and negative). The current investigators used both best single-day lags and polynomial distributed lags in the main analyses and sensitivity analyses although only the best lags were used for PM metrics ($NC_{0.01-0.1}$, $MC_{0.01-2.5}$, PM_{10}) and gaseous pollutants (SO_2 , NO_2 , CO) in their two-pollutant models. In their interpretation of the results, the HEI Review Committee used the entire sequence of lag effects and the polynomial distributed lag approach.

The investigators have reported a suggestion of a delayed effect for ultrafines versus an immediate effect for fines. The HEI Review Committee has some concern regarding statements about timing of effect. Although a delayed effect for ultrafines was suggested by the increase in weights for $NC_{0.01-0.1}$ from lag 0 to lag 4, two of the smaller ultrafine sizes had larger weights on day 0 than on day 5 ($NC_{0.01-0.03}$ and $NC_{0.05-0.1}$). Thus no consistent pattern emerged among the weights for number concentration to indicate a consistent temporal effect (delayed or immediate). Also, for mass concentration, the weights were roughly equivalent for day 0 and day 5. In summary, the HEI Review Committee felt that weight of evidence did not support statements regarding different timing of effects.

SENSITIVITY ANALYSES

In general, the HEI Review Committee felt the investigators did not fully evaluate their major findings in light of the results of their sensitivity analyses. The relative risks for $MC_{0.01-2.5}$ and PM_{10} decreased when SO_2 was added to the model, although this was less true for $NC_{0.01-0.1}$. Also, the investigators combined the best lags from the best single-day models (standard models and sensitivity models), implying that the findings were sensitive to modeling choices.

GASEOUS POLLUTANTS

Different interpretations from those of the investigators could be made regarding the point estimates of the gaseous pollutants. The same arguments used by the investigators to interpret the impact of gases on mortality could have been used for particles: (1) gaseous pollutants should not have a flat dose-response at high concentrations; (2) concentrations of gaseous pollutants were too low to worry about; and (3) gases were surrogates for other pollutants. Also, several relative risks for gaseous pollutants were above unity, including some that were statistically significant and some that had effect sizes of the same general magnitude as those for particulate matter.

PREVALENT VERSUS UNDERLYING CONDITION

The investigators chose to stratify cause-specific mortality based on prevalent diseases rather than underlying cause of death. Death certificate data are relatively reliable to identify cause of death, but such data do not reliably identify risk of death in a certain group, as indicated by conditions existing at the time of death. Accuracy of prevalent conditions depends upon whether the physician lists significant conditions present at death. Doctors differ in how conscientiously they include these prevalent conditions on the death certificate so the validity of these data varies.

CHARACTERIZATION OF EXPOSURE TO ULTRAFINE PARTICLES

The information required to characterize human exposure to ultrafines in Erfurt (the spatial distribution of ultrafines in Erfurt and the time course of a potential effect of ultrafines on human health) is not known. However, what is known about ultrafines in Erfurt raises questions about the ultrafines-mortality relation reported in the current study.

Ambient ultrafines are generated via combustion processes; in Erfurt the main combustion sources were

industry, domestic heating, and motor vehicle exhaust. As shown in the report, the ultrafine concentrations were high from Monday through Friday but decreased beginning Friday and continuing over the weekend. This pronounced day-of-the-week pattern of ultrafines suggests that automobile traffic (or mobile source) is the major source of ultrafines in Erfurt.

The life cycle of ultrafines raises the question of whether a single monitoring station measuring ultrafine levels can adequately represent the levels for the entire geographical area in which the population resides. The area of Erfurt is approximately 150 square kilometers. Under conditions of low wind velocity or stagnant weather conditions conducive to inversions, a gradient of ultrafine levels may occur across the study area if the mobile source density is not uniform where the people are located. Thus as distance increases between mobile sources (eg, traffic) and individuals (at work or at home), the exposure to ultrafines may decrease, raising uncertainty as to how well a single monitoring station represents the population's exposure to ultrafines. Cyrus and associates (1998) reported that concentrations of $PM_{2.5}$, PM_{10} , and other air quality parameters measured at the GSF site and other sites in Erfurt did not differ appreciably from each other. If so, a single monitoring station might represent exposure adequately for those pollutants measured; however, to know whether this homogeneity is true for ultrafines would require exposure comparisons specific to ultrafines, information that is currently not available.

SUMMARY AND CONCLUSIONS

This study was the first to investigate associations of mortality with detailed size categories of ultrafine and fine particles, and the results provide the scientific community with substantial new evidence of an association between ultrafines and human health. The investigators found comparable effects for ultrafine and fine particles and suggest a delayed effect for ultrafines versus an immediate effect for fines. The HEI Review Committee agreed with the authors' conclusions that associations were observed between mortality and ultrafines and fines, but the Committee did not find a consistent pattern indicating either a delayed or an immediate effect for these two size-fractionated metrics. The Committee also did not agree with the investigators' interpretation that the association of SO_2 with mortality was an artifact, given the similar magnitude of effect sizes between particulate matter and SO_2 and the persistence of an SO_2 effect in the two-pollutant analyses.

Analytic techniques developed by the investigators addressed several issues of global concern inherent to

epidemiologic studies. For example, instead of evaluating fines using $PM_{2.5}$, which contains elements of the smaller size indices, the investigators used the size-fractionated metric $MC_{0.01-2.5}$, which represents the mass calculated from particle number. Use of a more precise particle matter metric is a start toward addressing the issue of collinearity among complex mixtures of air pollutants, although the issue of dealing with other highly correlated air pollutants remains. Because the MAS calculated particle mass from particle counts, the artifactual formation of SO_4^{2-} in traditional filter-based PM samplers was avoided. Finally, earlier work in Erfurt suggests that measurement error for $PM_{2.5}$, PM_{10} , and other air quality parameters may not be a concern for fine particle air pollution but may still be an issue for the ultrafine fraction.

Despite these analytic strengths, the HEI Review Committee has concerns regarding the statistical analyses and interpretation. Performance of numerous statistical tests (as presented in this report) increases the likelihood of observing statistically significant results by chance alone. Also, the overall particulate matter findings were sensitive to confounders (influenza epidemics), other air pollutants (especially SO_2), and age at death. While the relative risks for $NC_{0.01-0.1}$ were relatively insensitive to the presence of gases, these rates increased for the youngest age group (< 70 years). Finally, results for both ultrafines and fines were highly sensitive to definition of lag (best single-day lag versus polynomial distributed lag). Therefore, the pattern of lag results did not support either a clear separation of effect or different timing of effect for ultrafines versus fines.

This study is a major contribution to the body of knowledge on actual particulate matter levels, and the results provide the first evidence that ultrafine particles as well as fine particles are associated with mortality. Despite the unique analytic techniques developed by the investigators, important limitations to the results remain (eg, interpretations regarding timing of effect). Although the ultrafine fraction has been shown to be associated with human mortality, no clear pattern of associations indicates relative or temporal differences between ultrafine and fine particles.

ACKNOWLEDGMENTS

The Health Review Committee thanks Dr JoAnn Ten Brinke for help in preparing the Commentary. Thanks also to Elizabeth Coolidge-Stolz, Sally Edwards, and Julia Campeti for editing, Frederic R Howe and Sybil N Carey for proofreading, and John B Abbott for desktop publishing the Investigators' Report and Commentary.

REFERENCES

- Castellani CM. 1993. Characterization of the atmospheric aerosol in an urban area and the vicinity of a main highway. In: ENEA Environment Department Meetings and Seminars Held in Bologna and Rome. INTO 7:35–55.
- Cyrus J, Heinrich J, Brauer M, Wichmann H-E. 1998. Spatial variability of acidic aerosols, sulfate, and PM_{10} in Erfurt, East Germany. *J Expo Anal Environ Epidemiol* 8:447–464.
- Ferin J, Oberdörster G, Penney DP, Soderholm SC, Gelein R, Piper HC. 1990. Increased pulmonary toxicity of ultrafine particles? I. Particle clearance, translocation, morphology. *J Aerosol Sci* 21:381–384.
- Ferin J, Oberdörster G, Penney DP. 1992. Pulmonary retention of ultrafine and fine particles in rats. *Am J Respir Cell Mol Biol* 6:535–542.
- Hughes LS, Cass GR, Jones J, Ames M, Olmec L. 1998. Physical and chemical characterization of atmospheric ultrafine particles in the Los Angeles area. *Environ Sci Technol* 32:1153–1161.
- Oberdörster G, Ferin J, Gelein R, Soderholm S, Finkelstein J. 1992. Role of alveolar macrophage in lung injury: Studies with ultrafine particles. *Environ Health Perspect* 97:193–199.
- Oberdörster G, Gelein RM, Ferin J, Weiss B. 1995. Association of particulate air pollution and acute mortality: Involvement of ultrafine particles? *Inhalation Toxicol* 7:111–124.
- Peters A, Wichmann HE, Tuch T, Heinrich J, Heyder J. 1997. Respiratory effects are associated with the number of ultrafine particles. *Am J Respir Crit Care Med* 155:1376–1383.
- Pekkanen J, Timonen KL, Ruuskanen J, Reponen A, Mirme A. 1997. Effects of ultrafine and fine particles in urban air on peak expiratory flow among children with asthmatic symptoms. *Environ Res* 74:24–33.
- Pope CA III, Dockery DW. 1999. Epidemiology of particle effects. In: *Air pollution and Health* (Holgate ST, Samet JM, Koren HS, Maynard RL, eds). Academic Press, Boston MA.
- Schlögl VR, Indlekofer G, Oelhafen P. 1987. Mikropartikelemissionen von Verbrennungsmotoren mit Abgasreinigung-Röntgen-Photoelektronenspektroskopie in der Umweltanalytik. *Angew Chem* 99:312–322.
- Tiittanen P, Timonen KL, Ruuskanen J, Mirme A, Pekkanen J. 1999. Fine particulate air pollution, resuspended road

dust and respiratory health among symptomatic children.
Eur Respir J 13:266–273.

US Environmental Protection Agency. 1996. Air Quality
Criteria for Particulate Matter. Document EPA/600/P-95/
001. Office of Research and Development, Washington DC.

Willeke K, Baron PA, eds. 1993. Aerosol Measurement—
Principles and Techniques and Applications. Van Nos-
trand Reinhold, New York NY.

RELATED HEI PUBLICATIONS: PARTICULATE MATTER

Report Number	Title	Principal Investigator	Publication Date*
Research Reports			
40	Retention Modeling of Diesel Exhaust Particles in Rats and Humans	CP Yu	1991
45	The Effects of Exercise on Dose and Dose Distribution of Inhaled Automotive Pollutants	MT Kleinman	1991
68	Pulmonary Toxicity of Inhaled Diesel Exhaust and Carbon Black in Chronically Exposed Rats		
	Part I. Neoplastic and Nonneoplastic Lung Lesions	JL Mauderly	1994
	Part II. DNA Damage	K Randerath	1995
	Part III. Examination of Possible Target Genes	SA Belinsky	1995
75	Ozone Exposure and Daily Mortality in Mexico City: A Time-Series Analysis	DP Loomis	1996
83	Daily Changes in Oxygen Saturation and Pulse Rate Associated with Particulate Air Pollution and Barometric Pressure	DW Dockery	1999
86	Statistical Methods for Epidemiologic Studies of the Health Effects of Air Pollution	W Navidi	1999
91	Mechanisms of Morbidity and Mortality from Exposure to Ambient Air Particles	JJ Godleski	2000
93	Effects of Concentrated Ambient Particles in Rats and Hamsters: An Exploratory Study	T Gordon	2000
94	The National Morbidity, Mortality, and Air Pollution Study	JM Samet	2000
	Part I. Methods and Methodologic Issues		
	Part II. Morbidity and Mortality from Air Pollution in the United States		
95	Association of Particulate Matter Components with Daily Mortality and Morbidity in Urban Populations	M Lippmann	2000
96	Acute Pulmonary Effects of Ultrafine Particles in Rats and Mice	G Oberdörster	2000
97	Identifying Subgroups of the General Population That May Be Susceptible to Short-Term Increases in Particulate Air Pollution: A Time-Series Study in Montreal, Quebec	M Goldberg	2000
99	A Case-Crossover Analysis of Fine Particulate Matter Air Pollution and Out-of-Hospital Sudden Cardiac Arrest (In press)	H Checkoway	2000

Continued

* Reports published since 1990.

Copies of these reports can be obtained by contacting the Health Effects Institute, 955 Massachusetts Avenue, Cambridge MA 02139. Phone (617) 876-6700 FAX (617) 876-6709 E-mail pubs@healtheffects.org www.healtheffects.org

RELATED HEI PUBLICATIONS: PARTICULATE MATTER

Research Reports

Report Number	Title	Principal Investigator	Publication Date*
------------------	-------	---------------------------	----------------------

Special Reports

Particulate Air Pollution and Daily Mortality: The Phase I Report of the Particle Epidemiology Evaluation Project

Phase I.A. Replication and Validation of Selected Studies

1995

Phase I.B. Analyses of the Effects of Weather and Multiple Air Pollutants

1997

Reanalysis of the Harvard Six Cities Study and the American Cancer Society Study of Particulate Air Pollution and Mortality: A Special Report of the Institute's Particle Epidemiology Reanalysis Project

2000

HEI Communications

5 Formation and Characterization of Particles: Report of the 1996 HEI Workshop

1997

8 The Health Effects of Fine Particles: Key Questions and the 2003 Review

1999

HEI Program Summaries

Research on Particulate Matter

1999

* Reports published since 1990.

Copies of these reports can be obtained by contacting the Health Effects Institute, 955 Massachusetts Avenue, Cambridge MA 02139. Phone (617) 876-6700 FAX (617) 876-6709 E-mail pubs@healtheffects.org www.healtheffects.org



BOARD OF DIRECTORS

Archibald Cox *Chair*

Carl M Loeb University Professor (Emeritus),
Harvard Law School

Donald Kennedy *Vice Chair*

Editor-in-Chief, *Science*; President (Emeritus) and Bing Professor of
Biological Sciences, Stanford University

Douglas Costle

Chairman of the Board and Distinguished Senior Fellow,
Institute for Sustainable Communities

HEALTH RESEARCH COMMITTEE

Mark J Utell *Chair*

Professor of Medicine and Environmental Medicine, University of
Rochester

Glen R Cass

Professor and Chairman, School of Earth and Atmospheric Sciences,
Georgia Institute of Technology

Peter B Farmer

Professor and Section Head, Medical Research Council Toxicology Unit,
University of Leicester

Seymour J Garte

Professor of Environmental and Community Medicine, Environmental
and Occupational Health Sciences Institute

Helmut Greim

Professor and Chairman of Toxicology, Technical University Munich and
GSF–National Research Center for Environment and Health

Rogene Henderson

Senior Scientist, Lovelace Respiratory Research Institute

Stephen I Rennard

Larson Professor, Department of Internal Medicine, University of
Nebraska Medical Center

HEALTH REVIEW COMMITTEE

Daniel C Tosteson *Chair*

Professor of Cell Biology, Dean Emeritus, Harvard Medical School

Ross Anderson

Professor and Head, Department of Public Health Sciences,
St George's Hospital Medical School, London University

John C Bailar III

Professor, Department of Health Studies, Biological Sciences Division,
and Harris School of Public Policy, The University of Chicago

Thomas W Kensler

Professor, Division of Toxicological Sciences, Department of
Environmental Sciences, Johns Hopkins University

Brian Leaderer

Professor, Department of Epidemiology and Public Health, Yale
University School of Medicine

OFFICERS & STAFF

Daniel S Greenbaum *President*

Robert M O'Keefe *Vice President*

Jane Warren *Director of Science*

Howard E Garsh *Director of Finance and Administration*

Sally Edwards *Director of Publications*

Richard M Cooper *Corporate Secretary*

Aaron J Cohen *Principal Scientist*

Maria G Costantini *Senior Scientist*

Bernard Jacobson *Senior Scientist*

Debra A Kaden *Senior Scientist*

Alice Huang

Senior Councilor for External Relations, California Institute of
Technology

Richard B Stewart

Professor, New York University School of Law

Robert M White

President (Emeritus), National Academy of Engineering, and Senior
Fellow, University Corporation for Atmospheric Research

Jonathan M Samet

Professor and Chairman, Department of Epidemiology, School of Public
Health, Johns Hopkins University

Robert F Sawyer

Class of 1935 Professor of Energy (Emeritus), Professor of the Graduate
School, University of California, Berkeley

Frank E Speizer

Edward H Kass Professor of Medicine, Channing Laboratory, Harvard
Medical School, and Department of Medicine, Brigham and Women's
Hospital

Gerald van Belle

Professor, Departments of Environmental Health and Statistics,
University of Washington

Clarice R Weinberg

Chief, Biostatistics Branch, Environmental Diseases and Medicine
Program, National Institute of Environmental Health Services

Thomas A Louis

Professor of Biostatistics, School of Public Health,
University of Minnesota

Edo D Pellizzari

Vice President for Analytical and Chemical Sciences,
Research Triangle Institute

Donald J Reed

Distinguished Professor of Biochemistry, Department of Biochemistry
and Biophysics, and Environmental Health Sciences Center,
Oregon State University

David J Riley

Professor of Medicine, University of Medicine and Dentistry of New
Jersey–Robert Wood Johnson Medical School

Sverre Vedal

Professor of Medicine, University of British Columbia

Geoffrey H Sunshine *Senior Scientist*

JoAnn Ten Brinke *Staff Scientist*

Annemoon van Erp *Staff Scientist*

Gail V Allosso *Office and Contracts Manager*

Terésa Fasulo *Senior Administrative Assistant*

L Virgi Hepner *Senior Scientific Editor*

Francine Marmenout *Senior Executive Assistant*

Teresina McGuire *Accounting Assistant*

Jacqueline C Rutledge *Controller*



HEALTH
EFFECTS
INSTITUTE

955 Massachusetts Avenue
Cambridge MA 02139 USA
+1-617-876-6700
www.healtheffects.org

RESEARCH
REPORT

Number 98
November 2000

